ASHESI UNIVERSITY

DESIGN AND ANALYSIS OF A LOW COST, DEPLOYABLE UNMANNED AERIAL VEHICLE FOR ENVIRONMENTAL SURVEILLANCE

APPLIED CAPSTONE PROJECT

B.Sc. Mechanical Engineering

Lloyd Teta

2021

ASHESI UNIVERSITY

DESIGN AND ANALYSIS OF A LOW COST, DEPLOYABLE UNMANNED AERIAL VEHICLE FOR ENVIRONMENTAL SURVEILLANCE

APPLIED CAPSTONE PROJECT

Capstone Project submitted to the Department of Engineering, Ashesi University in partial fulfilment of the requirements for the award of Bachelor of Science degree in Mechanical Engineering.

Lloyd Teta

2021

Declaration

I hereby declare that this capstone is the result of my own original work and that no part of it has been presented for another degree in this university or elsewhere.

Candidate's Signature:

……………………………………………………………………………………………

Candidate's Name:

Lloyd Teta
……………………………………………………………………………………………

Date:

23 May 2021
……………………………………………………………………………………………

I hereby declare that preparation and presentation of this capstone were supervised in accordance with the guidelines on supervision of capstone laid down by Ashesi University.

Supervisor's Signature:

……………………………………………………………………………………………

Supervisor's Name:

……………………………………………………………………………………………

Date:

……………………………………………………………………………………………

Acknowledgements

First, I would like to express my sincere gratitude to my supervisor, Dr. Heather Beem, for the continuous support, encouragement, guidance, and academic advice during this capstone project. She gave me timely and helpful feedback on the project on several occasions. To Dr. Stephen Kofi Armah, I would like to declare my earnest appreciation for the advice and guidance on the engineering design process. I also wish to show my gratitude to the Department of Engineering faculty, whose feedback was instrumental in discovering flaws and areas to develop upon in this work.

I want to thank my family for their immense support to undertake this project at home. Thank you for always encouraging me to follow my dreams. Also, not forgetting my friends and classmates whose encouragement and academic advice helped me undertake this project. Lastly, I would like to express my sincere gratitude to the Almighty God for giving me strength and seeing me through the hard times.

Abstract

Surveillance aircraft require long flight endurance and range to perform their task fully. An aircraft's flight endurance can be increased by lowering the aircraft's weight and increasing the UAV's wingspan. However, the challenges that arise with a long wingspan are increased weight and costs due to the addition of materials to the wing. Most importantly, it results in large volumes that take much storage space resulting in difficulties in storing and deploying multiple UAVs. This project discusses the design and analysis of a low-cost micro-UAV with collapsible wings made from lightweight, flexible fabric. The UAV designed in this paper weighs less than 300g and flies at an altitude of 200m and a flight endurance of approximately 45 minutes. Size optimisation was done in guidance with the mission and design requirements.

Flight endurance baseline was established by deriving a mathematical endurance model together with power sizing. The shape of the UAV was defined using configuration selection. This was followed by 3D modelling of parts and were assembled using SolidWorks software. To wrap the design, an XFLR5 software was used to analyse and select aerofoils and analyse the UAV's aerodynamic performance, Cl, Cd and Cl/Cd. The coefficient of lift of the aircraft when cruising is 0.455. Results from XFLR5 were compared with the analytically predicted values. Lastly, structural analysis (Finite Element Analysis (FEA)) was performed numerically (using SolidWorks) to determine the structural performance of the wing hinge to avoid failures due to static and fatigue torsional stresses. The critical point on the hinge had 0.74% damage and a safety factor of 2.258, showing that the hinge is unlikely to fail.

Keywords: UAV Design, Aerofoil, XFLR5, Flight Endurance

Table of Contents

Declaration i

Acknowledgements ii

Abstract iii

List of Tables viii

List of Figures ix

Nomenclature xii

Glossary xv

Chapter 1: Introduction 1

1.1. Background and Motivation 1

1.2. Classification of UAVs 2

1.3. Problem Definition 3

1.4. Proposed Solution 3

1.4. Hypothesis 4

1.5. Aims and Objectives. 4

1.6. Research Questions 4

1.7. Method of approach 5

1.8. Requirements and Parameters 5

1.8.1. Functional Requirements 5

1.8.2. Mission Requirements and Specification 6

Chapter 2: Literature Review 7

2.1. Related Works 7

2.1.1. Development of an In-Flight-Deployable Micro-UAV 7

2.1.2. Design, analysis and fabrication of micro class UAV 8

2.1.3. Design of a micro-scale deployable unmanned aerial vehicle 9

2.2. Types of Deployable Wings 11

2.2.1 Inflatable wing 11

2.2.2 Semi Rigid/ Rigid foldable wing 12

2.2.3 Rogallo wing 13

2.2.4 Membrane wing 16

2.3. UAV Materials and Manufacturing Methods 17

2.3.1. Composites 17

2.3.2 Polymers 18

2.3.3. Wood 19

Chapter 3: Conceptional Design and Analysis 20

3.1. UAV Design Specifications 20

3.2. Configuration Design and Selection 20

3.2.1. Tail Configuration 21

3.2.2. Wing Configuration 21

3.2.3. Wing Platform (shape viewed from top) Configuration. 22

3.2.4. Airframe Configuration 22

3.3. Deployable Wing Design 23

3.3.1. Proposed design 1: Folding wings 23

3.3.2. Proposed design 2: Collapsible/Flexible wings 25

3.3.3. Selection of Wing Design 26

3.3.4. Selected Design and Deployment system........ 26

3.3.5. Folding Mechanism........ 27

3.4. Material Selection 29

3.4.1 Wing and Tail........ 29

3.4.2. Support Rods........ 30

3.5. Wing sizing 30

3.5.1. Determination wingspan and chord length) 30

3.5.2. Fatigue (Determination of the hinge diameter) 31

3.6. Aircraft Structure Weight Estimation........ 32

3.6.1. Summary of weight Calculations........ 32

3.7. Electric Propulsion Design Considerations........ 33

3.7.1. Power System 34

3.8. Endurance-Maximisation Relations 35

3.8.1. Mathematical Model Formulation For Endurance 35

3.8.2. Motor Efficiency Consideration 40

3.9. Summary Power System Sizing........ 41

Chapter 4: Aerodynamic Design and Analysis 43

4.1. XFLR5 Overview 43

4.2. Stability Analysis 48

4.2.1. Estimating the position Avionics Components/container........ 48

4.2.2 Checking for Stability Using XFLR5 50

4.3 Analytical Prediction of Aircraft's Aerodynamic....................50

4.4. Aerodynamic Simulation using XFLR5. 52

4.4.1. Wing analysis....................52

4.4.2. Whole Aircraft Analysis 54

4.5. Comparisons: Analytical and Simulated Aerodynamic Results 60

Chapter 5: Cad Modelling and Numerical Analysis....................61

5.1. 3D Models....................61

5.2. FEA (Static and Fatigue) on the hinge....................62

5.3. FEA(Static) Wing Bending 64

Chapter 6: Conclusion....................66

6.1. Achievements 66

6.2. Limitations 67

6.3. Future Work 68

References 69

Appendix A: Sizing and Estimation....................77

A.1. Fatigue (Determination of the hinge diameter)....................77

A.2. Aircraft Structure Weight Estimation....................79

A.2.1. Weight of the wings....................79

A.2.2. Tail weight estimation....................80

A.2.3. Main carbon square rod support weight estimation....................80

Appendix B: FXLR5 Aerodynamic Results 81

Appendix C: CAD Files....................85

List of Tables

Table 1: Design Process 5

Table 2: UAV Mission Requirements and specifications 6

Table 3: Design Requirements 20

Table 4: Pugh Chart for tail configurations comparisons. 21

Table 5: Pugh chart for wing configurations comparisons. 22

Table 6: Pugh Chart showing the comparisons of the wing platform configurations 22

Table 7: Pugh chart for aircraft configurations considered for the drone. 23

Table 8: Pugh chart for the selection of deployable wing design. 26

Table 9: Decision matrix for material selection of the fabric 29

Table 10: Material Properties of Ripstop Nylon [29][30] 29

Table 11: Material Seletion Decision matrix 30

Table 12: Summary for the hinge diameter estimation 32

Table 13: Summary of Aircraft weight Estimations 32

Table 14: Motor Comparizons for Selection 40

Table 15: Summary of Component selection and sizing 42

Table 16: Matrix selection of aerofoil 48

Table 17: Centre of Gravity Determination 49

Table 18: Summary of Aircraft Performance 51

Table 19: Analytical vs XFLR5 values 60

Table 20: Summary of Static and Fatigue Analysis 64

Table 21: Summary results for wing bending analysis 65

List of Figures

Figure 1: Flight Path For Commercial airliner and Surveillance [6]...... 1

Figure 2: Classes of UAVs[32]...... 3

Figure 3: Deployed and folded UAV...... 8

Figure 4: Fabricated micro-UAV...... 9

Figure 5: Stowed and Deployed configurations...... 10

Figure 6: Normal Inflatable wing (b) rigidizable inflatable wing[36]...... 11

Figure 7: Indirect 3D printed hexagonal diamond structured inflatable wing[20]...... 12

Figure 8: (a) Folded state (b) transition state (c) deployed state [44]...... 13

Figure 9: Early version of para-wing[38]...... 14

Figure 10: Rogallo wing-Aerofoil Section[41]...... 14

Figure 11: Georgia Tech' DBF Rogallo wing[42]...... 15

Figure 12: Clarkson University Membrane wing[46]...... 16

Figure 13: University of Florida UAV with membrane wing[47]...... 17

Figure 14: Formation of fibre composite matrix [53]...... 18

Figure 15: Deign 1 Sketch...... 24

Figure 16: Detailed Sketch for Design 1 Folding Mechanism...... 24

Figure 17: Deign 2 Sketch...... 25

Figure 18: Detailed sketch of the chosen UAV...... 26

Figure 19: Folding Mechanism for the Selected Design...... 27

Figure 20: Hinge Visualisation in CAD software...... 27

Figure 21: Collapsing wing...... 28

Figure 22: Fully collapsed/Folded wing Skeleton...... 28

Figure 23: Block Diagram Layout for the Electric components...... 33

Figure 24: Detailed Layout of Electric components...... 33

Figure 25: Out View drawing for SPB463048 [34]...... 35

Figure 26: Free body diagram for a level flight[35] 35

Figure 27: Endurance vs Battery cell count [17] 39

Figure 28: Efficiency characteristics of Westport 22.7mm,20T/25ga motor [23] 41

Figure 29: 2D Aerofoil Plots 45

Figure 30: Cd against alpha 45

Figure 31 Plot of ratio of (Cl/Cd) against alpha 46

Figure 32: Plot of Cl against alpha 47

Figure 33 The plot of Cl) against Cd 47

Figure 34: 2D plot of the S5010 aerofoil 48

Figure 35: UAV Free Body Diagram 49

Figure 36 (a) CG before stability analysis (b) CG' at ¼ chord after shifting avionics box 49

Figure 37: 3D UAV Model in XFLR5 50

Figure 38: Modelled wing in FXLR5. 53

Figure 39: Snippet for the input data for analysis 53

Figure 40: Lift, downwash, viscous and induced drag 53

Figure 41: The viscous and induced drag 54

Figure 42: Model of an aircraft in XFLR5 55

Figure 43: UAV Lift distribution 56

Figure 44: CL vs Coefficient of Pressure and Pressure 56

Figure 45: Distribution of cp 57

Figure 46: Pressure Distribution 57

Figure 47: Induced drag distribution. 58

Figure 48: Cd vs Alpha and normal force 58

Figure 49: Streamlines on the aircraft 59

Figure 50: Surface velocity vector 59

Figure 51: Isometric view 61

Figure 52: Top View 61

Figure 53: Exploded View 61

Figure 54: Assembly drawing 62

Figure 55: Von Misses stresses (b) Static FOS 62

Figure 56: Material displacement 63

Figure 57: (a) the damage percentage   (b) Total life(number of circles) 63

Figure 58: Load Factor 63

Figure 59: (a)Wing deflections   (b)Von misses stresses 64

Figure 60: Factor of safety for the wing structure 65

Figure 61: DE-Goodman graph 79

Figure B.1:drag and lift 81

Figure B.2: Cl vs Wingspan 81

Figure B.3: Total drag vs Wingspan 82

Figure B.4: Induced drag vs Wingspan 82

Figure B.5: Aerofoil drag vs wingspan 82

Figure B.6: Streamlines 83

Figure B.7: All Aerodynamic Properties 83

Figure B.8: Surface Velocity vector 84

Figure C.1:Front View 85

Figure C.2: Isometric View 85

Figure C.3: Side View 85

Figure C.4: Assembly drawing 86

Nomenclature

Greek symbols

α	Angle of attack.
η_{ESC}	Electronic Speed Controller efficiency.
η_{motor}	Motor efficiency.
η_{Pro}	Propeller efficiency.
μ	Atmospheric dynamic viscosity.
ρ	Density.
σ	Stress.
σ_{yied}	Plasticity yield stress.

Roman symbols

$\bar{c}$	Mean aerodynamic chord.
AR	Aspect Ratio.
b	Wingspan.
c	Chord.
C_D	Three-dimensional drag coefficient.
C_L	Three-dimensional lift coefficient.
C_l	Two-dimensional lift coefficient.
C_{Do}	Three-dimensional zero lift drag coefficient.
C_{Di}	Three-dimensional lift induced drag coefficient.

D	Aircraft drag.
$\bar{E}$	specific energy of battery
E	Young's modulus.
e	Osvald factor.
h	Altitude.
Kv	RPM constant of a motor
L	Aircraft lift.
l	Length.
P_{flight}	Power of Flight
P_{bat}	Battery Power.
P_{pro}	Propulsive Power.
q	Lift force distribution.
Re	Reynolds Number.
S	Wing area.
T	Thrust.
t	Time.
t_{end}	Endurance.
$W_{ESCmotorprop}$	Weight of Power System
W_{bat}	Weight of the Battery.
$W_{airframe}$	Aircraft's Airframe Weight.

$W_{sensors}$ Weight of Sensors.

V Horizontal Velocity vector.

Glossary

BEC	Battery Eliminator Circuit
CAD	Computer Aided Design.
CFD	Computational Fluid Dynamics.
CG	Centre of Gravity.
ESC	Electronic Speed Controller.
FEA	Finite Element Analysis.
HALE	High Altitude Long Endurance.
LiPo	Lithium Polymer battery.
LLT	Lifting Line Theory
MALE	Medium Altitude Long Endurance.
MTOW	Maximum Take Of Weight.
MUAV	Micro & Mini UAV.
RPM	Revolutions Per Minute
TUAV	Tactical Unmanned Aerial Vehicle.
UAV	Unmanned Aerial Vehicle.
VTOL	Vertical Take-off and Landing

Chapter 1: Introduction

1.1. Background and Motivation

Several Unmanned Aerial Vehicles (UAVs) popularly known as automated drones have are fast developing in Africa. Unmanned Aerial Vehicles have recently gained attention due to their ability to perform trailblazing tasks such as food and medical delivery, photography, agriculture, construction, mining and environmental monitoring and surveillance [8]. More importantly are used in disaster relief, as well as in dangerous military missions where there is a high risk of losing lives. Due to their small size in nature, UAVs are considered quicker, less cost and efficient than manned aircraft like helicopters as they can reach confined areas where a human cannot easily reach [9]. UAVs have better maneuverability hence are more suitable for sophisticated missions. The figure below shows differences in the mission profiles for commercial airline and that of surveillance UAV. Despite the increase in demand for UAV operation, there are stringent policies on the UAVs operation for human safety measures. As a result, researchers are conducting experiments to find ways to make the technology more feasible, efficient and less costly.

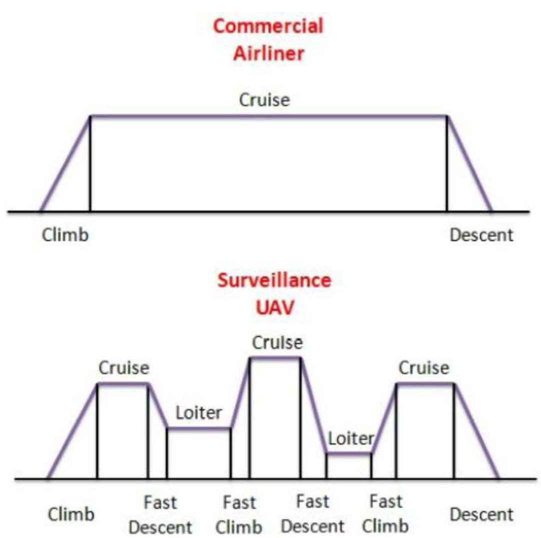

Figure 1: Flight Path For Commercial airliner and Surveillance [6]

This project focused on the context of Sub-Saharan Africa. The technology of using UAVs for different uses is fast developing in different African Countries. A notable example is the use of drones by Zipline to deliver lifesaving medicines in Ghana and Rwanda. Drone revenue in Africa is expected to reach US$625 million by 2025[10]. In Ghana, startup companies such as SKT AeroShuttle are manufacturing UAVs for Agriculture and other specific purposes [11]. More importantly, the government of Ghana are using drones for surveillance missions such as gathering data against illegal mining [12]. One of the critical requirements for surveillance planes is high flight endurance and range to fully perform their task [4]. Flight endurance is the longest time taken by an aircraft in before landing, whereas range is the largest distance travelled by plane before landing [5]. Study shows that lowering the aircraft's weight as well as increasing the wingspan of a UAV increases its endurance [6].

1.2. Classification of UAVs

Unmanned Airial vehicles are classified basing on different characteristics such as flight range, endurance, velocity, payload weight, as well the uav's size. Several classes are used to categorise these uavs. These are Micro & Mini UAV(MUAV), Tactical Unmanned Aerial Vehicle (TUAL), Vertical Take-off and Landing (VTOL), Medium Altitude Long Endurance(MALE) and High Altitude Long Endurance(HALE. The MUAV has a range of 0-75km, altitude 1000ft and payload capacity of 0-5kg. TUAV has a flight range of 0-100km, altitude of up to 15000ft, and a payload capacity of 1-150kg. VTOL class has a range of 0-250km, altitude of up to 18000ft and payload capacity of 1-150kg. Last but not least, the MALE category has a range of 100-5000km, an altitude 1000ft to more than 40000ft and a payload capacity of 60-400kg. Finally the HALE class has a flight range of 1000-to more than 10000km, an altitude of exceeding 40000ft and a ppayload capacity of 400-2000kg.)[32]

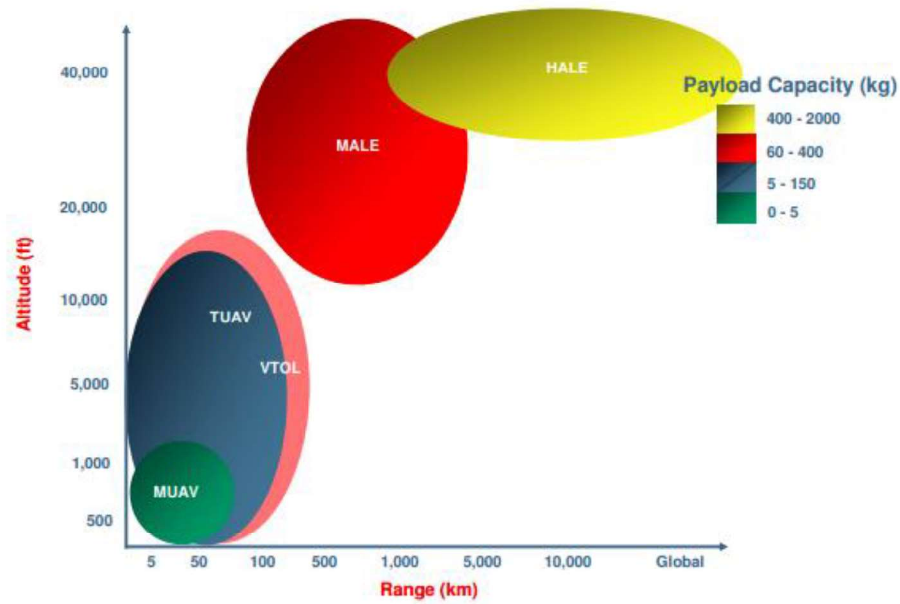

Figure 2: Classes of UAVs[32]

1.3. Problem Definition

Increasing an aircraft's wingspan can help increase flight endurance needed for surveillance. However, the challenges that arise with a long wingspan are increased weight and costs due to the addition of materials to the wing. It is expensive to perform surveillance operations successfully; thus, the lack of resources and funds threatens to hinder the technological advancement of UAVs in Africa [13]. Other disadvantages of a long wingspan are storage problems. It takes ample storage space and makes it challenging for African drone companies to deploy UAVs in large numbers, especially in space-restricted applications such as air, hand launch and marines[7][45]. Thus, this project is motivated by the need to increase flight endurance for the UAV without trading off its less weight and cost.

1.4. Proposed Solution

This capstone project aims to design and fabricate a low cost and storage efficient UAV by fabricating collapsible aircraft structures. This will potentially be done by modelling and developing a micro-UAV possible to perform better than the available average-sized UAVs.

The smaller size will result in the cut of manufacturing resources as well as cost. The micro-design will be accompanied by a flexible wing design capable of collapsing when storing and unfolding for rapid deployment in flight. The project will also explore different fabrication methods that will enable the low-cost manufacturing of the proposed model to reduce the costs further.

1.4. Hypothesis

With proper design parameters, there is the smallest permissible size for UAV where it has the same or better flight performances than that of the average-sized UAVs.

1.5. Aims and Objectives.

Primary Objective: to design and analyse a low cost, micro-UAV with collapsible wings capable of deployment.

Specific:

- Select aircraft configuration that suits the design requirements.
- Design the folding mechanism of the UAV.
- Design a small-sized UAV by carrying out wing and fuselage sizing.
- Model a low-cost propulsion system of the UAV.
- Minimise the cost of the UAV through material selection.
- Model all UAV parts using SolidWorks!
- Perform Finite Element Analysis on critical parts and aerodynamic characteristics for the UAV using XFLR5 and compare with analytical values.

1.6. Research Questions

- What are the mechanisms for collapsing/folding the wing?
- What are the disadvantages of the existing deployable UAV designs?
- What are the materials used in deployable structures?

1.7. Method of approach

To achieve the objectives of this capstone project below is an outline of the steps that will be followed.

Detailed design process
Design and Specifications of the mission profile requirements
Design Matrix, Configuration Selection (tail and wing)
Design and Sizing Considerations, Reynold’s number
Propulsion system Analysis
Collapsible Wing Structure Design
Design Matrix -Material selection
Cad modelling and simulation
Prototyping
Static, Aerodynamic and Flight Testing
Data Analysis
And conclusion.

Table 1: Design Process

1.8. Requirements and Parameters

1.8.1. Functional Requirements

The UAV must perform the following listed function requirements for it to fulfil the design objectives.

1. It should be able to be collapsible.
2. High long-range capabilities
3. Should be able to self-lock into flight configuration.
4. Be capable of deploying/operating from high altitude flights.
5. Should have high flight endurance.
6. Should be able to carry a small atmospheric sensing payload.
7. Should be able to carry an autopilot and communication system.

1.8.2. Mission Requirements and Specification

The mission requirements govern the UAV design. The following table shows the mission requirements of the UAV to be modelled. The values are inspired by some of the existing UAVs on the market, with some specifications improved to better the current values[33].

Mission Parameter	Expected performance
Endurance	>45 min
Operating Altitude	200 m
Manoeuvrability	Turning radius of $\leq 1km$
Range	≥20 km
Cruising speed	$10m/s \leq v \leq 20\ m/s$
Re number	<60000

Table 2: UAV Mission Requirements and specifications

Chapter 2: Literature Review

Deployable UAV can adjust their structure or size to perform a required task. This allows storing and deploying them in large numbers [1].

2.1. Related Works

Different designs of deployable UAVs have been proposed, and many successful tests prove that unmanned aerial vehicles are becoming more efficient and less costly. This paper studies and evaluates works of literature related to the objective of this project. The scope explored are previous and current design, materials used as well as manufacturing processes. Knowledge from the study shows that researchers proposed designs to achieve the criterion of a deployable UAV. This ranges from foldable wings, inflatable and compliant wings, as well as micro UAVs. Related work was summarised and analysed to save as a reference for the future design of this project.

2.1.1. Development of an In-Flight-Deployable Micro-UAV

The article by Tao and Hansman developed a surveillance micro-UAV capable of being deployed from a host aircraft flying at an altitude of 35 000 feet [17]. Also, the UAV system, which would carry atmospheric sensing payload and an autopilot and communication system, was designed to achieve maximum endurance. The researchers outline that the smaller battery yields a lower flight endurance due to the reduction of energy carried, whereas having a larger battery result in the increased wing loading and drag; hence endurance also decreases. Thus, through well outlined mathematical modelling, they optimised the battery size basing on the wing configuration, which met the packaging constraints. Also, to increase endurance, they carried out an experimental analysis to determine the wing and fuselage's best geometrical layout and position. Lastly, they designed the wing folding mechanism as well as fabricating and testing the prototype.

Figure 3: Deployed and folded UAV

The authors gave an in-depth analysis of the experiments carried out and stability and the aerodynamic tests performed. They also did well as they explicitly state the materials used for the sub-components of the UAV, which highlighted how they determined the weight of the subsystem and ensured lightweight. However, using an expensive Kevlar may not be economically sustainable for African drone companies that may need to adapt the design idea. Overall, the article is of much use to my capstone project. It outlined some of the essential

parameters that may need to considered in this project to increase the UAV's flight endurance.

2.1.2. Design, analysis and fabrication of micro class UAV

In this paper, the authors discuss the design and analytical approach for the UAV [19]. The purpose of the study was to construct a UAV with high structural strength with a possible lightweight. Their design process consisted of selecting fuselage configuration with better capabilities such as lift capacity, stability and ease of construction. They also performed aerofoil analysis, and they chose the one with the highest lifting capabilities at a low Reynolds number. The research carried out further investigation to reach optimum sizing and operating efficiency. These included thrust analysis, servo sizing, drag and lift analysis. The static loading of the wing was simulated and analysed using ANSYS software. Uniform load was applied along the wingspan, and they concluded that the wing will not break and is within safe limits.

The authors used balsa wood for the wing, fuselage and tail, claiming it is strong and lightweight.

Figure 4: Fabricated micro-UAV

Although the researchers performed analytical and simulations to test their hypothesis, there is no evidence of the experimental approach of physical tests actually to prove if their design work. Moreover, they did not explicitly show the material strength analysis and compared to back the claim that balsa wood is better in terms of strength and reduced weight.

2.1.3. Design of a micro-scale deployable unmanned aerial vehicle

In their paper, the authors Alioto, Bittitta, Epps, Nguyen, Yahaghi and Mourtos, presented the design of a micro-scale, autonomous unmanned aerial vehicle that is capable of being deployed from a cylindrical tube and withstand high wind conditions [18]. The researchers focused on designing the configurations of the aircraft as well as a unique deployment capability.

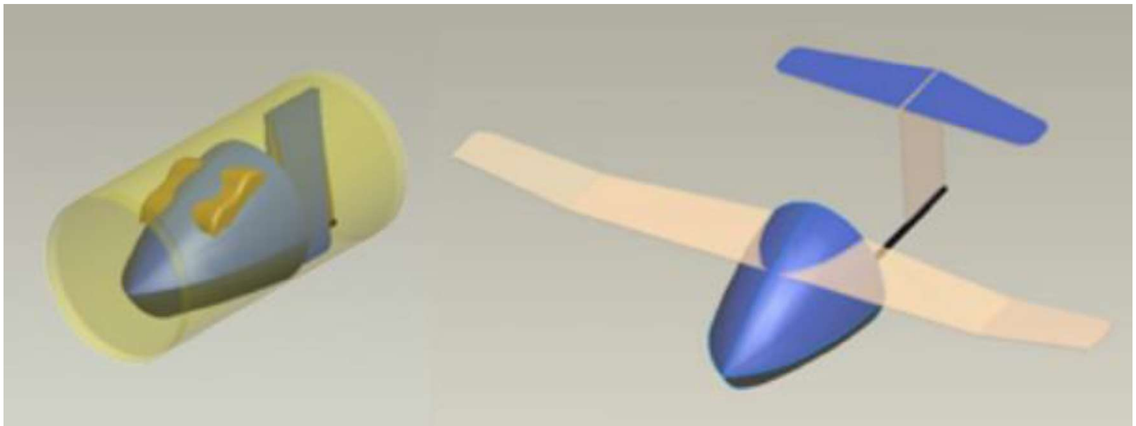

Figure 5: Stowed and Deployed configurations

The researchers performed tail configuration selection to find a way of minimising the size of the UAV when storing. As a result, they chose a T-tail configuration which demonstrated that the horizontal stabiliser could be folded down towards the tail. The fuselage was designed to house the autopilot and the inflation system, with the rest of the tail made of a carbon fibre tail boom capable of rolling to reduce its length. They also used the inflatable structure for the wing design. They abandoned the favoured technique of multi-chambered inflatable wing structure, which help provide shape and the stiffness of the wing. According to their research, the bumpy profile provided by the inflated tubes improves the aerodynamic performance of the aircraft. However, the authors claimed that this design is intricate, and the small tube diameters may be challenging to implement in micro-UAVs; hence they opted for a single large chamber. Their system consisted of a wing core that was an open foam cut into a shape of an aerofoil and then a PVC fabric adhered to the foam. The primary purpose of the foam was to provide stiffness and maintain the shape of the wing. The design offers a simple manufacturing process of the wing, and also, the foam and PVC are low-cost materials. However, the authors outlined that the disadvantage of this design is that when inflated, the foam partially delaminated from the core resulting in lost wing shape, which affects the aerodynamic characteristics of the wing. Thus, more research on a possible adhesive or technique is required.

2.2. Types of Deployable Wings

2.2.1 Inflatable wing

Inflatable wings have emerged as an alternate wing design solution for situations where wings need to be stowed when storing the aircraft. It is being used as an alternative to the traditional wing design of a folding mechanism for the same application of stowing the UAV when not in use. They have found applications in planetary exploration due to the low volume to weight packing ratio. Although inflatable wings are conceptually possible in almost any aircraft size, they are most appropriate for developing micro to medium scale UAVs [37].

A UAV that uses inflatable wings is deployable manually or autonomously pumping air into the wing before the flight. When the wing is inflated, it becomes rigid and stiff for flight. Previous research experiments show the success in the rigidization of inflatable wings for

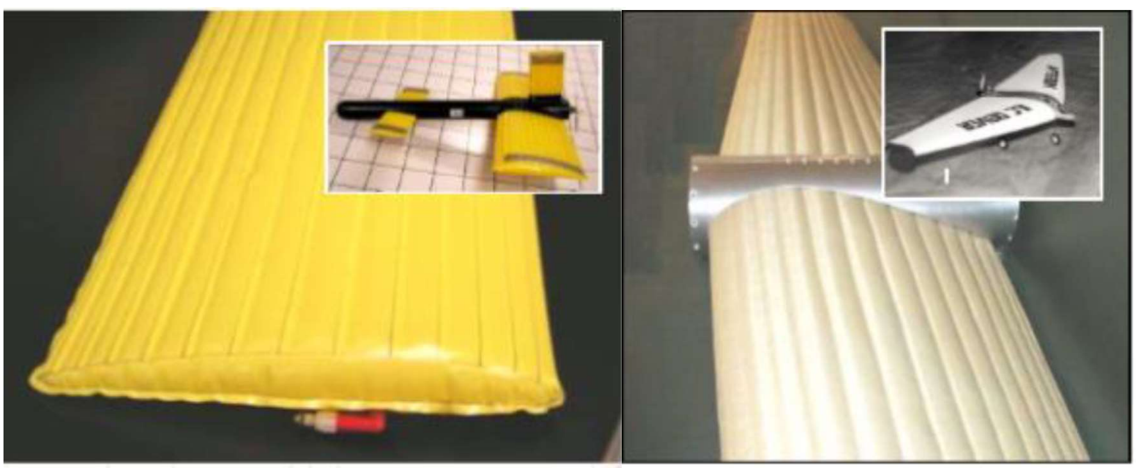

flight.

Figure 6: Normal Inflatable wing (b) rigidizable inflatable wing[36]

The design offers a better alternative to the foldable wing as it has less weight and is storage efficient by rolling the deflated wing firmly. However, the disadvantage is that when a fault occurs on an inflatable wing, it can lose its shape resulting in loss of flight. Current researchers use expensive and robust material for the inflatable wing to curb this challenge, such as Kevlar [3]. The lack of resources, funds and skills have delayed Africa to catch up with the technology of manufacturing and using massively deployable UAVs. As a result, there is a necessity for a redesigned structure that will allow Africa to deploy Unmanned Aerial Vehicles.

In the research paper, “Inflatable Wing Design for Micro UAVs using Indirect 3D Printing”, the authors proposed a new design of an inflatable wing to address challenges encountered in the previous and existing techniques of inflatable wings [20]. The new inflatable design consists of a networked lattice of a hexagonal diamond structure made of a flexible silicon rubber material.

Figure 7: Indirect 3D printed hexagonal diamond structured inflatable wing[20]

According to the authors, the purpose of the lattice structure is to conform to the desired shape of the wing and carrying the potion of the load exerted on the wing. They claimed that their proposed design increases aerodynamic performances and decreases the weight and complexity of the wing. The study outlines a manufacturing approach of using “indirect 3D printing” to fabricate their proposed design. The “indirect 3D printing” fabrication process starts by creating a 3D printed mould in a structure of hexagonal lattices. The silicon rubber is then injected and cast. The authors argued that this method has the advantage of direct three printing because the final product will not have different layers (monolithic part) instead of having different layers that pose a problem of failure in critical components affected by defects in the bonding of separated layers.

2.2.2 Semi Rigid/ Rigid foldable wing

Rigid foldable wings are probably the first and the oldest deployable technology. The wing is rigid and has high stiffness, which is maintained throughout the wing. The stiffness helps preserve the shape of the aerofoil section and cannot be easily altered during flight. The deployable semi-rigid wing designs are foldable wings that can be stowed for storage and unfolded when the plane is ready to fly. They were mainly used in rockets and missiles, where they would be deployed at a certain altitude in flight. However, this design technology has several flaws that prompted for more inventions of new deployable wings. First, foldable rigid wings have a high volume packing to weight ratio; therefore, they are heavy, resulting in a reduction in flight endurance [2]. They are not suitable for medium and micro-UAVs due to the presence of complex mechanical components and connections such as joins, bolts and nuts. These extra components add extra weight to the UAV, which is not cost-effective. Even when stowed, they still consume a considerable storage volume; hence they are quite difficult to store/deploy many UAVs at once.

Furthermore, semi-rigid wings are not suitable for low Reynolds number as they are susceptible to adverse pressure gradients that result in the reduction of flight performance [43]. Also, rigid wings are intricate in designing a morphable wing. The figure below shows the deployment process of a rigid tandem wing.

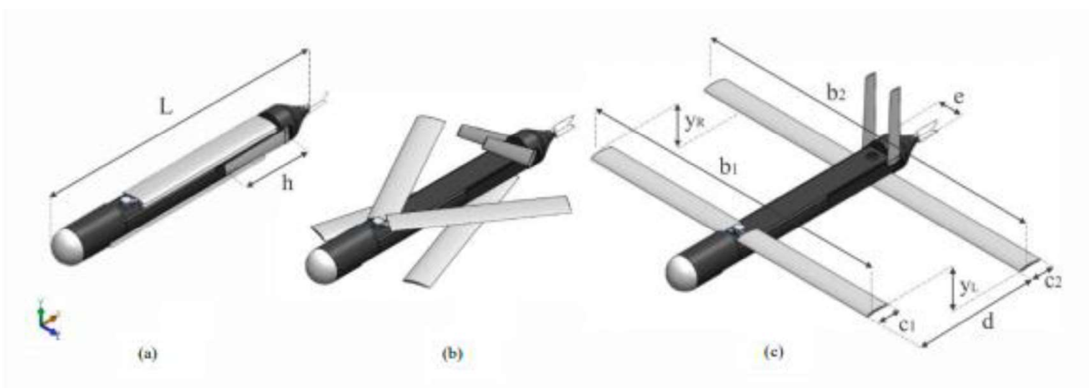

Figure 8: (a) Folded state (b) transition state (c) deployed state [44]

2.2.3 Rogallo wing

In 1945, with the help of his wife, Dr. Francis Rogallo, an aeronautical engineer of the National Aeronautics & Space Administration (NASA), developed a flexible wing kite called the "Flexi-Kite". NASA initially used the wing as a recovery system for capsules and spacecraft landing

[39]. Many developments were made, and currently, a partial conical-shaped surface pointed forward are now termed synonymously as Rogallo Wing after inventor Francis Rogallo. Its shape is in the form of an aerofoil curve that can flex in the wind, giving it favourable aerodynamic characteristics as it is less susceptible to turbulence. The engine was later attached to the wing, and the first powered manned Rogallo wing test was done in 1945. It is also argued that Dr Francis made a significant contribution to the development of the currently famous "Delta Wing" [39].

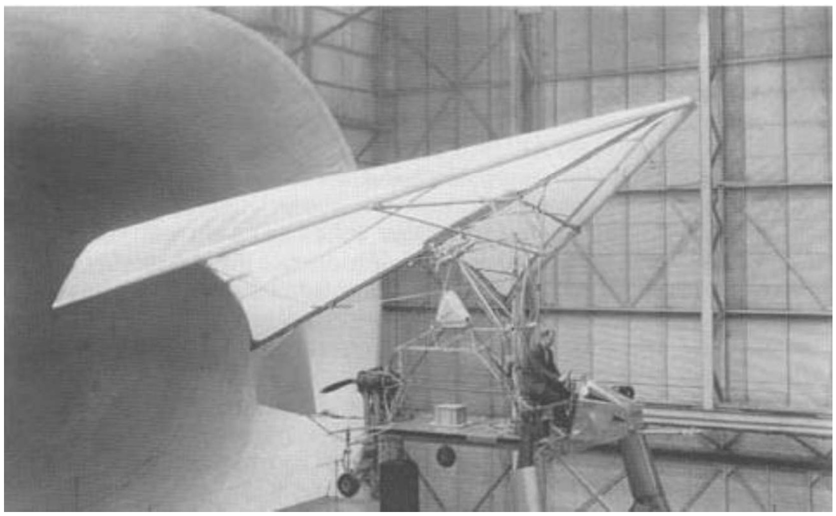

Figure 9: Early version of para-wing[38]

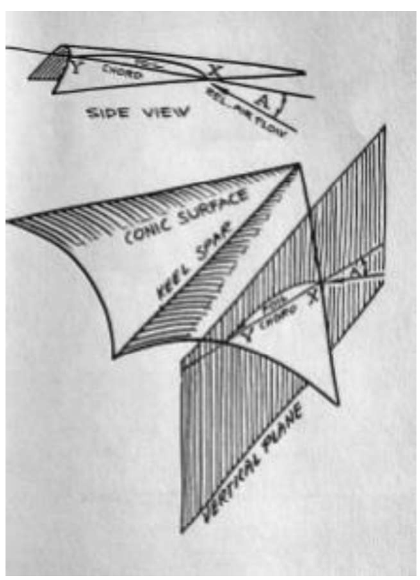

Figure 10: Rogallo wing-Aerofoil Section[41]

Rogallo wing has many advantages such as light weight, which makes it power consumption efficient and long flight endurances. Also, it is low cost in manufacturing and design as it uses low-cost material such as few metal bars and inexpensive fabric. Flexibility makes it easier for the wing to warp there by increasing UAV's aerodynamic performance. However, though the Rogallo wing offers optimum performances, it has several flaws, so it is not used in bigger aircraft. Due to its shape, the engines are mounted on the wings; hence, the aircraft is restricted to single-engine or inline engines. Still on this, the landing gear is mounted and retracted into the wing, making it challenging to design for flexible wings. Lastly, it poses a safety issue as sometimes the flexible wings may fail to deploy during inflight deployment tasks [40].

However, Rogallo wing has found applications in unmanned aerial vehicles due to their ability to flex. The use of Rogallo wing in UAVs has helped avoid some of the limitations outlined above as medium UAVs such as safety and micro-UAVs use propellers instead of engines and no need for landing gears. One example is a Rogallo UAV designed by students at the Georgia Institute of Technology for their DBF competition. This design was awarded number 2 in the design competition.

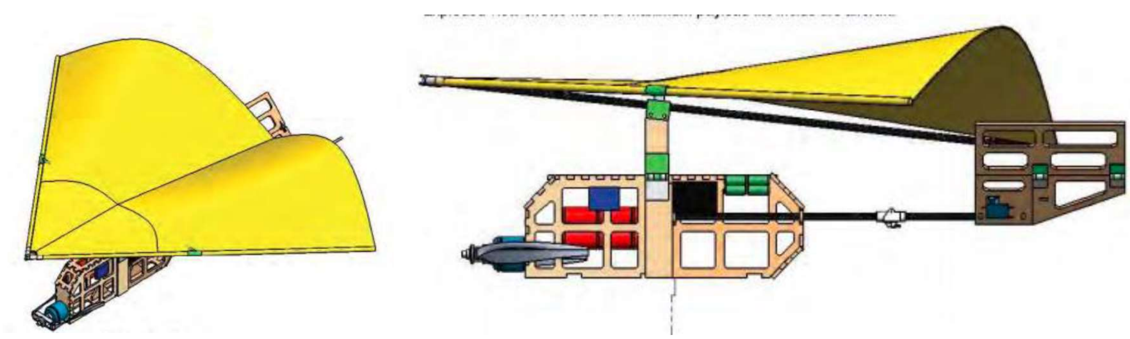

Figure 11: Georgia Tech' DBF Rogallo wing[42]

The UAV can collapse when storing and automatic deploy when inflight. Four carbon fibre rods were used to make triangular support that makes the Rogallo wing. It was then covered by ripstop nylon fabric owing to its strength and light weight. Through calculations derived from NASA data and function, the authors derived the aerodynamic characteristics of the UAV with a lift coefficient as high as 0.75. The fuselage was made using Balsa wood, and maximum stress was calculated using Euler-Bernoulli equations. They found that their Rogallo wing design withstands a total weight of 2.005 pounds [42].

2.2.4 Membrane wing

"Membrane wings are flexible wings that are rigid enough to resist aerodynamic forces and

provide lift while retaining the flexibility required to allow the wing to conform to its environment. Are flexible that they can wrap around the fuselage" [43]. It was first developed at Clarkson University.

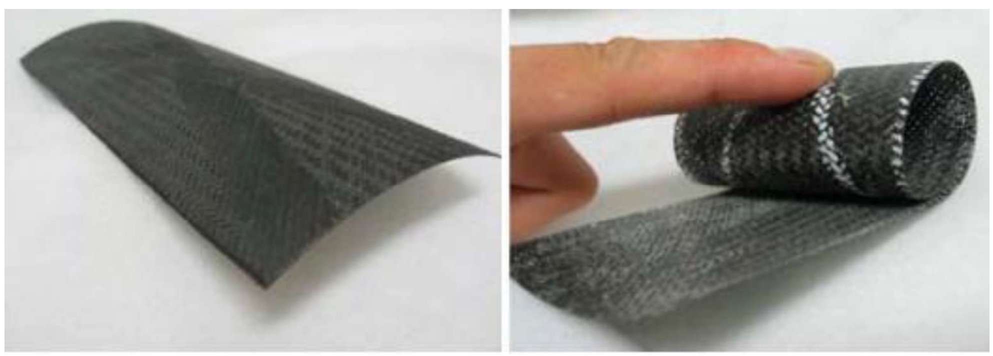

Figure 12: Clarkson University Membrane wing[46]

Several aerodynamic tests were carried out, and the wing had an optimum performance. However, it was discovered that it was difficult to deploy when flying at high velocities or greater angle of attack. The researchers argued that it was due to the lack of stiffness on the wing [46]. This limitation reduces its application to most UAVs.

When used in UAVs, the membrane wing has a high strength to overcome buckling due to flight load stresses. It also has several advantages over the conventional rigid foldable wing. It is lightweight than the conventional rigid wing and since it is flexible, this type of wing gives wings morphing developments and innovation possibilities. As said before, membrane wing is quite suitable for micro to medium UAVs as they are lighter. Human-crewed and commercial aircraft have large masses; hence the weight can cause buckling during flight. Several micro-

UAV with membrane wings were developed. Below shows a figure of the flexible membrane wing designed by the University of Florida.

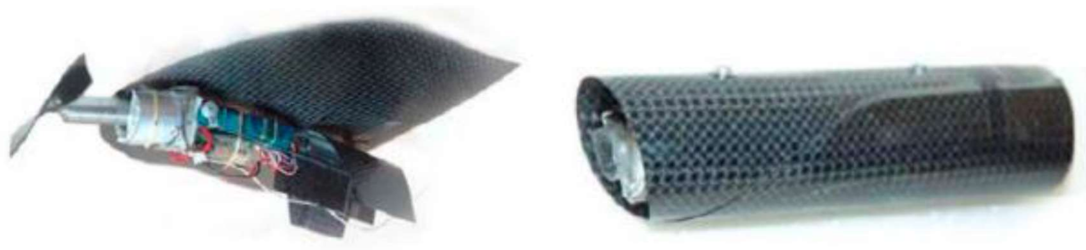

Figure 13: University of Florida UAV with membrane wing[47]

2.3. UAV Materials and Manufacturing Methods

2.3.1. Composites

Composites can be defined as a material structure consisting of two macroscopically identifiable materials with different physical and chemical properties working together to accomplish a superior property than their respective individual properties [52]. Composites have found application in Aerospace due to their superior properties. The most interesting composite if the Fibre Reinforced Polymer composite (FRP). The reinforcing fibre provides the stiffness and strength of the polymer matrix thus help avoid wear and cracks. Some of the common fibres are carbon, glass, basalt and natural fibres. On the other hand, the polymer matrix, helps to avoid external damage by distributing the stress along the fibres [53].

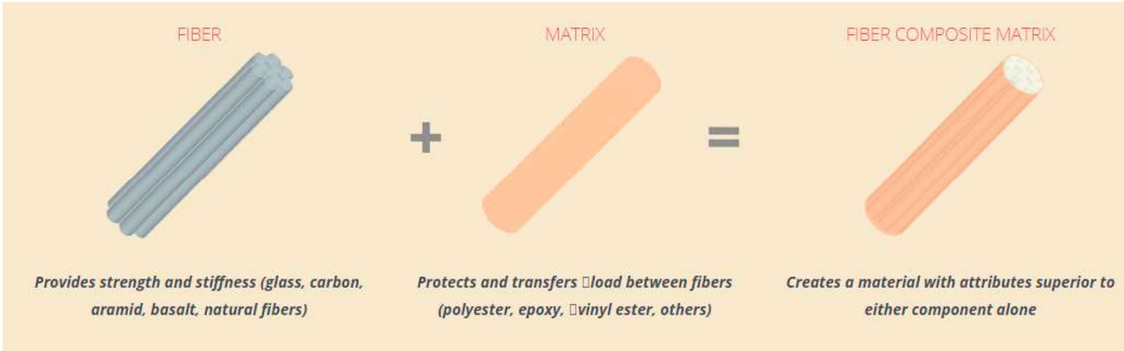

Figure 14: Formation of fibre composite matrix [53]

The most common composite in Aerospace it the Carbon Fibre Reinforced Polymer (CFRP). This is made from a polymer matrix that is reinforced with a carbon fibre. They are considered to be low cost, have high load carrying capacity, high strength, low density, high toughness, high hardness, low damage tolerance, low friction coefficient and good wear resistance, chemical and dimensional stability and corrosion resistance [54]. It has high modulus of elasticity in the ranges between 120-580 GPa and the tensile strength in the ranges 1.7 to 3.6 GPa. It also has strain at break of 0.5-1.9 percent [55].

2.3.2 Polymers

Polymers is a substance or ma made up repeated molecules called monomers. Polymers are light with a certain degree of strength hence their application in aerospace. Other important properties are that they are resistant to chemicals and are insulators for thermal and electricity [51]. As material and manufacturing processes is also crucial for my project, I read a paper entitled, "Application of 3D Printing Technology for Designing Light-weight Unmanned Aerial Vehicle Wing Structures" [21]. The authors started by investigating different structures used for wings such as foams, honeycombs and truss lattice. They found that the 3D lattices are superior than both foams and honeycombs as it has higher strength and light weight. As a result, the research's focus was to identify the lattice structure with the favourable elastic performance for deployable UAV wing design. According to the authors, "lattice structures consist of repeating units of identical skeleton structures of geometric three-dimensional shapes such as a polyhedron arranged in a regular pattern." Their proposed lattices structures for testing were 3D Kagome, pyramidal and the hexagonal diamond. With polypropylene as a selected material, the structures were fabricated using Objet 350 3D printer. This method of fabrication is less expensive and is more flexible as the lattice structures can be easily produced from CAD files. They performed compression tests to investigate the structure that can withstand high stresses. The results proved that the Kagome structure has the highest load structure hence their proposed inflatable wing design maximises flexibility as well as the advantage of having compliant mechanism.

2.3.3. Wood

There are many varieties of woods although are classified in three categories namely hard, soft and engineered wood. Hard woods are dense hence have very high strength and are durable. Examples of hard woods are Alder, Aspen and Balsa wood. Soft woods are less dense thus they are less strong, durable and cost than the hard woods. Engineered woods are woods that are machined and hence have new and different properties to the original material. An example of an engineered wood is plywood [48].

Woods have found application in aerospace structures and manufacturing due to their favourable characteristics. Some of the desirable characteristics are that they are abundant which makes them cheap. They are also light weight which is an important characteristic for aerospace materials. Lastly woods are biodegradable hence are environmentally friendly. The most type of wood used for aircraft structure is the Balsa wood. Although it is a hard wood, it is very light weight unlike most of the hard woods hence its great application for building drone aircrafts [49]. It has good stiffness to weight ratio. Balsa wood has strong axial stresses(tension) than in lateral direction. It has an elastic modulus as high as and an ultimate strength [50].

Chapter 3: Conceptional Design and Analysis

This chapter presents the solution and the conceptional design of the deployable uav.

To archive the design specifications, this project seeks to:

1. Design a micro unmanned aerial vehicle capable of carrying sensing load for environmental monitoring.
2. Design retractable wings that are capable of being deployed manually when about to fly.

3.1. UAV Design Specifications

After identifying the issues to address and determining the project's objective, the design specifications were developed to serve as a guideline for the selection of various configuration and components as well as design decisions.

Design Parameter	Baseline Requirement
Aircraft's skeleton weight	$45\text{g} - 90\text{g}$
Total weight (including the sensors)	$\leq 300\text{g}$
Number of motors	≤ 2
Wingspan	$350mm - 500mm$
Aircraft Length	$\leq 300mm$

Table 3: Design Requirements

3.2. Configuration Design and Selection

The mission requirements inform the choice of configuration. The criterion are thoroughly chosen to meet the project's objectives. These are cost, weight, manufacturability and foldability. Weight are assigned to each criteria depending the importance to the specific configuration. The design matrix charts are used to select the best configuration. Four main configurations examined are for wing, tail, wing platform and aircraft airframe.

3.2.1. Tail Configuration

The main purpose of the tail section of a conventional aircraft is to provides stability for the aircraft. It also serves as a surface control, with the rudder and elevator attached to it. The two controls yaw and the pitch of the aircraft respectively. From the research, the main tail configurations are, the conventional tail configuration, V-Tail and T-tail.

Criteria	**Weight**	**Conventional** 	**V-tail** 	**T-tail** 
Cost	0.30	2	2	1
Weight	0.30	2	2	1
Foldability	0.10	1	2	1
Stability	0.20	2	0	1
Total	**1.00**	**1.7**	**1.4**	**0.9**

Table 4: Pugh Chart for tail configurations comparisons.

From the matrix table, the V tail configuration has a better score for cost, foldability and weight; however, the conventional tail has an overall performance as it is more stable hence is selected.

3.2.2. Wing Configuration

The three main wing configurations are low wing, high wing and mid wing. The low wing means the wing is below the midline of the fuselage, while mid wind is at the midline of the fuselage. Lastly the high wing is located at the top of the fuselage. Different wing configurations offer different aerodynamic characteristics, hence the pugh chart was also used to select the configuration that best suit the outline criterion.

Criteria	**Weight**	**Low wing** 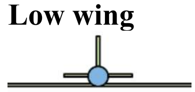	**Mid wing** 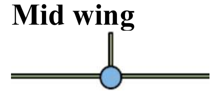	**High wing** 
Stability	0.3	0	1	2
Manufacturability	0.3	2	1	2

Ground clearance	0.1	0	1	2
Foldability	0.3	1	0	2
Total	**1**	**1**	**0.7**	**2**

Table 5: Pugh chart for wing configurations comparisons.

The merit of choosing the wing configuration are stability, manufacturability, ground clearance and foldability. The high wing configuration scored the highest hence is selected for the uav.

3.2.3. Wing Platform (shape viewed from top) Configuration.

The main purpose of the wings are to provide overall lift for the aircraft. It also serves as a housing surface for the ailerons, flaps, Spoiler and Slats. The two controls the aircraft's roll, lift and drag. Different wing shapes have different characteristics. The three main platform configurations considered are, the conventional (rectangle configuration, Tapered and Prismatic wing section.

Criteria	Weight	Rectangle 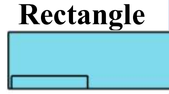	Tapered 	Prismatic Mid-Section 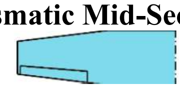
Aerodynamic	0.30	1	2	1
Weight	0.30	0	2	1
Foldability	0.10	1	2	1
Manufacturability	0.20	2	1	0
Total	**1.00**	**0.8**	**1.7**	**0.7**

Table 6: Pugh Chart showing the comparisons of the wing platform configurations

Four selection criterions used are Aerodynamic performance, Weight, Foldability and Manufacturability. Tapered wing is selected as it has overall best figure of merits.

3.2.4. Airframe Configuration

The airframe of a uav is the main hollow body that houses the sensors, electronics and also hold the other parts of the aircraft together such as wings and tail. It also provides lift and drag for the uav. The airframe configurations explored in this study are, conventional, biplane and flying wing. Conventional has one wing, whereas biplane has a wing above and another below the fuselage. A flying wing has whole body made of the wing. It sometimes usually has low aspect ration.

Criteria	**Weight**	**Conventional** 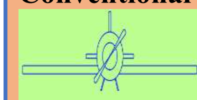	**Biplane** 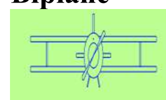	**Flying Wing** 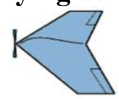
Weight	0.3	1	1	2
Manufacturability	0.2	2	1	0
Cost	0.1	2	1	2
Aerodynamics	0.1	2	0	2
Foldability	0.3	2	0	2
Total	**1**	**1.7**	**0.6**	**1.6**

Table 7: Pugh chart for aircraft configurations considered for the drone.

The conventional fuselage configuration was selected. The configuration selection was used design the aircraft's specifications shown below.

3.3. Deployable Wing Design

This section talks about the design of the deployable wing. Many designs were brainstormed and eliminated until 2 best designs. The 2 designs are illustrated below and a design matrix with criterion will be used to select the best design.

3.3.1. Proposed design 1: Folding wings

This design uses the idea of hinges that allow the wings to fold towards the fuselage when storing and deploy when flying. It is made of a rigid wing.

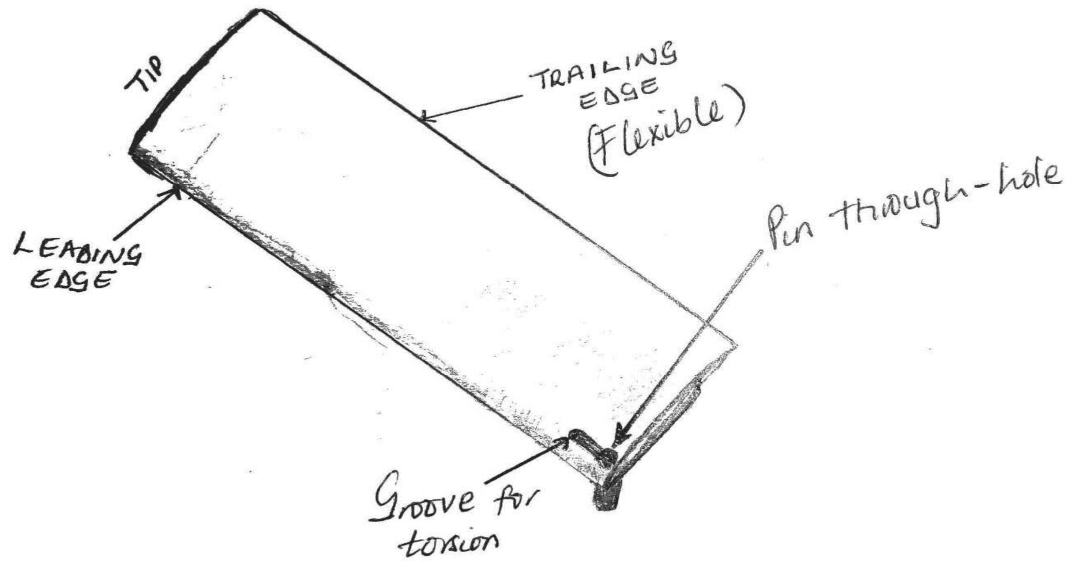

Figure 15: Deign 1 Sketch

The wing has a hole where a torsion tube(pin) is inserted. A rod or a torsion bundle is inserted through the wing pin which is then glued in the groove on top of the wing. The groove is used so as to maintain the smoothness of the wing surface to avoid altering aerodynamic characteristics of the wing. The trailing edge is thin and flexible made by using a material such as carbon fibre fabric.

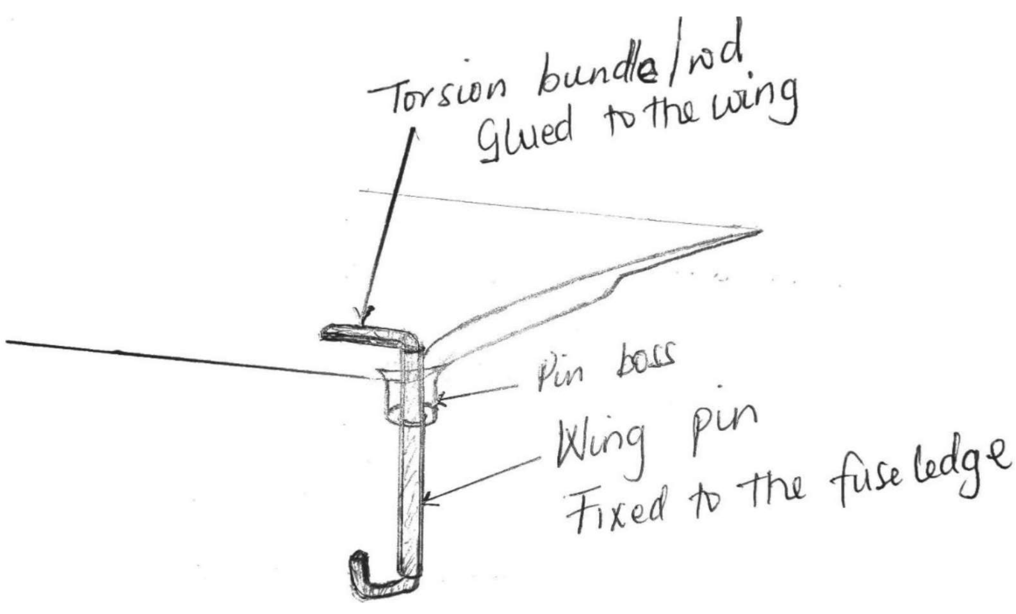

Figure 16: Detailed Sketch for Design 1 Folding Mechanism

The figure above shows the bend rod/torsion bundle glued on the wing's groove. The wing pin (a tube) is fixed and glued to the fuselage. The filleted pin boss helps to transfer the bending stress to the wing pin tube. The rod rotates/torsion bundle twist inside the wing pin and supports the lift force of the aircraft.

3.3.2. Proposed design 2: Collapsible/Flexible wings

The proposed solution uses flexible fabric for the wing material. I consist of front and back support of a rigid rod that allows the wing to maintain its shape. The fabric is wrapped around the support rods are made air tight.

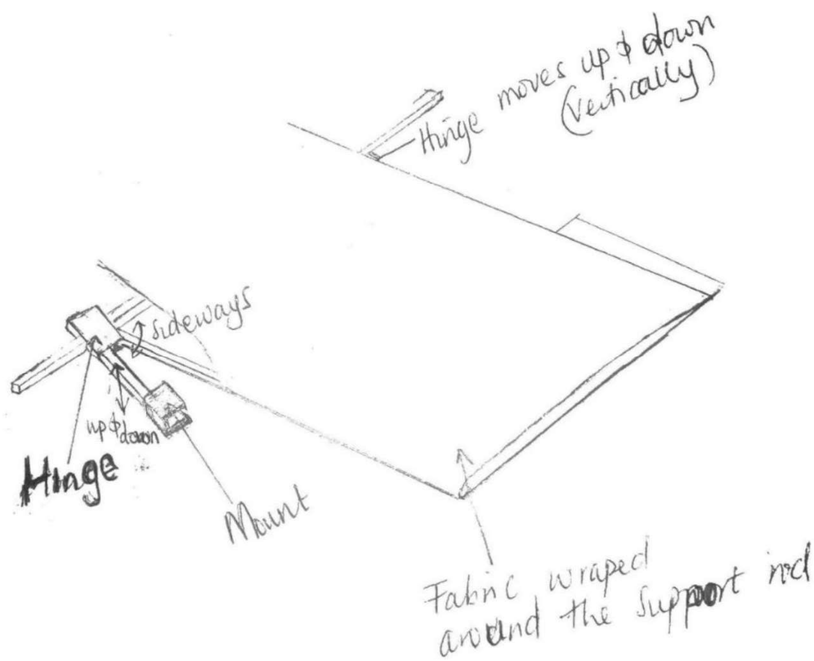

Figure 17: Deign 2 Sketch

Carbon fibre square rods is used as the tail boom and also help to mount the fuselage. At the leading edge there is a support rod with a mount fixed on it. This support is hinged at the tail boom and fixed in such that it allows it to rotate vertically(up-down). The leading-edge rod is also hinged but can rotate horizontally from front to back. The leading-edge rod can be stowed to the aircraft's fuselage when storing. Likewise, when deployed, the rod is mounted to the support rod.

3.3.3. Selection of Wing Design

Factors considered when selecting the deployable wing design are driven by the objectives, and design specification. The criterion considered are weight, manufacturability, cost and foldability. Weight is assigned in accordance to the importance and relevant to project's objectives.

Criteria	Weight	Design 1	Design 2
Weight	0.4	1	2
Manufacturability	0.3	2	1
Cost	0.2	2	2
Foldability	0.1	1	2
Total	**1.0**	**1.5**	**1.7**

Table 8: Pugh chart for the selection of deployable wing design.

The score are tightly close showing that any of these 2 can fulfil the project's objective to some extent. However, Design 2 edged out Design 1 with a narrow score difference of 0.2 and design 2 is selected as a result.

3.3.4. Selected Design and Deployment system

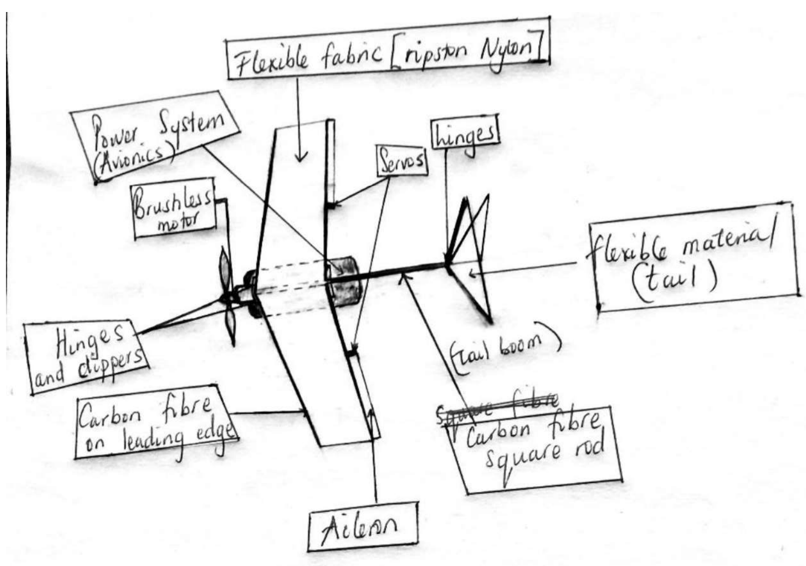

Figure 18: Detailed sketch of the chosen UAV

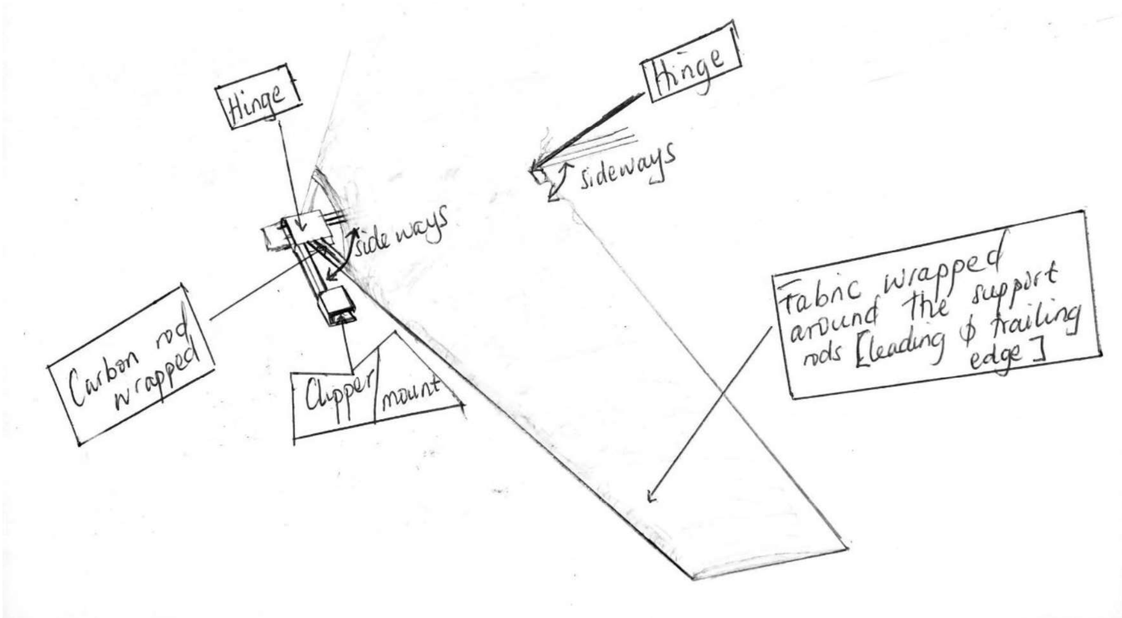

Figure 19: Folding Mechanism for the Selected Design

3.3.5. Folding Mechanism

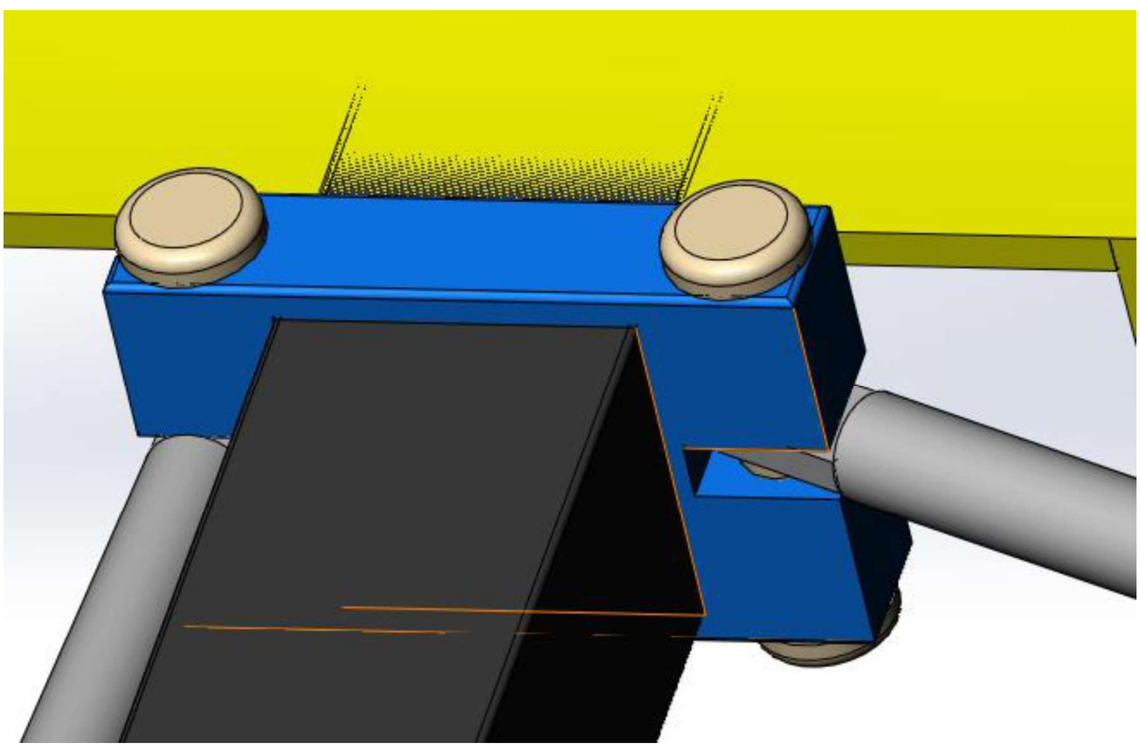

Figure 20: Hinge Visualisation in CAD software

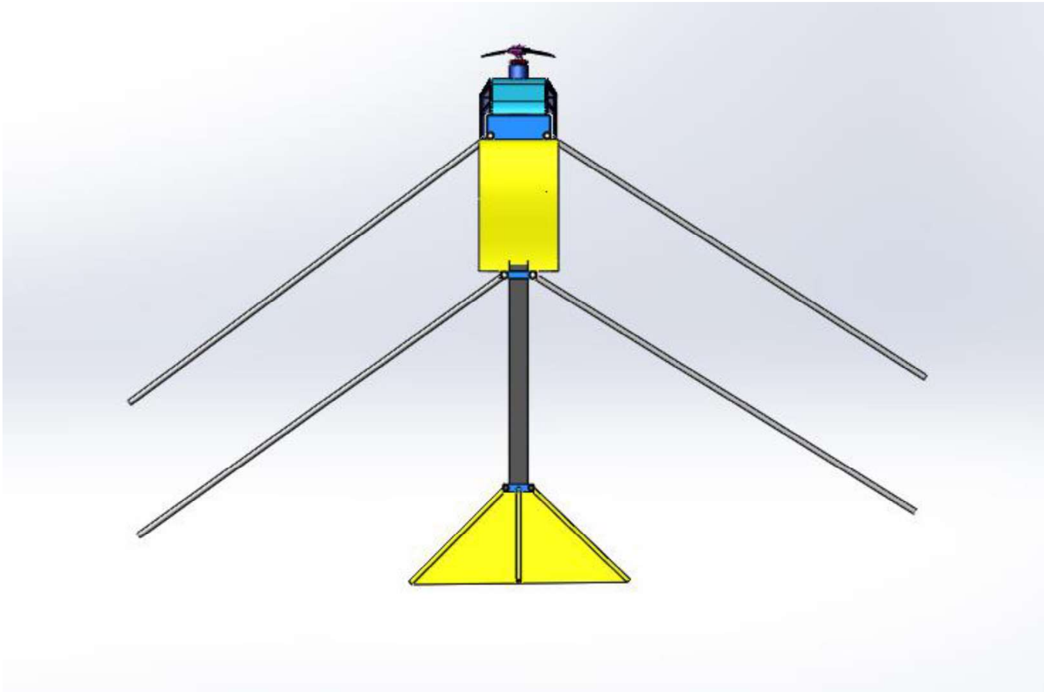

Figure 21: Collapsing wing

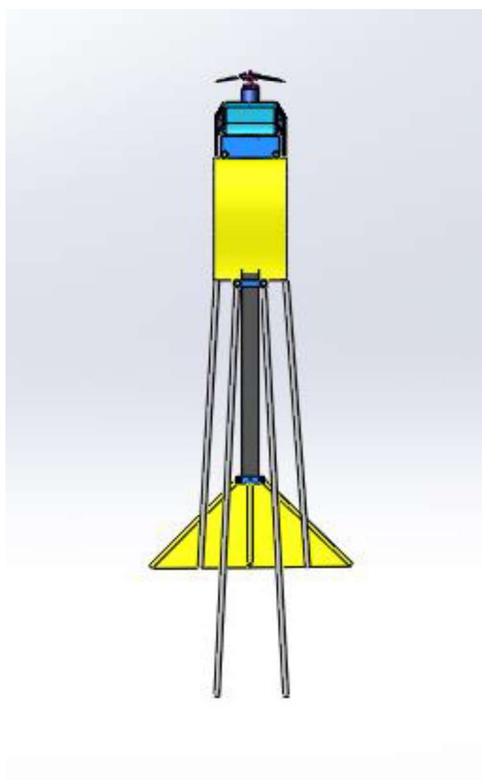

Figure 22: Fully collapsed/Folded wing Skeleton

3.4. Material Selection

Design matrix are also used to select structural material for the wing. The aircraft consist of the skeleton made from rods. The wing and the tail are then covered by a flexible fabric material.

3.4.1 Wing and Tail

From research, the materials usually used to design aerospace structure are Nylon, Kevlar and PVC.

Evaluation Criteria	7 Denier Ripstop Nylon	Kevlar	PVC
Manufacturability	2	1	2
Cost	1	1	3
Light weight	4	3	1
Strength	2	1	2
Durability	1	1	1
Total	**10**	**7**	**9**

Table 9: Decision matrix for material selection of the fabric

From the table above, Ripstop Nylon scored the highest followed by PVC and lastly Kevlar. Since Nylon and PVC have almost the same score, I will use both of them for prototyping and the final material will be selected based on the results of the physical tests on the prototype.

Material Properties	Ripstop Nylon Fabric
Finish/Coating	highwater/wind resistance
breathability	None
abrasion	resistance
Density	0.76g/cm3
Weight	0.000024 g/mm2
Thickness	0.03302 mm

Table 10: Material Properties of Ripstop Nylon [29][30]

3.4.2. Support Rods

Below are the materials used for the aircraft skeletal system or fuselage. These are balsa wood class iv, aluminium 6061, reinforced carbon fibre, glass fibre and PVC(hard).

Material Name	Weight/density	Impact strength	Water resistivity	**Cost**	Total
Balsa wood Class IV	**3**	**1**	**1**	**5**	**10**
Aluminium 6061	**2**	**3**	**3**	**3**	**11**
G Carbon Fibre	**3**	**5**	**3**	**2**	**13**
Glass fibre	**3**	**4**	**3**	**2**	**12**
PVC(hard)	**3**	**2**	**3**	**4**	**12**

Table 11: Material Seletion Decision matrix

Reinforced was selected as it has higher tensile strength and young modulus which is a great requirement for the parts that experience fatigue.

3.5. Wing sizing

3.5.1. Determination wingspan and chord length)

One of the objectives is to design micro-UAV, the mission requirements were considered when sizing the wing. Below are flight conditions as well parameters such as Aspect Ratio earlier defined to be between 7.5 and 8.5. The UAV will be operating at low Reynolds number hence it will have high viscous forces and less inertia forces. Values used to design the wing sizes are:

Using properties table at high altitude, h = 200m

Density, ρ = 1.202 kg/m^3

Dynamic viscosity of fluid $\mu = 1.783 \times 10^{-5}$ kg/m-s

Kinematic=0.0014833611m2/s =$1.48 \times 10^{-3} m2/s$

Average cruising velocity, V = 45km/hr = 15 m/s

Aspect Ratio was defined at , $AR = 8$

Reynold's number was defined at , Re = 61235.26

Calculating chord length, c using Re

Using the formular, $Re = \frac{\rho Vc}{\mu}$

Making the chord length the subject, $c = \frac{Re \times \mu}{\rho V} = \frac{61235.26 \times 1.783 \times 10^{-5}}{1.202 \times 15} = 0.0606\ m = 60.6mm$

Calculating the wingspan, b using AR

Since $AR = 8 = \frac{wingspan\ length(b)^2}{Wing\ area(S)} = \frac{b^2}{bc} = \frac{b}{c} = \frac{b}{60mm}$

Therefore $b = 60 \times 8 = 480mm$

Thus the refined maximum wing area $S = 480mm \times 60mm = 28800mm^2 = 0.0288m^2$

3.5.2. Fatigue (Determination of the hinge diameter)

For alternating stresses with X_{min} and X_{max}, where X is any type of loading

Alternating Loading, $X_a = \frac{1}{2}(X_{max} - X_{min})$

Mean Loading, $X_m = \frac{1}{2}(X_{max} + X_{min})$

Design Equation chosen: Modified Goodman.

Failure by fatigue $= \frac{1}{n} = \frac{\tau_m}{S_{us}} + \frac{\tau_a}{S_f}$

Failure by Yield $= \frac{1}{n} = \frac{\tau_m}{S_{ys}} + \frac{\tau_a}{S_{ys}}$

Refer to the **Appendix A.1** for detail calculations.

Load Analysis	$T \sim (-9.23, 9.23) Nmm$ $T_m = 0$ $T_a = 9.23\ Nmm$	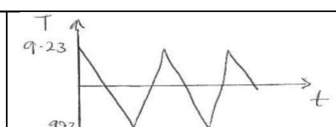
Stress Analysis	CP: At the walls	$\tau_m = \frac{16T_m}{\pi d^3} = 0$ $\tau_a = \frac{16T_a}{\pi d^3} = \frac{47.01}{d^3}\ MPa$
Material Properties	Material Type: Carbon fibre low grade	$S_{ut} = 7MPa;\ S_{yt} = 6.62MPa$ $S_{us} = 0.8S_{ut} = 5.6MPa$ $S_{ys} = 0.5777S_{yt} = 3.82MPa$ $S_f = 3.5\ MPa$
Design Equation and Solution	DE: *Modified Goodman*	Operating Point, $P\left(0, \frac{47.01}{d^3}\right)$ Safety factor = 2

Failure by Fatigue	$\frac{1}{n}=\frac{\tau_m}{S_{us}}+\frac{\tau_a}{S_f}=\frac{1}{2}=\frac{47.01}{3.5d^3}$	$d^3=\frac{47.01\times 2}{3.5}$ therefore d = 4.99mm
Failure by Yield	$\frac{1}{n}=\frac{\tau_m}{S_{ys}}+\frac{\tau_a}{S_{ys}}=\frac{1}{2}=\frac{47.01}{3.82d^3}$	$d^3=\frac{47.01\times 2}{3.5}$ therefore d = 4.91mm
Conclusion	Failure by Fatigue	N(actual) = 2.01

Table 12: Summary for the hinge diameter estimation

3.6. Aircraft Structure Weight Estimation

After material selection and determining the sizes of the aircraft components, the mass of each component is calculated using the traditional formula:

$Mass = density(\rho) \times volume(V)$

The density is of each component is known since the material has been selected.

3.6.1. Summary of weight Calculations

See Appendix A.2 for detail calculation.

Part		Area/Volume mm^2 *or* mm^3	Density g/mm^3 or g/mm^2	Weight *grams*	Total weight *(grams)*
Wing	Ripstop Nylon	$69663.72mm^2$	$0.000024g/mm^2$	1.672	**17.1**
	Rod	$6785.84mm^3$	$0.002267\ g/mm^3$	15.38	
Tail	Ripstop Nylon	$9210mm^2$	$0.000024g/mm^2$	0.221	**2.1**
	Rod	$823.1mm^3$	$0.002267\ g/mm^3$	1.865	
Main support (empennage)		$20000mm^3$	$0.002267\ g/mm^3$	45.3	**45.3**
Hinges		$2426.1mm^3$	$0.002267\ g/mm^3$	5.5	**5.5**
Total					**70**

Table 13: Summary of Aircraft weight Estimations

3.7. Electric Propulsion Design Considerations

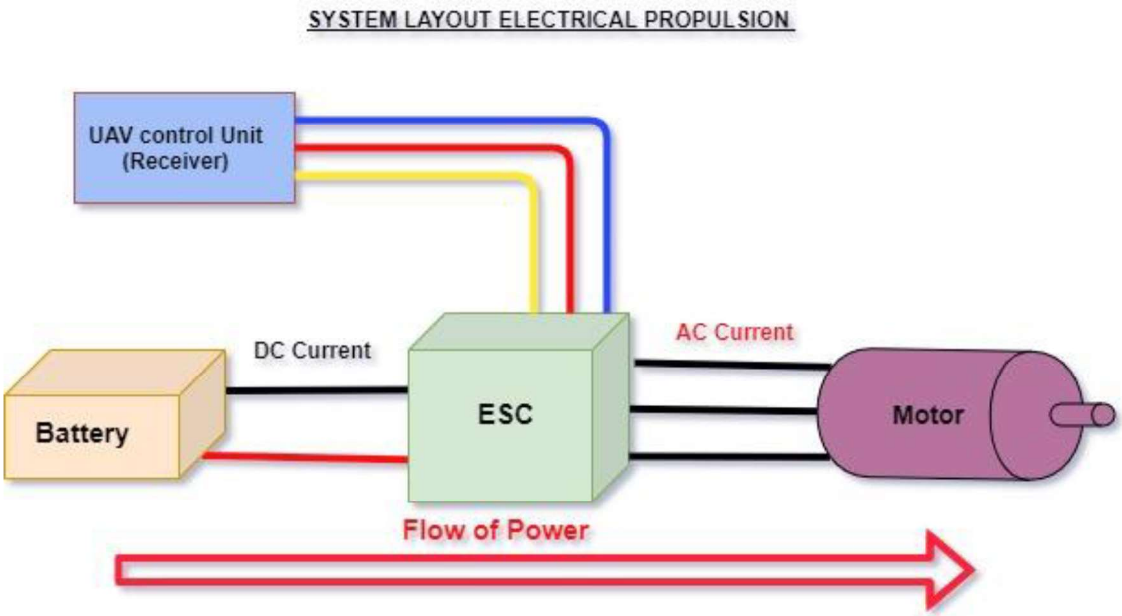

Figure 23: Block Diagram Layout for the Electric components

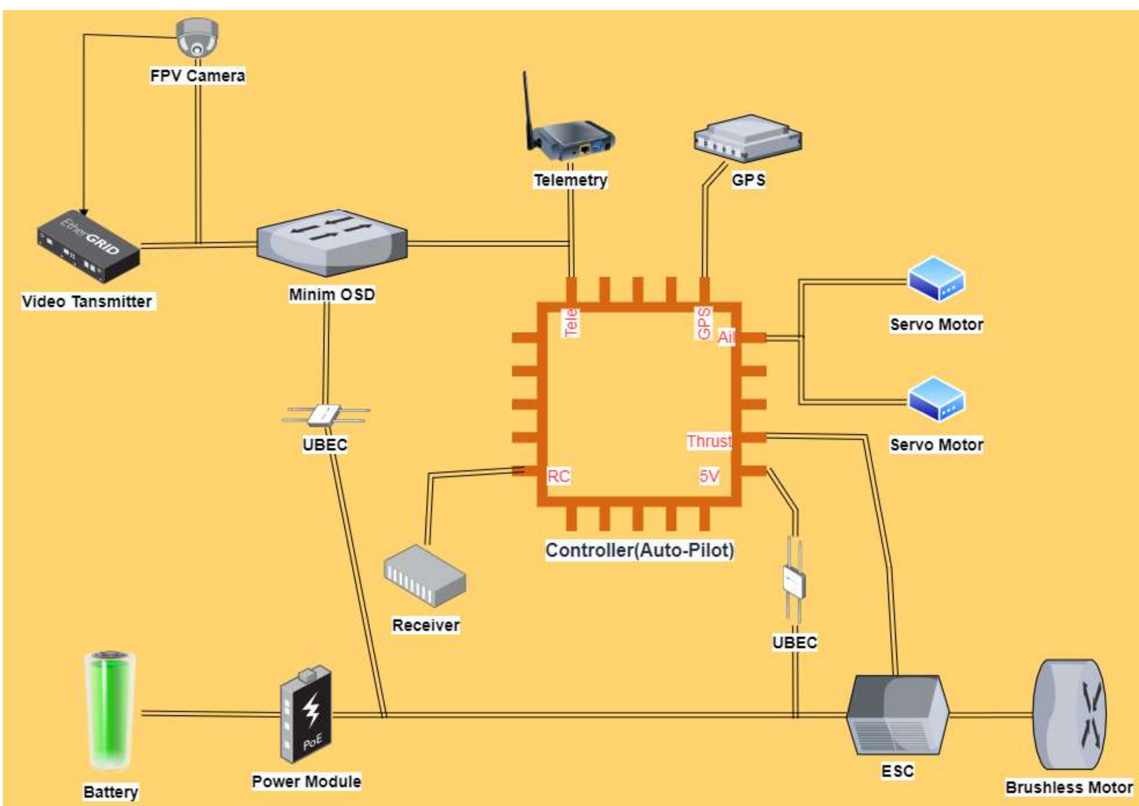

Figure 24: Detailed Layout of Electric components

One of the main design considerations of an aircraft is its propulsion system. It consists of three main components which are the battery, the electronic speed controller (ESC) and the electric motor. The brushless ESC will be used as it is lighter in weight and it supplies higher power performance as compared to the brushed ESC. Consequently, the brushless electrical motor will be used for this project's propulsion system. The purpose of battery is to provide DC power to the electronic speed controller. The ESC controls and regulate the speed and direction of the electrical motor by reading the signal provided by control unit(receiver). The three components need to be scaled so as to reduce the overall wight while increase its efficiency.

3.7.1. Power System

A lithium-polymer cell was selected because it has high specific energy density, a property that is high important to electric flying vehicles [31]. However, it is imperative to note that the use of solid battery, unlike liquid that reduce its weight when providing power; the weight of the battery does not change when the energy is being used. This means that an aircraft carries a constant weight of the battery during the course of the mission which in turn affect the aircraft's endurance. Hence careful propulsion design was performed in the preceding sections.

Lipo batteries can bought as a battery pack with cell configurations already fixed. Battery cells can also be bought separately, and the configuration is determined by the designer basing on the performance that best suit the UAV design. In this project, where the sizes, weight are to be minimised to maximise endurance, separate battery cells will be explored and the maximum number of battery cells will be considered based on the derived equation below. Lipo cell selected for this project is a SPB463048. This Rechargeable Li-ion Polymer Battery has a nominal voltage of 3.7V, a nominal capacity of 700 mAh. It also has volumetric and mass energy densities of 391Wh/l and 192Wh/kg respectively. LiPo battery cell with dimensions 5.5×24×65.5 mm is around 16g.

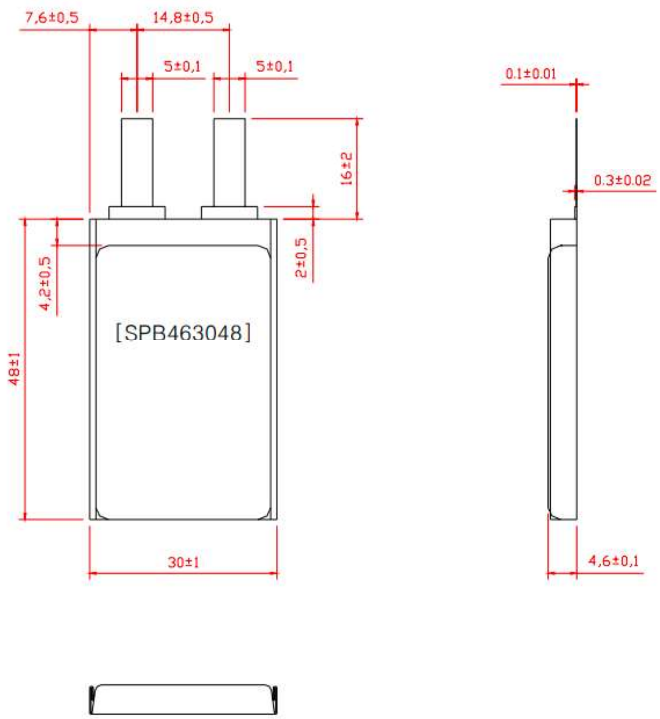

Figure 25: Out View drawing for SPB463048 [34]

3.8. Endurance-Maximisation Relations

Under this section, the relationship between the aircraft's endurance with its geometric and aerodynamic parameters were established. The newton's laws of motion in conjunction with energy equations were used to derive the equations. Several assumptions were made to arrive at the desired parameters.

3.8.1. Mathematical Model Formulation For Endurance

The governing equation of a level flight were used to derive the equation for endurance.

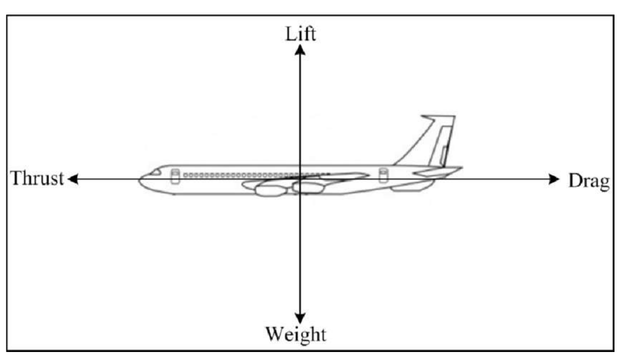

Figure 26: Free body diagram for a level flight[35]

For a level flight

Weight(W) = Lift(L)

Thrust(T) = Drag(D)

$$W = L = \frac{1}{2}\rho V^2 S C_L \qquad \text{Equation 1}$$

$$T = D = \frac{1}{2}\rho V^2 S C_D \qquad \text{Equation 2}$$

$$q = \frac{1}{2}\rho V^2 \qquad \text{Equation 3}$$

For an aircraft with a wing area, S, the total lift, L becomes;

$$W = L = qSC_L \qquad \text{Equation 4}$$

$$T = D = qSC_D \qquad \text{Equation 5}$$

When the equation 1 is substituted into the equation 2 and making the coefficient of lift C_L, the subject, the equation becomes,

$$C_L = \frac{2W}{\rho V^2 S} \qquad \text{Equation 6}$$

The aspect ratio of the aircraft, AR which is the ratio of the square of cord length, b to the total wing area, S.

$$AR = \frac{b^2}{S} \qquad \text{Equation 7}$$

The drag coefficient for the aircraft is the total of the parasite drag C_{do} and the induced drag

$$C_D = C_{do} + \frac{C_l^2}{\pi e AR} \qquad \text{Equation 8}$$

Substituting equation 8 into the equation 5 result in the following expression.

$$D = q\left[(SC_{do} + \frac{SC_l^2}{\pi e AR}\right] \quad = qSC_{do} + \frac{W^2}{q\pi e b^2} \qquad \text{Equation 9}$$

For an aircraft flying on a level with a steady velocity, V, the power required to propel it is the product of the velocity and the drag force as shown in the equation below.

$$Power\ of\ flight, P_{flight} = Drag\ force\ \times Velocity \qquad Equation\ 10$$

$$P_{flight} = DV = \left[qSC_{do} + \frac{W^2}{q\pi eb^2}\right] \times V \qquad Equation\ 11$$

However, the propulsive power can be calculated directly using the power system of the battery. Thus, the battery power P_{bat} is related to the propulsive power P_{prop} as shown on equation 12

$$P_{prop} = \eta_{motor}\eta_{ESC}\eta_{Pro}P_{bat} \qquad Equation\ 12$$

The power required for flight P_{flight} should be equal to the power supplied by the battery.

$$P_{flight} = P_{prop} \qquad Equation\ 13$$

$$P_{bat} = \frac{1}{\eta_{motor}\eta_{ESC}\eta_{Pro}}\left[qSC_{do} + \frac{W^2}{q\pi eb^2}\right] \times V \qquad Equation\ 14$$

The power provided by the battery is calculated using the above relationship. On the other hand, the energy, E provided by the battery is calculated using the battery's specific energy, $\bar{E}$, which is the defined as the energy per unit weight of the battery. The average specific energy of a lithium-polymer battery is 59390 J/N[17]. Thus,

$$\bar{E} = \frac{E_{bat}}{W_{bat}} \qquad Equation\ 15$$

Making the E the subject gives equation 16

$$E_{bat} = W_{bat}\bar{E} \qquad Equation\ 16$$

Power is the rate if change of energy, thus since the expressions for energy and power of the battery are derived, the expression for the endurance time, t_{endu} is deduced as shown in the equation 17

$$t_{endu} = \frac{E_{bat}}{P_{bat}} = \frac{W_{bat}\bar{E}}{\frac{1}{\eta_{motor}\eta_{ESC}\eta_{Pro}}\left[qSC_{do}+\frac{W^2}{q\pi eb^2}\right]V} = \frac{\eta_{motor}\eta_{ESC}\eta_{Pro}}{\left[qSC_{do}+\frac{W^2}{q\pi eb^2}\right]V}W_{bat}\bar{E} \qquad \textit{Equation 17}$$

Taking the reciprocate of equation 17 gives equation 18

$$\frac{1}{t_{endu}} = \frac{V}{(\eta_{motor}\eta_{ESC}\eta_{Pro})\bar{E}}\left[\frac{qSC_{do}}{W_{bat}} + \frac{W^2}{q\pi eb^2 W_{bat}}\right] \qquad \textit{Equation 18}$$

As shown previously, the total weight of the aircraft is;

$$W = W_{ESCmotorprop} + W_{bat} + W_{airframe} + W_{sensors} \qquad \textit{Equation 19}$$

To understand between the effects of the battery weight and weight of the sensors on the UAV's endurance, each weight component is broken down into weight fractions by dividing by the total weight as shown in equation 19

$$\frac{W}{W} = 1 = \frac{W_{ESCmotorprop}}{W} + \frac{W_{bat}}{W} + \frac{W_{airframe}}{W} + \frac{W_{sensors}}{W} \qquad \textit{Equation 20}$$

Introducing a non dimensionless term, f which is the ratio of the component's weight to the total weight of the UAV.

$$1 = f_{ESCmotorprop} + f_{bat} + f_{airframe} + f_{sensors} \qquad \textit{Equation 21}$$

When the terms for sensors and battery from Eq 20 and Eq 21 are substituted in the equation 18 the result is shown in equation 22

$$\frac{1}{t_{endu}} = \frac{V}{(\eta_{motor}\eta_{ESC}\eta_{Pro})\bar{E}}\left[\frac{1}{\frac{C_L}{C_{do}}f_{bat}} + \frac{W_{sensors}}{q\pi eb^2 f_{bat}f_{sensors}}\right] \qquad \textit{Equation 22}$$

The equation 22 show the various UAV parameters that influence the aircraft performance. Analysing the equation 22 from left to right, the expression shows that for an aircraft to have high endurance, it should fly at low velocities as required by the mission requirement stated previously. It should also use highly efficient propulsion components as well as a battery that has high specific energy. The first term of the expression in the square bracket show that the endurance can be maximised by maximising the aerodynamic efficiency $\frac{C_L}{C_{do}}$. The last term (induced drag) is affected by the square of the span as well as weight of the sensors. The relationship shows that to maximise endurance, the span loading, $\frac{W_{sensors}}{b^2}$ should be minimised. It is also shown that the endurance of the aircraft is independent of the battery capacity. Battery sizing analysis was performed to increase the flight endurance of the aircraft. From above data and the derived equation $Eq\ 3.20$ a graph of light endurance was plotted against the weight of the battery cells. The count of battery cells are quantised hence each node represent a possible solution to the number of required cells.

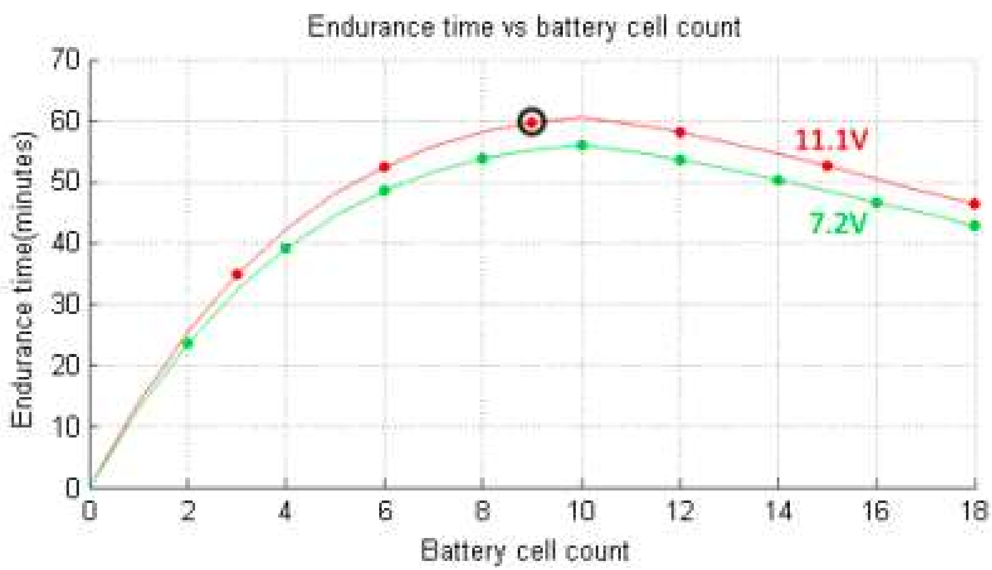

Figure 27: Endurance vs Battery cell count [17]

The 11. 1V and 7.2V voltages are important because these are the possible voltages the battery pack can have. Nominally, 3 lithium-polymer cells in series generates 11.1V and 2 cells in series generates 7.4V. Because the cell count is quantized, and battery packs are made with parallel groups of cells in series, only cell counts divisible by 2 or 3 can be achieved. A plot of system endurance vs. battery cell count is shown below in Figure 35. The solid nodes on the plot are the achievable configurations.

3.8.2. Motor Efficiency Consideration

A brushless motor is used in this project. This is because it has numerous advantages such as easy to control, reduced noise, high efficiency, reliable and it last long (it has no brush abrasion).

In selecting a motor, the recommended Kv rating was calculated from the relationship.

$$RPM = Kv \times volt \qquad 3.3.2$$

Where Kv is the constant velocity of the motor [26]. Thus 1 Kv mean 1 revolution per minute. A higher KV rating means a higher top speed but less torque, while a lower KV rating means powerful torque but a lower top speed. For surveillance micro-UAVs, the average RPM is estimated to be around 9000-14500 RPM thus.

$$Kv = \frac{RPM}{volt} = \frac{14500}{11.1} = 1306Kv$$

Several motors were analysed from the table below.

Motor	Weight	Kv	Max Amps	Diameter	Length	Shaft Dia
ELE - C20 KV2100	19g	1800	8	22.2mm	22mm	3mm
Suppo - A2204-14	19g	1570	7.5	27.6mm	18.8mm	3mm
Westport - 22.7mm, 20T/25ga	22g	1325	6	26.6mm	11.5mm	3mm
Westport - 22.7mm, 17T/25ga	22g	1605	6	26.6mm	11.5mm	3mm
Westport - 22.7mm, 15T/25ga	22g	1790	8	26.6mm	11.5mm	3mm
Westport - 22.7mm 20T/26ga	22g	1270	6			
Motrolfly - 2203-1350 v2	18g	1315	5	28mm	13.7mm	3mm
Motrolfly - 2203-1600 v2	18g	1645	7	28mm	13.7mm	3mm
E-power - GC GT2203-1560	20g	1805	6	27.6mm	19.5mm	3mm
SunnySky - X2204-21	22g	1875	7	27mm	18.9mm	3mm

Table 14: Motor Comparizons for Selection

The motor "Westport - 22.7mm, 20T/25ga" was selected as it has high efficient of 80% when 2 series and 75% when 2 series as shown on the graph below

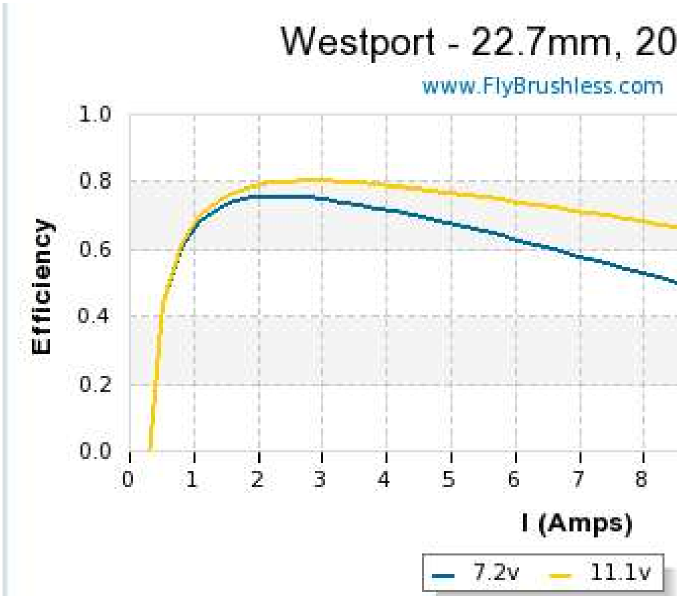

Figure 28: Efficiency characteristics of Westport 22.7mm,20T/25ga motor [23]

Specifications: Westport - 22.7mm, 20T/25ga

- Type: Outrunner
- Weight: 22.00g (0.78oz)
- Diameter: 26.60mm (1.05in)
- Length: 11.50mm (0.45in)
- Shaft Diameter: 3.00mm (0.12in)
- Maximum Amps: 6
- Kv: 1325

3.9. Summary Power System Sizing

Power System

- Cell voltage = 3.7 V
- Cell capacity = 700-mAh
- Cell dimensions = 5.5mm × 24mm × 65.5mm.
- Energy density of the battery E = 52,800 J/N, as measured by a cold-temperature −20°C discharge test [22].

- Motor efficiency = 80% for a 3-series and 75% for a 2-series battery configuration[23].
- Efficiency of the electronic speed controller = 89%[24]
- Propeller efficiency = 70% [25].

Masses

1. The weight of the onboard sensor system is assumed to be 22g
2. Weight of airframe as calculated above to be 70g
3. Weight of power system (electronic speed controller, propeller and brushless motor) is assumed to be 30g
4. Weight of each battery cell is assumed to be 16g (16×9= 126g)

Total weight = 126+30+70+22 = 248g

Thus $weight\ of\ an\ aircraft\ = 248g\ =\ 2.43288N$

Parameter		Specification
wingspan		480 mm = 0.48 m
Length		180 mm
Empty Weight		248g
Mean Aerodynamic Chord MAC		50mm and 70 mm 60.556mm
Configuration	Wing	High wing
	Tail	Conventional
	Fuselage	Conventional
Propulsion type		Electric motor(1950 KV)
Controls		Autonomous/ remoter controller/manual

Table 15: Summary of Component selection and sizing

Chapter 4: Aerodynamic Design and Analysis

This chapter start with analysis of aerofoils in the XFLR5 with the best performer selected for the UAV design. This is followed by stability calculations and analysis to ensure the aircraft remain stable when it changes yaw, roll or pitching moment. Lastly aerodynamic performance will be predicted analytically before using the software to simulate aerodynamic values for the aircraft.

4.1. XFLR5 Overview

An XFLR5 "is a software is an analysis tool for aerofoils, wings and planes operating at low Reynolds Numbers. It includes: XFoil's Direct and Inverse analysis capabilities and Wing design and analysis capabilities based on the Lifting Line Theory, on the Vortex Lattice Method, and on a 3D Panel Method" [28].

There are several steps taken when analysing using XFLR5.

1. **Direct Foil design**

Aerofoils can be designed using the B-Splines or Splined Point found in an internal crude module. For a B-Splines, Upper and lower surfaces of the aerofoil are smooth and are determined by a single and separate B-Spline; whereas for Spline Points emphasise on greater control over the geometry.

However the design of aerofoil is not the best option as there are other alternatives such as importing designed aerofoils or aerofoil data from the Aerospace database.

2. **XFoil Direct Analysis**

It is performed to analyse the aerodynamic performance of the 2D aerofoils. Values need to converge when the Xfoil direct analysis is ran. The Operating Points are created are stored in the current polar object. The Reynold's number, the March number as well as the range of angle of attack are defined. After launching the analysis, if the XFoil has converged the coefficient of pressure will automatically appear and different graphs of Cl, CD can be analysed.

3. **Wing and plane design**

Firstly, the 3D wing is defined as a set of panels. Parameter that defines the wing are inputted such as wingspan, root and tip chords as well as the angles for dihedral shapes. An analysis can be carried on the wing only using the Lifting Line Theory (LLT). This analysis takes parameters such flying altitude, velocity, air density as well as the Reynold's number. It as some limitations for 3D bodies or dihedral wings and tail hence an alternative analysis call VLM is used. This also used for the analysis of the full designed aircraft(3D Model)

4.2. Aerofoil Selection

For surveillance where the flaps will always on their original position, the aerofoil selected should have low drag at zero angle of attack.

Aerofoil selection was based on the known aerodynamic characteristics. The goal is to select the most optimum aerofoil from the predetermined collection of aerofoils. The online Aerofoil Tool is used to compare these predetermined aerofoils. The Reynold's number, Re, as well as the aerofoil type was needed to generate the aerodynamic characteristic of these aerofoils.

From research, the most dominance aerofoils designed to operate at low Reynold's number and low speed are: Eppler 193, S5010, Mh 45 and Mh 60

The data coordinates of the above aerofoils were downloaded from the Illinois University department of Aerospace database [27]. The coordinates system of the aerofoil was downloaded as .dat files. Using an XFLR5 software, the data was imported into the software for analysis.

The fig below show plotted aerofoils and each legend show respective aerofoil as well as the important information about each aerofoil such as the aerofoil thickness and camber.

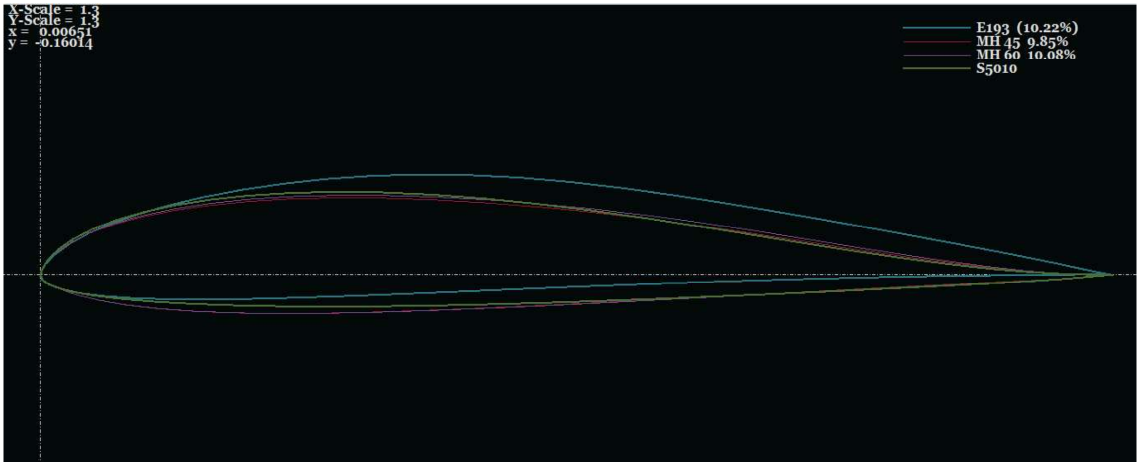

Figure 29: 2D Aerofoil Plots

Using XFLR5, an aerofoil analysis was performed to understand the aerodynamic characteristics of each aerofoil and help choose the best at low Reynold's number. Since the designed aircraft will be flying at calculated Reynold's number of 61300, the values were inputted into the software to get the best aerofoil operating in these conditions.

Below are the plots for the aerodynamic characteristics of the aerofoils at Re = 61300.

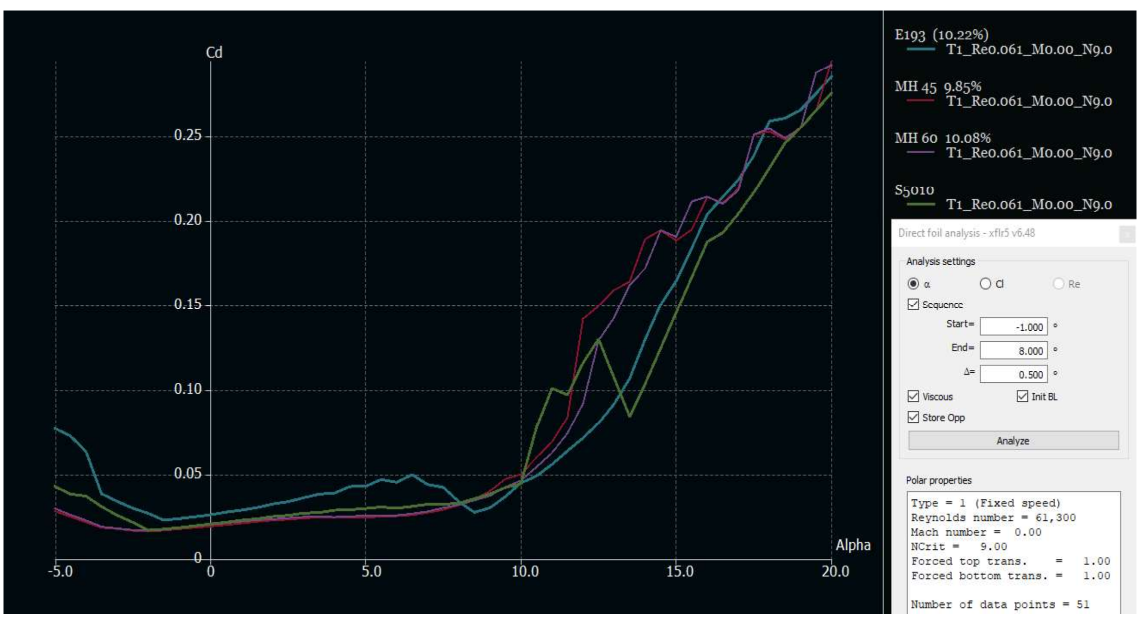

Figure 30: Cd against alpha

The designed aircraft is made for surveillance purposes hence it will be mostly flying at zero or very low angle of attack. Hence there is need of an aerofoil with low drag force at zero angle of attack. From fig 1, MH 45,MH 60 and s5010 have approximately same and lowest drag coefficient at zero angle of attack.

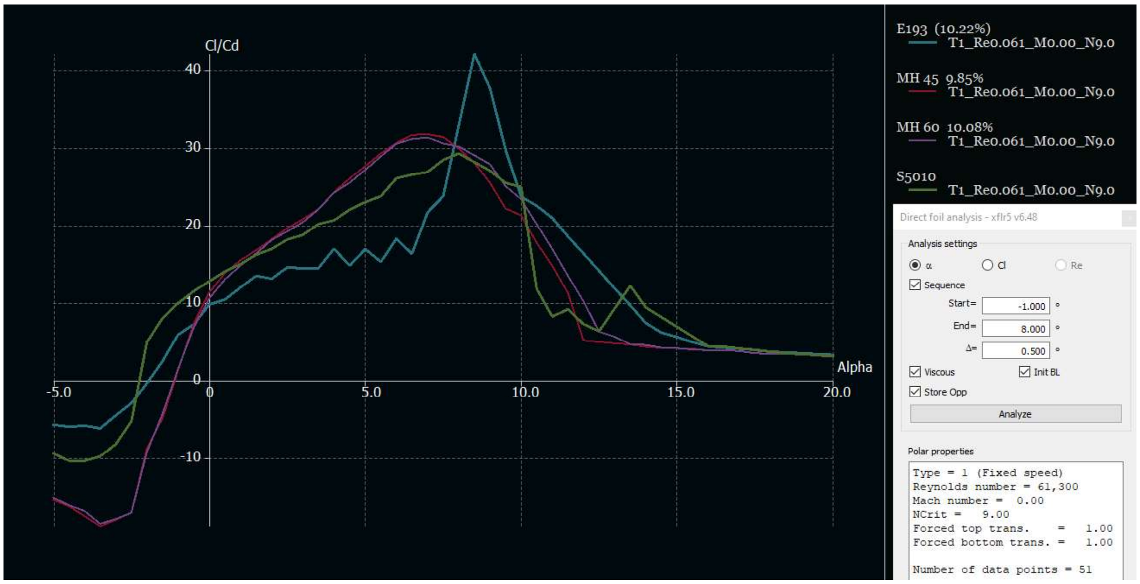

Figure 31 Plot of ratio of (Cl/Cd) against alpha

An aerofoil with high Cl/Cd at zero angle is attack is desirable as it will be easy for the aircraft to gain lift without need of high power or thrust.

Fig 2 graph show that the aerofoil s 5010 has higher Cl/Cd ratio at zero angle of attack. It is also worth to note that Eppler 193 has the highest ratio at large angle of attack with stall angle of approximately 8 degrees. However, Eppler is not the most suitable for the purpose of this project as UAV will be flying at very low angle of attack.

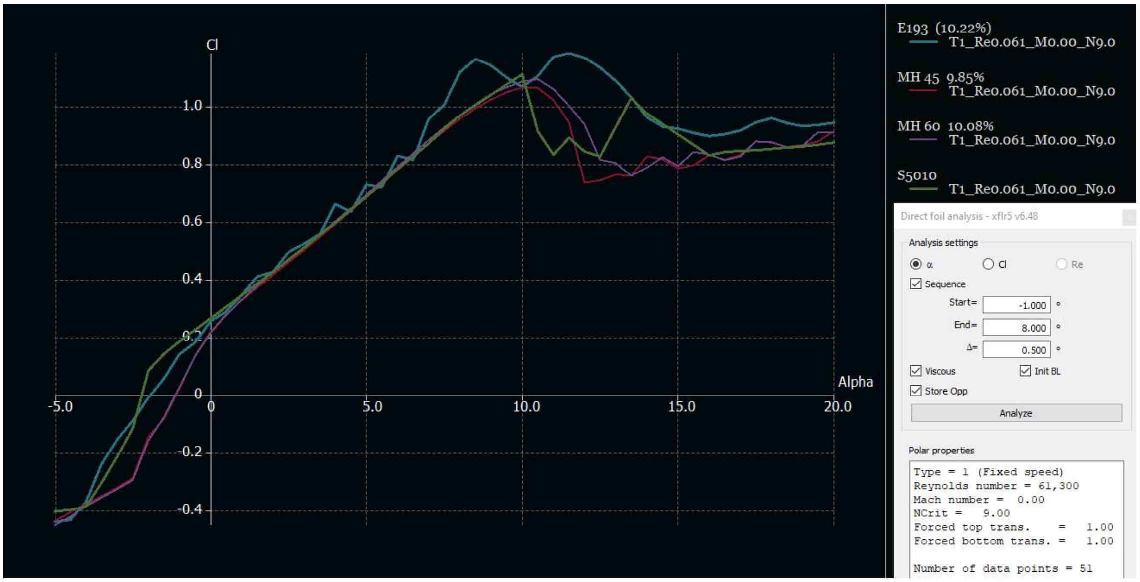

Figure 32: Plot of Cl against alpha

Fig 3 show that aerofoils s5010 and E193 have higher Cl at zero angle of attack with the s5010 having slightly higher value. Hence an aerofoil with high Cl at zero angle of attack is desired to help aid lift.

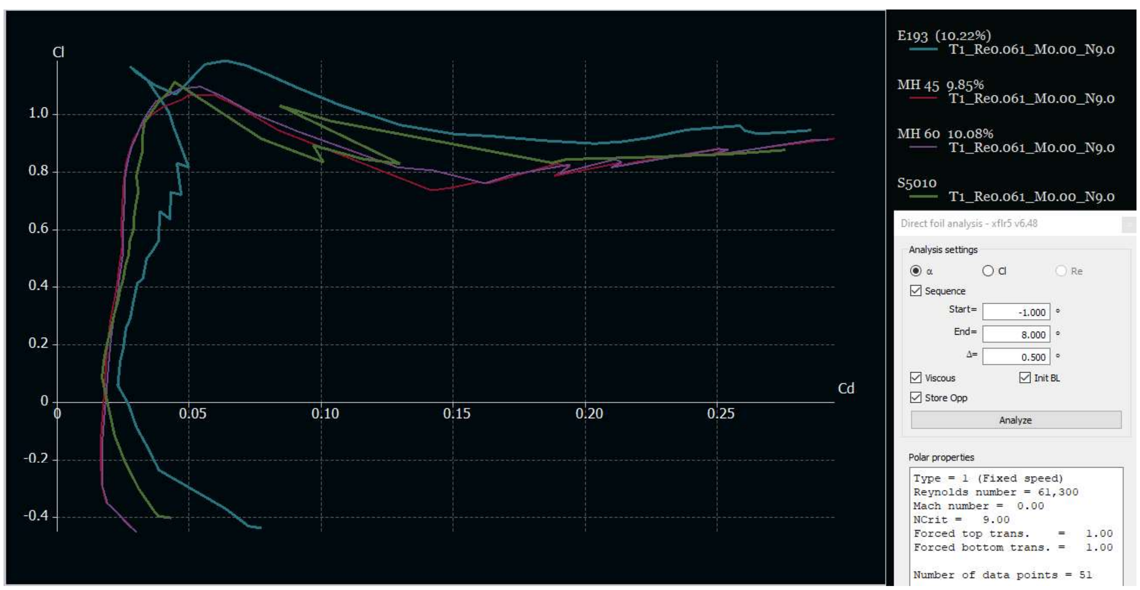

Figure 33 The plot of Cl) against Cd

The aerodynamic characteristics of the aerofoils are summarised on table below

Aerofoil	@ Cl =0	MH 45	S 5010	MH60	Eppler 193
Cl vs Cd	**Cd**	0.018	0.019	0.019	0.026
Cl vs alpha	**Cl**	0.21	0.26	0.21	0.25

Cl/Cd vs alpha	Cl/Cd	11	13	10.8	10
Cd v Alpha	Cd	0.019	0.022	0.018	0.024

Table 16: Matrix selection of aerofoil

The data analysed above show that S5010 has the best overall performance and was therefore chosen for the design of the wing.

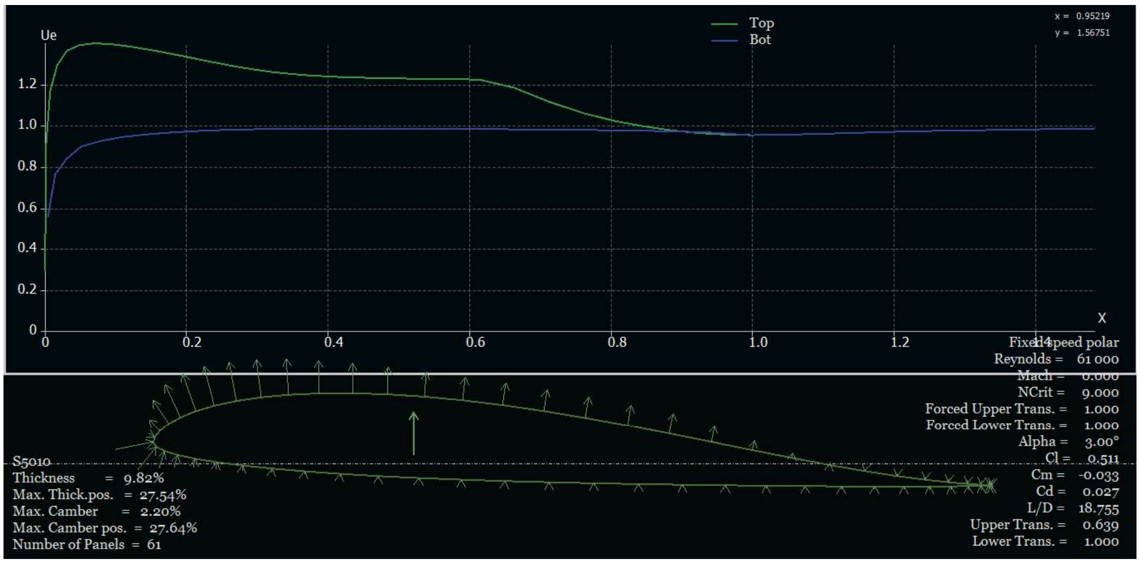

Figure 34: 2D plot of the S5010 aerofoil

4.2. Stability Analysis

Stability of an aircraft is determined by the centre of gravity. Centre of gravity of the point where the total weight of the aircraft is considered to act. For an aircraft, it is a point where if an aircraft is suspended at that point it can balance. For a flying aircraft, the centre of gravity should be further forward of the centre of pressure to maintain stability. Centre of pressure is the point where the resultant total lift act and it changes when the angle of attack changes. From research the centre of gravity should be within 15% to 35% of the MAC i.e 25%< (X_cg-X_leading edge)/100 <35%.

4.2.1. Estimating the position Avionics Components/container

Moments of force were used. XFLR5 software were used to assign the above calculated to their respective parts. The centre of gravity of the total weight was assumed to be the quarter chord that is (1/4 × 60mm =15mm) from the leading edge. All the coordinates in the software are measured from the origin where the leading edge aligns. At the leading edge, a datum line of reference was used to determine the centre of gravity. The centre of gravity of the skeletal aircraft is 79.397mm from datum. The point to position the centre of gravity of the avionics system was calculated using moment of forces.

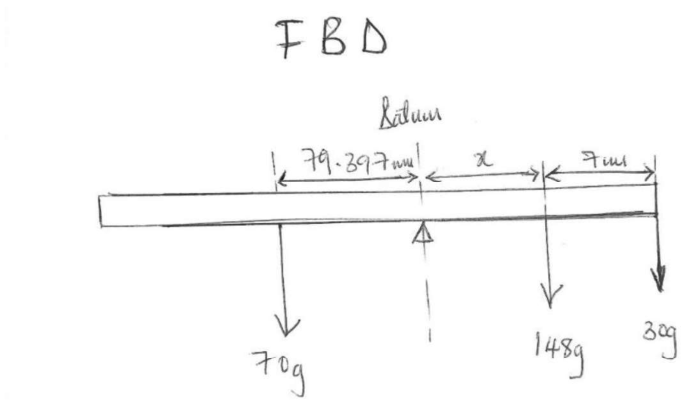

Figure 35: UAV Free Body Diagram

Component	Mass/g	CG(X from the pivot/mm	Moments/g-mm
Skeletal aircraft	70	79.397	5557.79
Electronic components	148	x	148x
Electric motor	30	x+7	(x+7)30
Whole aircraft	248	15mm	3720mm

Table 17: Centre of Gravity Determination

Calculating for x:
$148x + (x+7)30 = 5557.79 - 3720$
$x = 9.144mm$
Thus, the centre of gravity avionics components will be placed 9.14mm forward of the leading edge. As result the position of the avionics box had to be shifted forward as shown below.

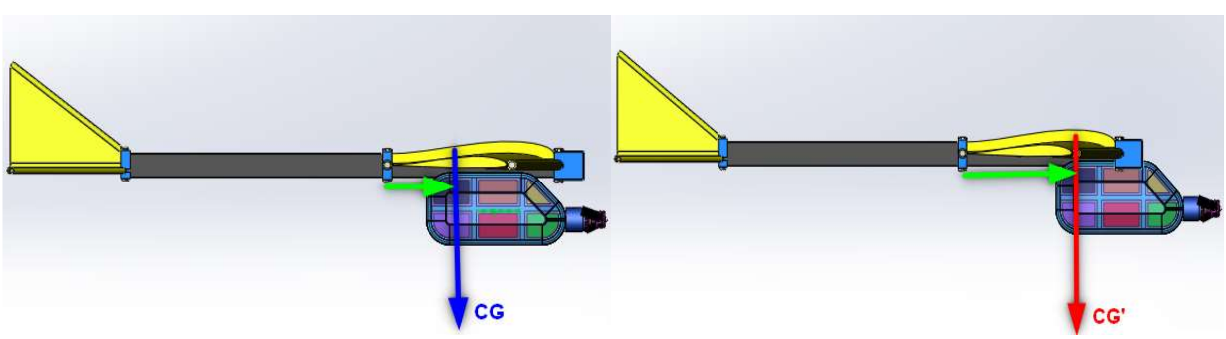

Figure 36 (a) CG before stability analysis (b) CG' at ¼ chord after shifting avionics box

4.2.2 Checking for Stability Using XFLR5

After determining the CG position for the avionics components, each weight and its respective centre of gravity position was inputted in the XFLR5 software for to check if indeed the aircraft is stable.

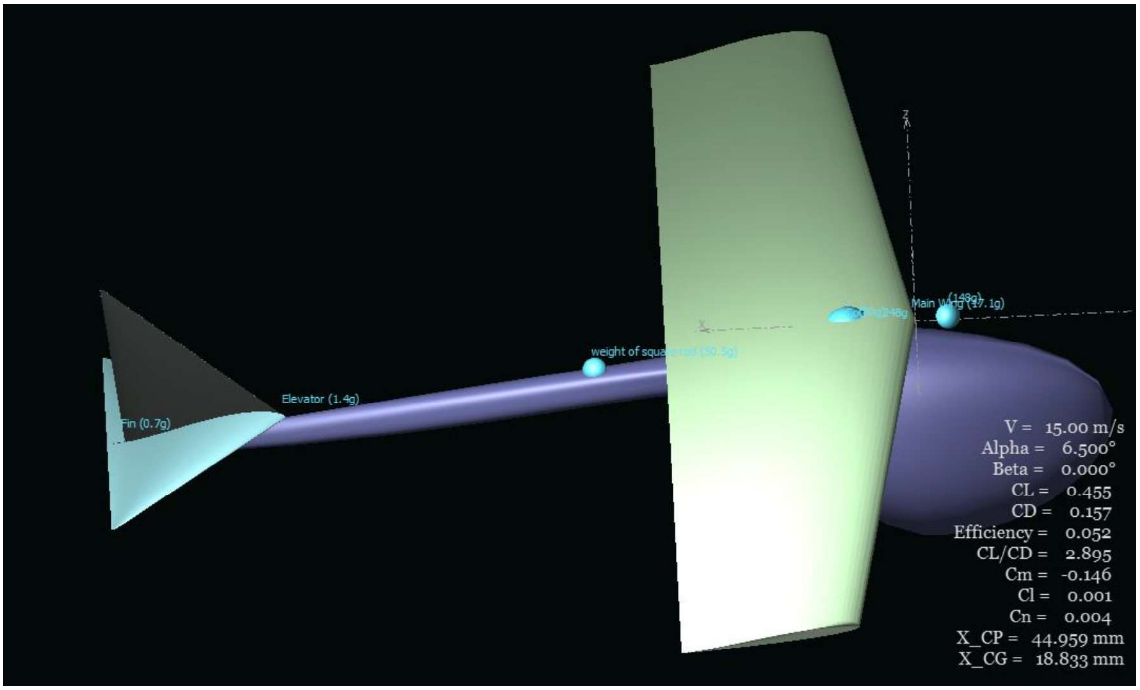

Figure 37: 3D UAV Model in XFLR5

X_CG=18.833mm; MAC=60.556

%of MAC = $\frac{18.833}{60.55} \times 100 = 31.1\%$. the %MAC is within the range of 25% -35% hence the aircraft is stable.

4.3 Analytical Prediction of Aircraft's Aerodynamic

The aircraft's aerodynamic parameters such as, Cl, Cd, Cl/Cd where predicted analytically. The derived mathematical model eq 3.4 to 3.15 are used together with sizes determined in chapter 3.

- $\bar{E} = 52800J/N$
- $W_{bat} = 126\text{g} = 1.23606\text{N}$
- $Endurance = 45\ min = 2700\ seconds$

- $V_{cruise} = 15m/s$
- Efficient factor e for the aerofoil = 0.95
- $Weight\ of\ an\ aircraft\ = 248g\ =\ 2.43288N$
- $t_{endu} = \frac{E_{bat}}{P_{bat}}$ therefore $P_{bat} = \frac{E_{bat}}{t_{endu}}$
- But $E_{bat} = W_{bat}\bar{E} = 1.23606 \times 52800 = 65263.968\,J$
- $P_{bat} = \frac{E_{bat}}{t_{endu}} = \frac{65263.968}{2700} = 24.17\,Watts$
- $P_{flight} = P_{prop} = \eta_{motor}\eta_{ESC}\eta_{Pro}P_{bat} = 0.7 \times 0.89 \times 0.8 \times 24.17 = 12.05\,Watts$
- Since $P_{flight} = Drag\ force\ \times Velocity$
- Therefore $D = \frac{P_{flight}}{Velocity} = \frac{12.05}{15} = 0.803N$
- Since $\frac{C_l}{C_d} = \frac{L}{D} = \frac{2.43}{0.803} = 3.0291$
- But $C_L = \frac{2W}{\rho V^2 S} = \frac{2\times 2.43288}{1.202\times 15^2\times 0.0288} = 0.501$
- Calculating the coefficient C_D since C_L and $\frac{C_l}{C_d}$ are known
- $C_D = \frac{C_L}{(\frac{C_l}{C_d})} = \frac{0.501}{3.0291} = 0.165$
- $C_{do} = C_D - \frac{SC_l^2}{\pi eAR} = 0.165 - \frac{0.50109^2}{\pi\times 0.5\times 8} = 0.132$

Below is a table showing the prediction of the designed UAV aerodynamic performance.

Data	Symbol	Value
Battery Power	P_{bat}	$24.17\,Watts$
Propulsion Power	P_{prop}	$12.05\,Watts$
Flight Endurance	t_{endu}	$45\,min = 2700\,seconds$
Lift	L	$2.43288N$
Drag	D	$0.803N$

Table 18: Summary of Aircraft Performance

4.4. Aerodynamic Simulation using XFLR5.

In engineering design, analytical values are more accurate than simulation values. However, from research, an XFLR5 gives values that are close to the wind tunnel results. The analytical approach for determining aerodynamic characteristics of an aircraft are always less accurate because they not consider all the variables such as geometry and change is centre of pressure. Analytical would only give more accurate values when all these variables are considered, however including all these variables results in a complex equation that is difficult to solve analytically, hence wind tunnel experiments is crucial in determining the aerodynamic performance of an aircraft. Since there was no wind tunnel testing, XFLR5 was used to determine the values. Before, adding the fuselage and the tail; wing analysis was performed to see the behaviour of the wings.

4.4.1. Wing analysis

Lower aspect ratio of a wing result in high induced drag coefficient and low lift due to high vortex, hence as shown in the wing sizing section, this wing was designed have higher aspect ratio which is expected to have low induced drag and high lift.

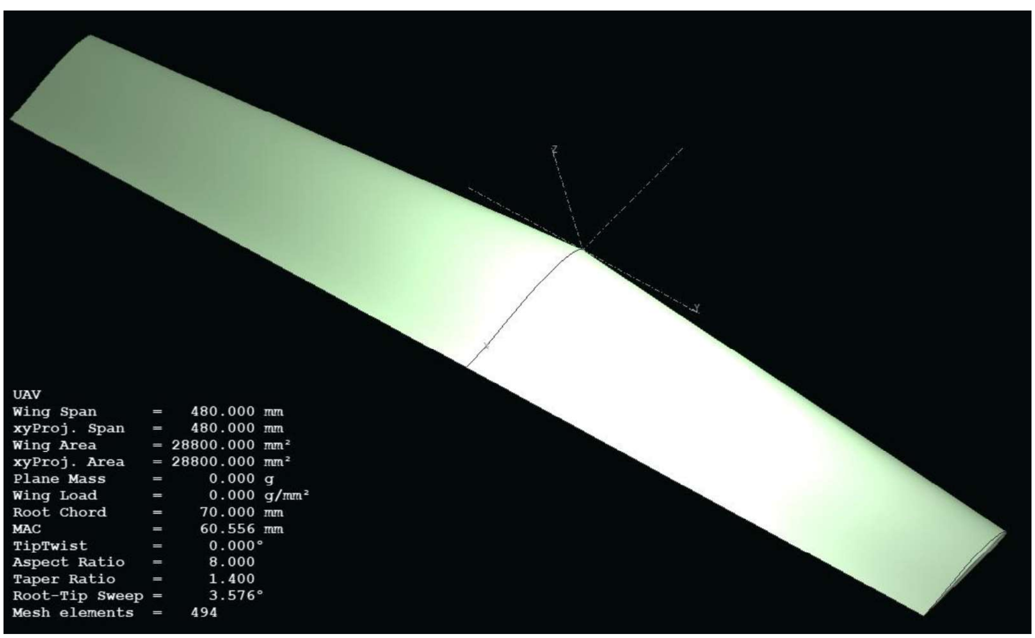

Figure 38: Modelled wing in FXLR5.

Using the XFLR5 for analysis, the flight data that are UAV velocity, air density, altitude, and kinematic viscosity were inputted into the system and launched. Type 1 was used for easy analysis. Since it is for surveillance, the UAV is assumed to fly with a constant speed

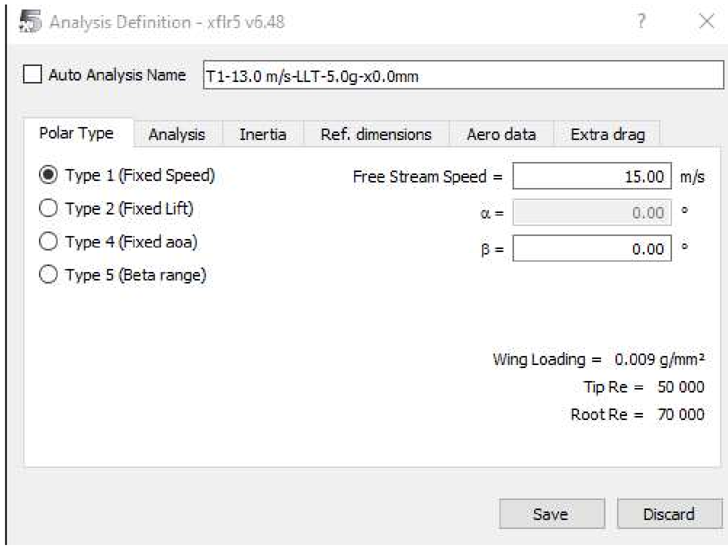

Figure 39: Snippet for the input data for analysis

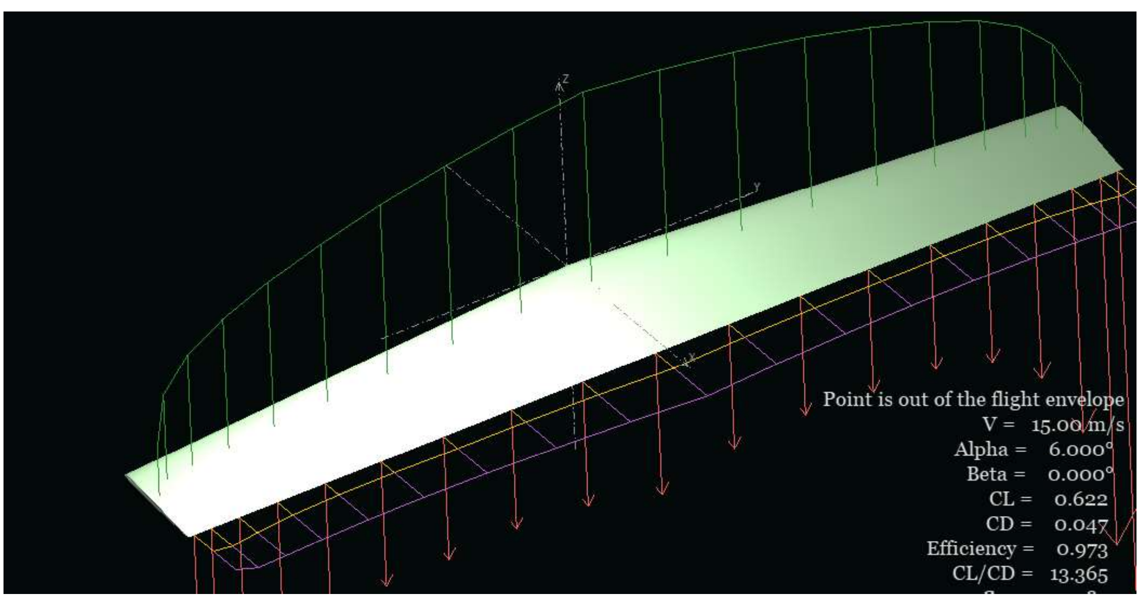

Figure 40: Lift, downwash, viscous and induced drag

The aerofoil has optimum performance at angle of attack of 6^0. At that angle of attack the coefficient of lift(Cl) and drag (Cd) are 0.633 and 0.046 respectively. As a result, the ratio of Cl/Cd is about 13.841.

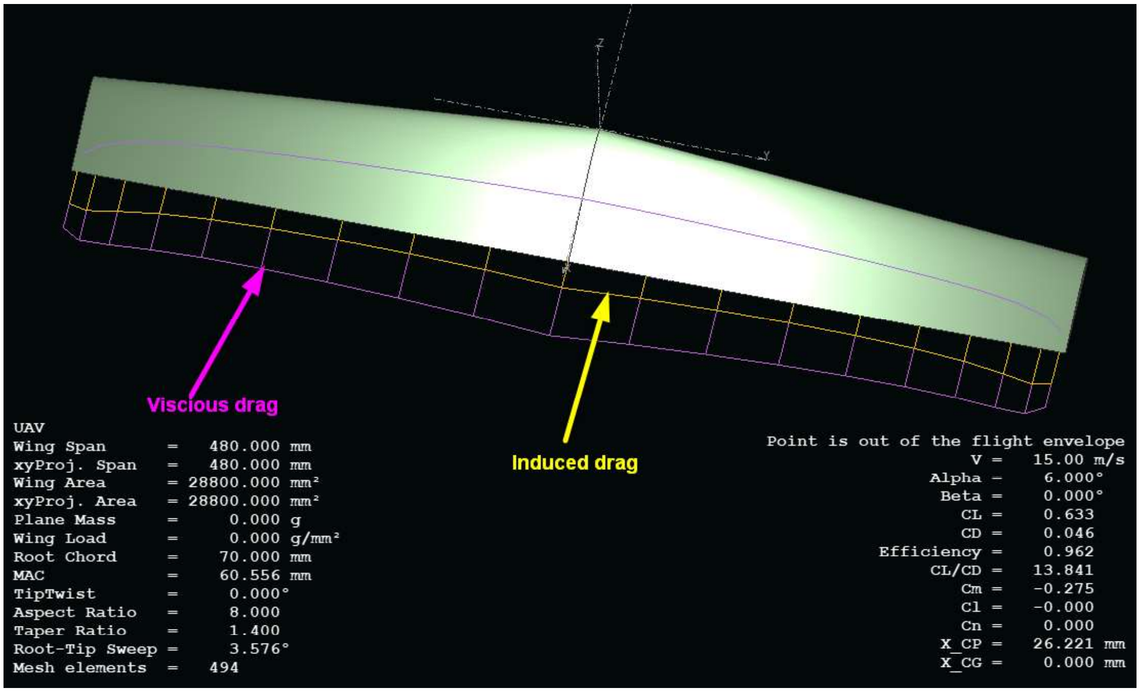

Figure 41: The viscous and induced drag

As expected, the induced drag(indicated in yellow) is low due to the tapered shape as well as the high aspect ratio. However, viscous forces are significant resulting in high viscous drag indicated in purple. Refer to **Appendix B** for induced, viscous and total drag distribution quantities.

4.4.2. Whole Aircraft Analysis

The chosen aerofoil was applied, and all the derived dimensions weights where assigned to their respective parts. An aircraft model was created.

The fig below shows that the UAV, will weigh 247.7g, tail volume of 0.352, and mesh elements of 809.

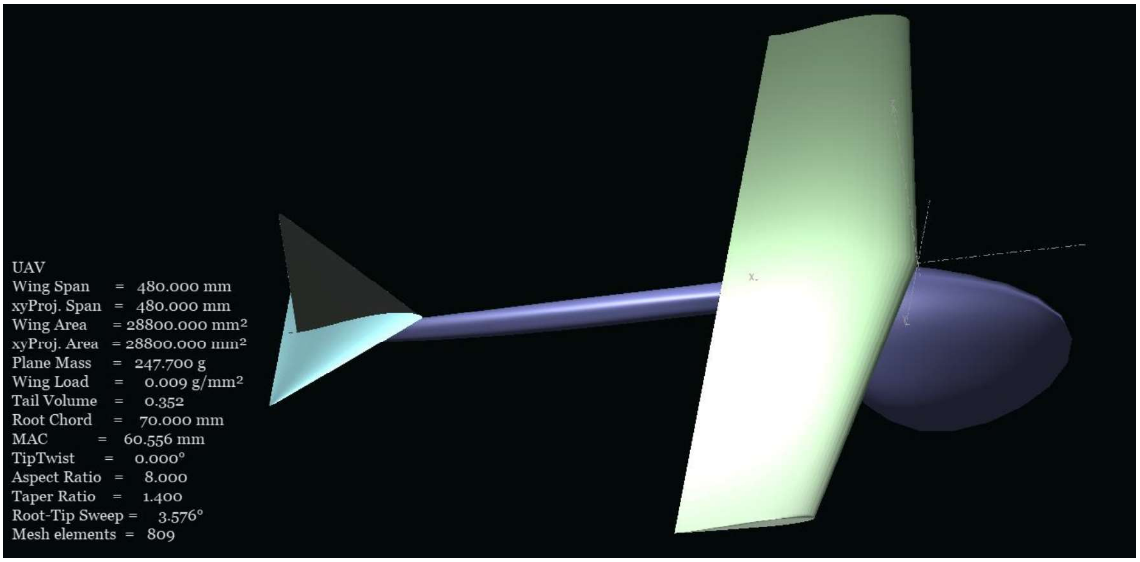

Figure 42: Model of an aircraft in XFLR5

Lift

The aircraft's overall lift was analysed. The lift distribution (in green) is positive at the wing and tail while on the longitudinal below the fin it is negative. However, overall, the aircraft has positive lift with a coefficient of lift (Cl) of 0.455.

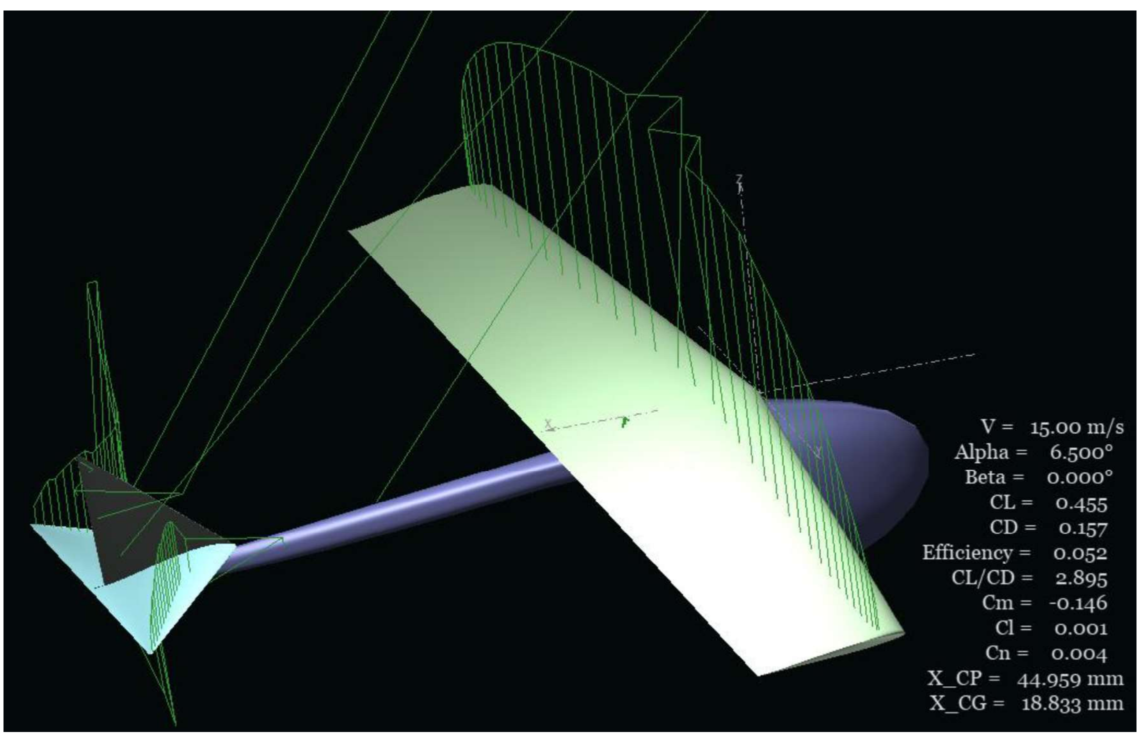

Figure 43: UAV Lift distribution

Also graphs of the Cl to CD and Alpha are analysed. The fig below shows that when Alpha=0, CL=0, CD = 0.058. Thus, the Cdo= 0.058. Also, the aircraft has high stall angle denoting to its high stability as the second graph show that the coefficient of lift increases as the angle of attack increases in excess of 20^0.

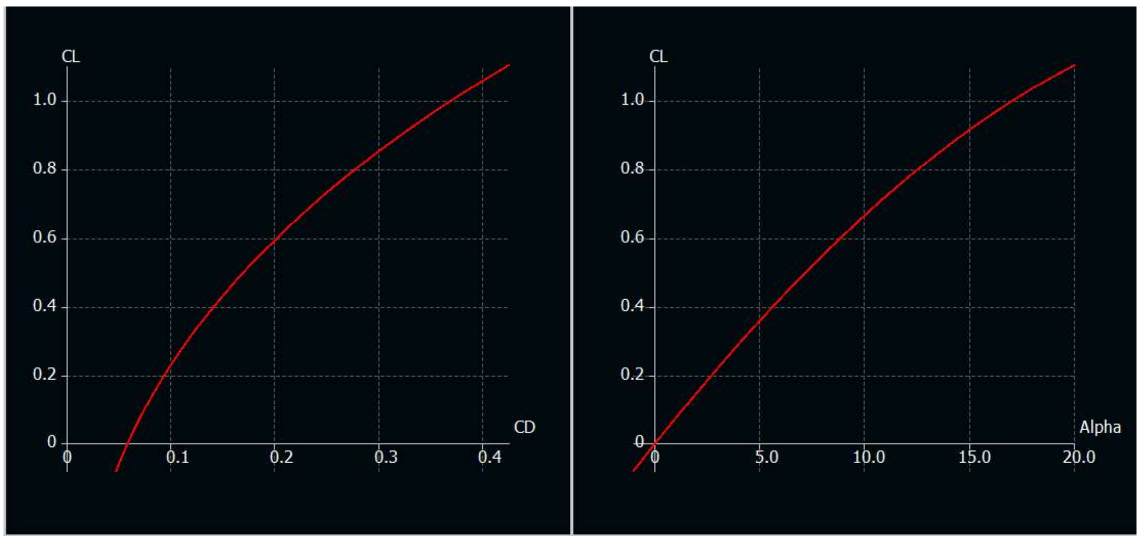

Figure 44: CL vs Coefficient of Pressure and Pressure

The fig below shows that the coefficient of pressure of the top surface to be around -2.01 while at the leading edge is 2.7. The negative value show that the resultant pressure is going upwards thereby providing lift.

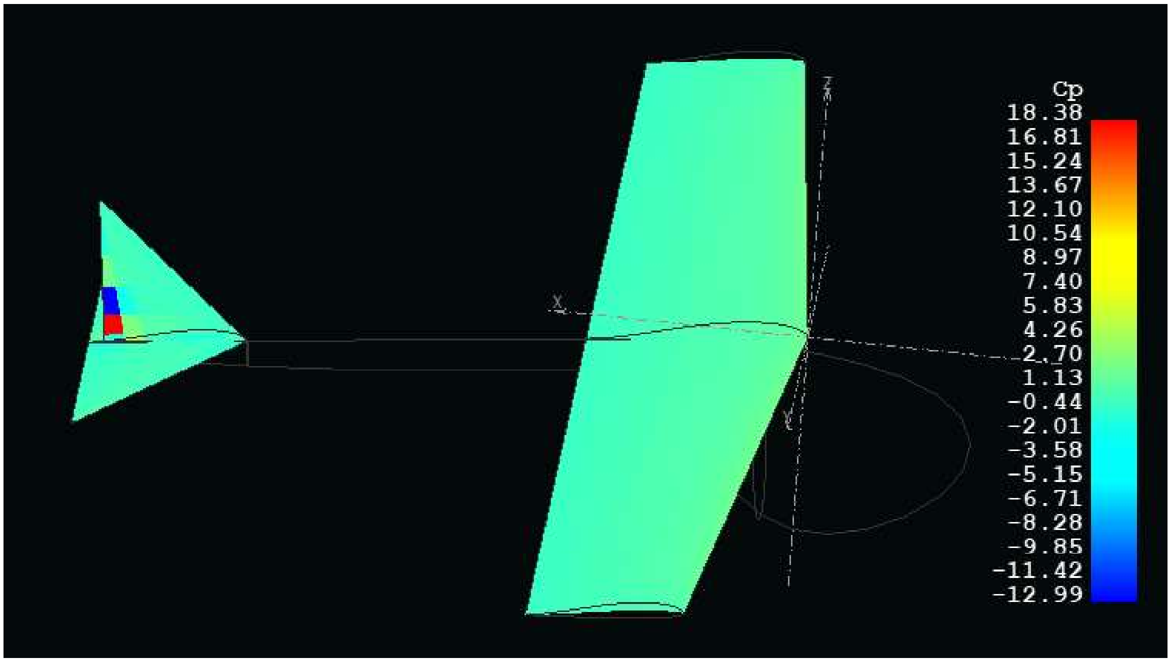

Figure 45: Distribution of cp

For better analysis and easy visualisation, the pressure distribution is plotted on the aircraft.

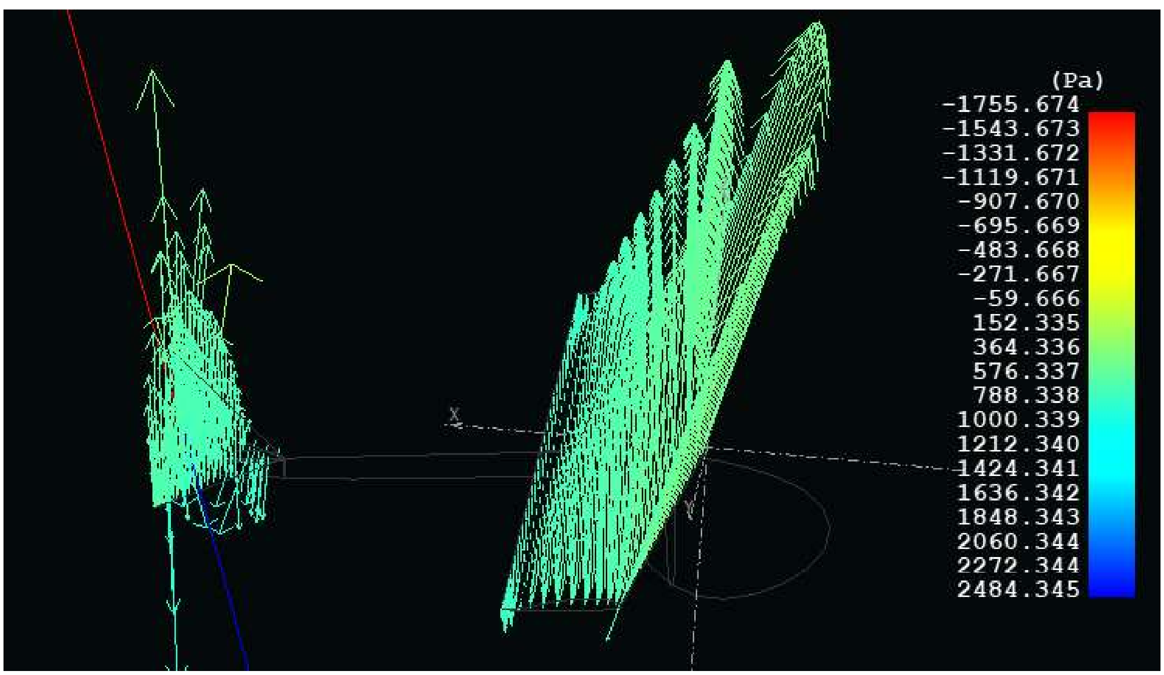

Figure 46: Pressure Distribution

Using colour distribution, the aircraft receives a pressure of around (-ve)1755.67 MPa.

Drag

The fig below show the distribution of the induced drag.

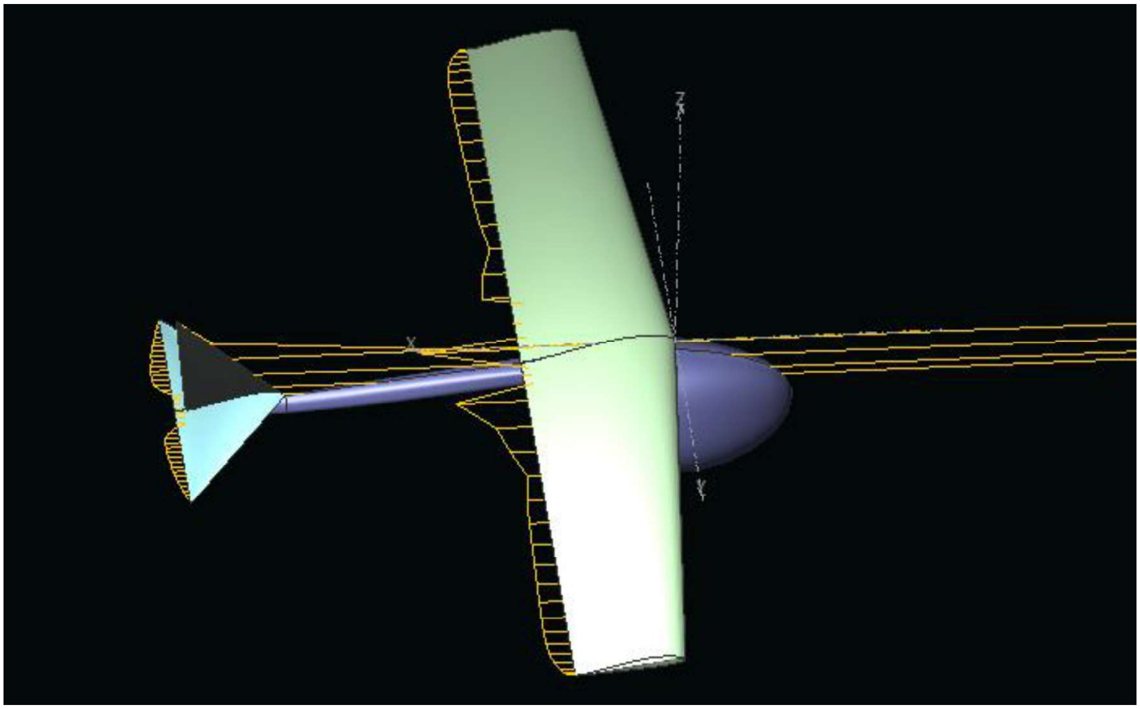

Figure 47: Induced drag distribution.

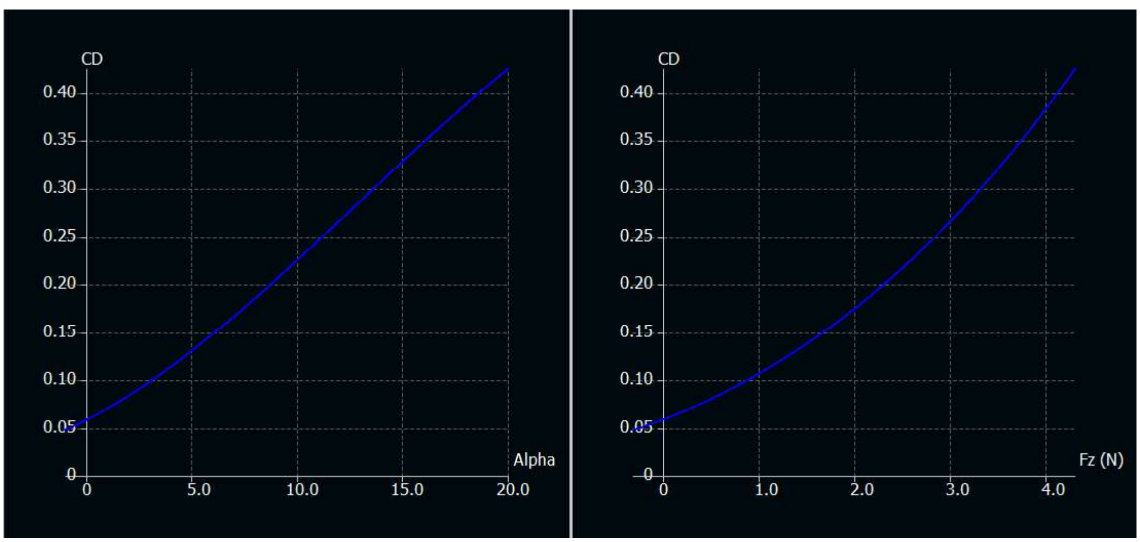

Figure 48: Cd vs Alpha and normal force

The induced drag is increasing as both the angle of attack and the normal force are increasing.

The drag is not zero when the independent variables (Alpha/Fz) is zero.

Streamlines

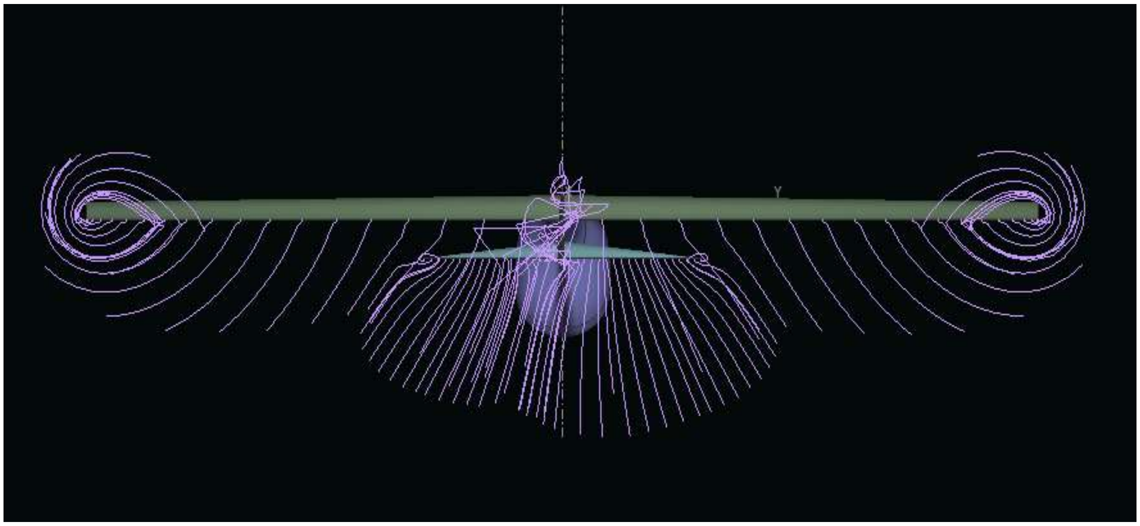

Figure 49: Streamlines on the aircraft

The above model show the vortices formed at the wing tips, elevator tips as well as at the fin.

Surface Velocity

The fig below show surface velocity with some velocity vector deflected off the tail

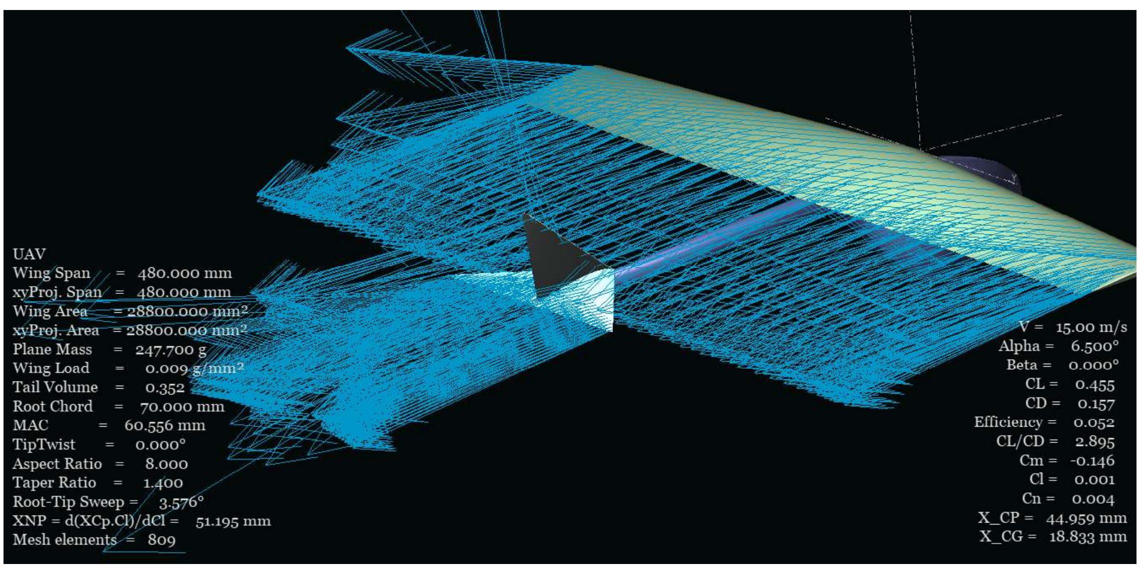

Figure 50: Surface velocity vector

4.5. Comparisons: Analytical and Simulated Aerodynamic Results

Data	Symbol	Analytical	XFLR5 values	% increase
Coefficient of Lift	C_L	0.501	0.455	9.2
Coefficient of drag	C_D	0.165	0.157	4.84
Coefficient of induced drag	C_{do}	0.132	0.058	56
Lift to Drag ratio	$\frac{C_L}{C_D}$	3.0291	2.895	4.43

Table 19: Analytical vs XFLR5 values

The general trend is that all the values from the software are lesser than the predicted analytical values. Hence all the percentage shown above are percentage decrease. As stated initially the simulation values are closer to the wind tunnel values hence conclusion will be mainly drawn from the XFLR5 results.

There is no much decrease for the CL, CD and CL/CD with respective %difference of 9.2, 4.84 and 4.43. However, this is a huge difference in the Cdo. This is because there were many estimations made to reach to that value. It would have been a worry if the XFLR5 Cdo value had increased, however the small value is more desired that the predicted value. The small value from XFLR5 indicate the good design and component selection done in chapter 3 which had the aim of reducing drag. Hence in overall, the UAV aerodynamic performance is are in good range to ensure lift, long endurance and stability.

Chapter 5: Cad Modelling and Numerical Analysis

The sketched design is modelled in SolidWorks to show the detailed design of the UAV.

5.1. 3D Models

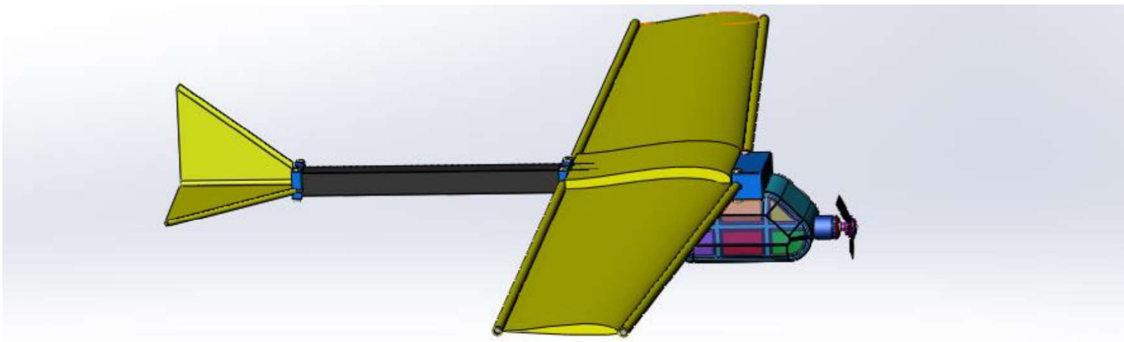

Figure 51: Isometric view

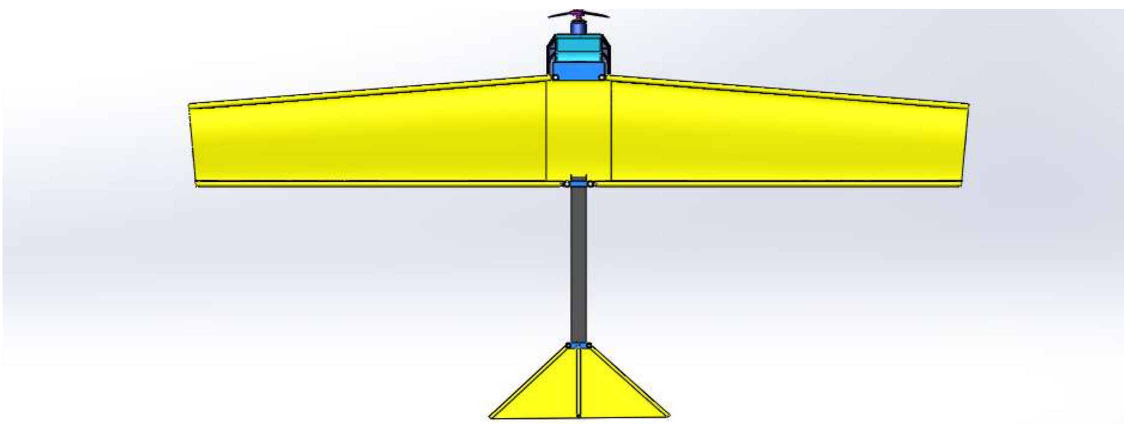

Figure 52: Top View

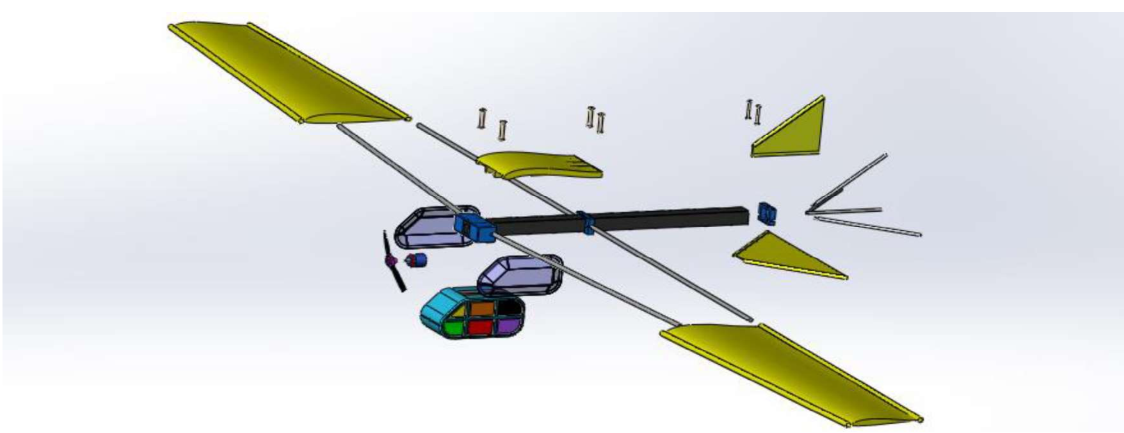

Figure 53: Exploded View

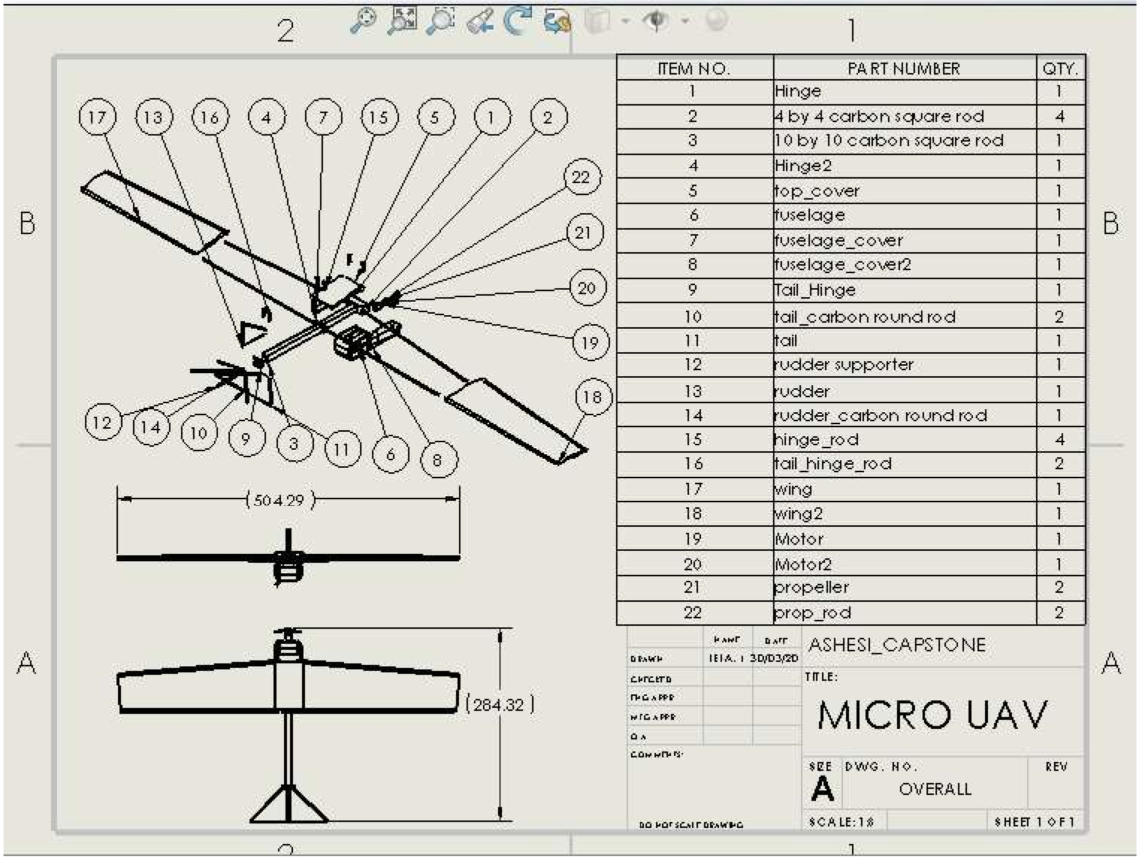

Figure 54: Assembly drawing

For more CAD models, see **Appendix C.**

5.2. FEA (Static and Fatigue) on the hinge

The torque of 9.23Nmm calculated in chapter 3 were applied. Same material properties were defined. Figure 55(a and b) show the von misses stresses and factor of safety after running static analysis.

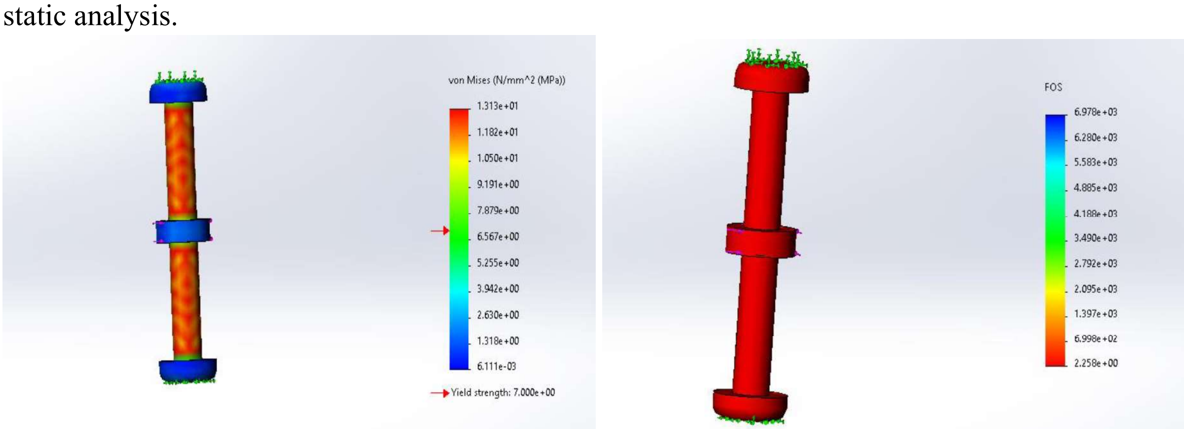

Figure 55: Von Misses stresses (b) Static FOS

Figure 56 show the material displacement. The values range from 1e-30 to 1.399e-02mm

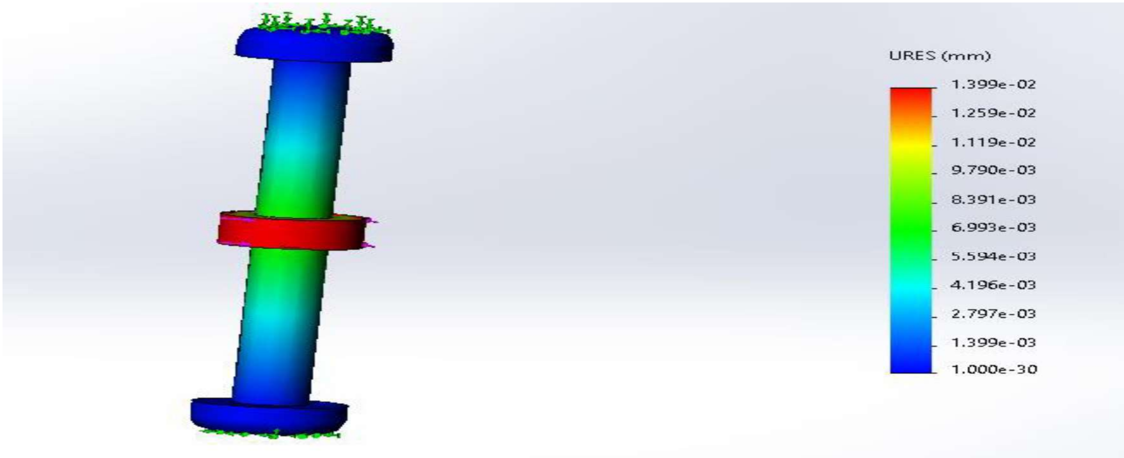

Figure 56: Material displacement

Fatigue Analysis

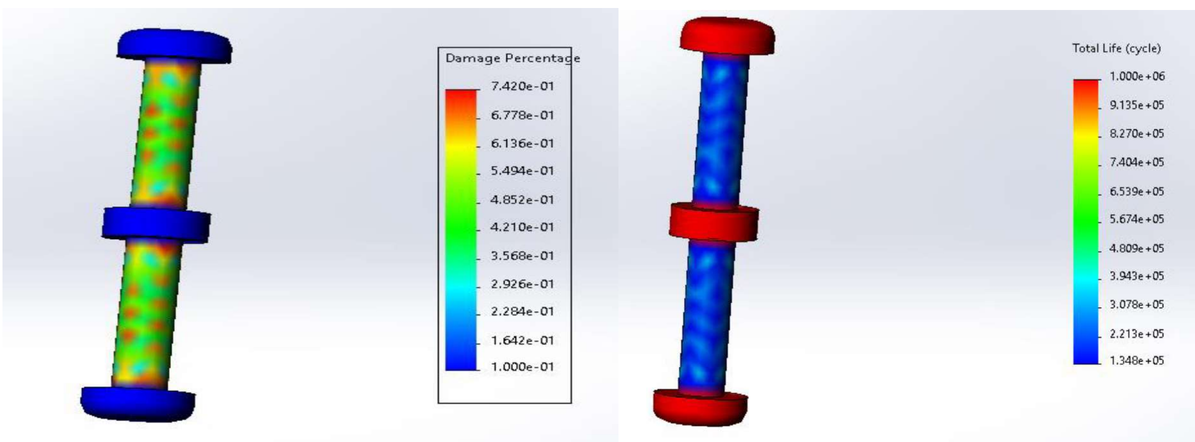

Figure 57: (a) the damage percentage **(b) Total life(number of circles)**

Figure 58: Load Factor

Maximum Stress	13.13 MPA
FOS	2.258
URES	0.0139mm
Damage %	0.74
Load factor	0.732

Table 20: Summary of Static and Fatigue Analysis

The factor of safety of 2.258 show that the hinge shaft was properly designed. The displacement is 0.0139mm which is insignificant hence will not alter the shaft diameter. Also the damage factor of 0.74% show that it is unlikely to fail.

5.3. FEA(Static) Wing Bending

The total weight of the aircraft calculated was 2.3N. This force together with an additional of 1.7N(total of 4N) were applied at the tip end of the wing. Since the wing shape is maintained by the rods and the force was applied to the tip of the rods. The fabric was hidden to for proper viewing of the bending and deflection of the wing structure.

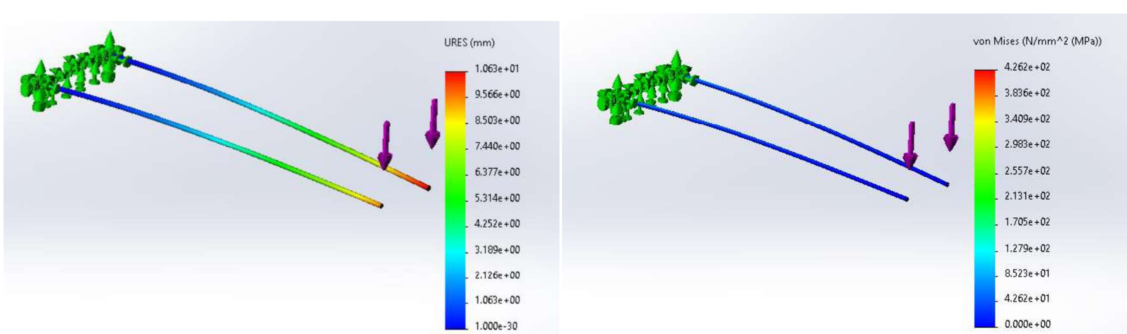

Figure 59: (a)Wing deflections (b)Von misses stresses

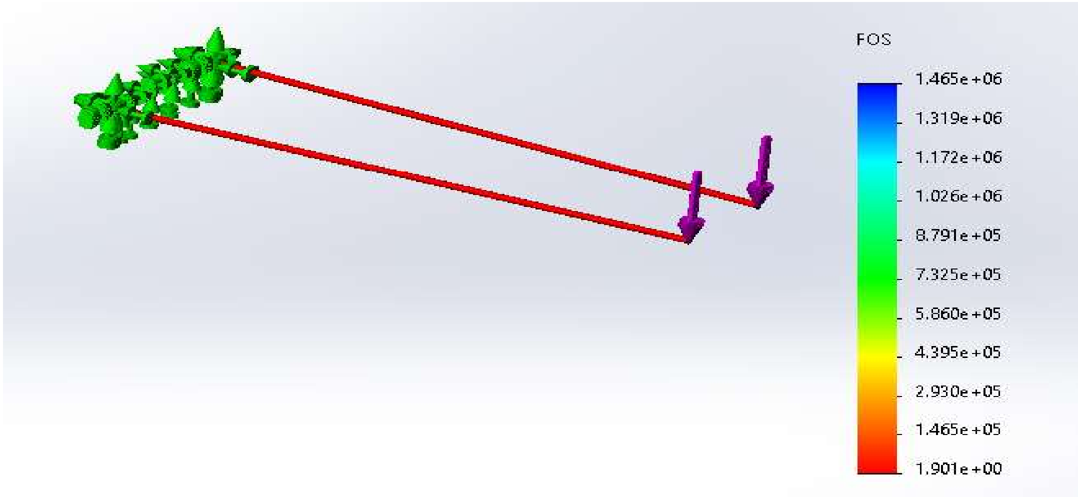

Figure 60: Factor of safety for the wing structure

The table shows the static results.

Maximum Stress	42.6 MPA
FOS	1.9
URES	10.63 mm

Table 21: Summary results for wing bending analysis

The wing is stiff as displacement of 10.63mm is optimum and the FoS is within an acceptable range. Low value is proper for aircrafts where light weight is of much importance.

Chapter 6: Conclusion

6.1. Achievements

The micro-UAV capable deploying and collapsing wing was successfully designed and analysed. The ability of the designed UAV to stow/fold wings meet this project mission requirement were the UAV is designed for surveillance hence can be launched at much space constrained places such as airdrop from mother/carrier aircraft.

Component's selection ensured a low-cost design and structural analysis proved the static and fatigue stresses to within the limit and that the micro-UAV is capable sustaining these stresses for long. The aircraft parts sizing as well as material selection ensured that total weight of the UAV lie withing the range of not exceed the 300g weight baseline requirement. Also the sizing optimisation ensured that the aircraft has high aspect ratio, a property that increases flight endurance of the UAV. Despites its high AR, the micro-UAV was successfully designed with a length of 70mm.

A lightweight UAV designed requirement was achieved due to the proposed design that use an ultra-light weight ripstop nylon fabric and carbon fibre rods, hence would reduce battery power consumption thereby increasing flight endurance.

The low-cost UAV was achieved through material selection criteria where cost was considered for each decision hence the material selected are cheap and are accessible to the African drone companies. Low cost was also achieved through the design of a small sized UAV hence helped reduce he amount of materials used thereby cutting the UAV's costs.

Propulsion system optimisation ensure selection of small and cheap components (battery, esc and motor) that suits the proposed micro design.

Despite the aircraft small size in nature, it proved to have optimum aerodynamic performance for long flight endurance. The performances were confirmed from the results found after running simulation on XFLR5. Control surfaces that are flaps, ailerons, and rudders were not analysed and since that the UAV had better CL values, it gives a satisfying insight that if the control surfaces are added, the aerodynamic characteristics of the UAV will be much improved.

6.2. Limitations

During the course of this project, several challenges the hinder the project completion were faced. Although some of the limitations hindered the success of the project, alternatives were devised to ensure the project objectives are met. Firstly, designing the exact aerofoil and making tapered wing in SolidWorks were a great challenge. Fortunately, aerofoil data was provided on the internet as an open source. Using the SolidWorks importation tool, the aer0foil cross-section was created in SolidWorks and was then resized to suit design specifications.

Restrictions due the Covid 19 pandemic and the national lockdown greatly affected the project and some of the vital decisions were made as a result of this challenge. First there was no access lab and equipment for fabrication as all non-essential shops were closed and movement was restricted. The initial aim was to fabricate the UAV however, full simulation was considered as an alternative. Moreover, even if the UAV was built, there are no local wind tunnel equipment to test the UAV's aerodynamic performance. Fortunately, an XFLR5 software that specifically made for UAVS was taken advantage of and was used to simulate aerodynamic characteristics of the UAV.

Unfortunately, XFLR5 does not support the importation of 3D models from CAD software such as SolidWorks. Modelling the exact the design made in SolidWorks in XFLR5 was a challenge. Extra in detail modelling had to be done to imitate CAD model in XFLR5. This is because aerodynamic of an aircraft is sensitive hence a small geometrical change would alter performances.

Although theoretically and analytically proved, it is difficult to conclude if the designed micro unmanned aerial vehicle is capable of flying and carrying sensing load for environmental monitoring. Lastly frequent power cuts derailed the completion of the capstone.

6.3. Future Work

Due to some of the challenges mentioned above, some of the initial project objectives were not carried out.

- First there is need to perform an in detail CFD analysis on the advanced control surfaces such as ailerons, flaps and just to mention a few.
- In high regard, there is need to build a physical UAV using the selected material. Stability testing is also vital as it also determines the performance of the aircraft. Structural stiffness test, wing loading and bending has to be carried out to understand structural performance when acted upon by external forces.
- Wind tunnel test is imperative to analyse the aircraft aerodynamic performance. Also, flight testing and most importantly endurance testing need to be tested and confirmed.
- The aircraft designed has deployable wings, however this paper did not design the automatic deployment system of the wings. Future work can consider developing a self-locking deployment wings with feedback system so that the UAV can be dropped and automatically deploy into the flight configuration.
- It also necessary to design a deployment tube that houses a collapsed wing aircraft is this would allow a massive deployment of the UAVs.

References

[1] Y. E. Tan and S. K. Moon, "Inflatable wing design for micro UAVs using indirect 3D printing," 2014 11th International Conference on Ubiquitous Robots and Ambient Intelligence (URAI), Kuala Lumpur, 2014, pp. 545-546, doi: 10.1109/URAI.2014.7057386.

[2] N. J., “Design of a micro-scale deployable unmanned aerial vehicle,” Sjsu.edu. [Online]. Available: https://www.sjsu.edu/people/nikos.mourtos/docs/micro%20UAV.pdf. [Accessed: 06-Oct-2020].

[3] J. D. Jacob, A. Simpson, & S Smith, “Design and Flight Testing of Inflatable Wings with Wing Warping” (SAE Technical Paper No. 2005-01–3392), https://doi.org/10.4271/2005-01-3392, pp. 3, 2005.

[4] A. Olorunlomerue and A. O. Agbeyangi, “Review on UAVs used for Aerial Surveillance.”

[5] Mit.edu. [Online]. Available: https://web.mit.edu/16.unified/www/FALL/thermodynamics/notes/node99.html. [Accessed: 06-Oct-2020].

[6] V. P. Galantai, “Design and analysis of morphing wing for unmanned aerial vehicles,” Utoronto.ca. [Online]. Available: https://tspace.library.utoronto.ca/bitstream/1807/33722/3/Galantai_Vlad_P_201011_MASc_thesis.pdf. [Accessed: 06-Oct-2020].

[7] S. D. Landon, “Development of deployable wings for small unmanned aerial vehicles using compliant mechanisms,” Byu.edu. [Online]. Available: https://scholarsarchive.byu.edu/cgi/viewcontent.cgi?article=1951&context=etd. [Accessed: 06-Oct-2020].

[8] S. Moon, Y. Tan, J Hwang and Yoon, Y., Application of 3D Printing Technology for Designing Lightweight Unmanned Aerial Vehicle Wing Structures. International Journal of Precision Engineering and Manufacturing-Green Technology, 1, 223–228, 2014. https://doi.org/10.1007/s40684-014-0028-x

[9] S. Chiesa, D. Camatti, S. Corpino, M. Pasquino, and N. Viola, “Hypothesis about cost-effective unmanned offensive airplane vehicles,” Aircr. des., vol. 3, no. 3, pp. 151–165, 2000.

[10] “Commercial drone market revenue projection - MENA 2025,” Statista.com. [Online]. Available: https://www.statista.com/statistics/607897/commercial-drone-market-revenues-in-middle-east-and-africa-projection/. [Accessed: 06-Oct-2020].

[11] “SKT Aeroshutter,” Sktaeroshutter.com, 24-Oct-2019. [Online]. Available: https://www.sktaeroshutter.com/. [Accessed: 06-Oct-2020].

[12] GhanaWeb, “Government to use drones to fight Galamsey - Frimpong-Boateng,” Ghanaweb.com, 18-Aug-2018. [Online]. Available: https://www.ghanaweb.com/GhanaHomePage/NewsArchive/Government-to-use-drones-to-fight-Galamsey-Frimpong-Boateng-677673. [Accessed: 06-Oct-2020].

[13] African Development Bank, “Industrialize Africa,” Afdb.org, 08-Jun-2019. [Online]. Available: https://www.afdb.org/en/the-high-5/industrialize-africa. [Accessed: 06-Oct-2020].

[14] J. Rowe, S. Smith, A. Simpson, J. Jacob, and S. Scarborough, "Development of a finite element model of warping inflatable wings," in 47th AIAA/ASME/ASCE/AHS/ASC Structures, Structural Dynamics, and Materials Conference 14th AIAA/ASME/AHS Adaptive Structures Conference 7th, 2006.

[15] S. D. Landon, "Development of deployable wings for small unmanned aerial vehicles using compliant mechanisms," Byu.edu. [Online]. Available: https://scholarsarchive.byu.edu/cgi/viewcontent.cgi?article=1951&context=etd. [Accessed: 13-Oct-2020].

[16] V. P. Galantai, "Design and analysis of morphing wing for unmanned aerial vehicles," Utoronto.ca. [Online]. Available: https://tspace.library.utoronto.ca/bitstream/1807/33722/3/Galantai_Vlad_P_201011_MASc_thesis.pdf. [Accessed: 13-Oct-2020].

[17] T. S. Tao and R. J. Hansman, "Development of an in-flight-deployable micro-UAV," in *54th AIAA Aerospace Sciences Meeting*, 2016

[18] N. J., "Design of a micro-scale deployable unmanned aerial vehicle," *Sjsu.edu*. [Online]. Available: https://www.sjsu.edu/people/nikos.mourtos/docs/micro%20UAV.pdf. [Accessed: 12-Oct-2020].

[19] R. R. Vannarth, S. Kulkarni, and K. Mallikharjuna, "Design, analysis and fabrication of micro class uav," *Ijamejournals.com*. [Online]. Available: http://ijamejournals.com/pdf/rpm11175.pdf. [Accessed: 12-Oct-2020].

[20] Y. E. Tan and S. K. Moon, "Inflatable wing design for micro UAVs using indirect 3D printing," in *2014 11th International Conference on Ubiquitous Robots and Ambient Intelligence (URAI)*, 2014, pp. 545–546.

[21] S. K. Moon, Y. E. Tan, J. Hwang, and Y.-J. Yoon, "Application of 3D printing technology for designing light-weight unmanned aerial vehicle wing structures," *Int. J. Precis. Eng. Manuf.-Green Technol.*, vol. 1, no. 3, pp. 223–228, 2014.

[22] MIT, "Low Cost UAV Sampling Test System Critical Design Review" [Accessed: 12-Oct-2020].

[23] "Westport - 22.7mm, 20T/25ga - FlyBrushless.com," Flybrushless.com. [Online]. Available: http://www.flybrushless.com/motor/view/278. [Accessed: 26-Jan-2021]. [23] "Westport - 22.7mm, 20T/25ga - FlyBrushless.com," Flybrushless.com. [Online]. Available: http://www.flybrushless.com/motor/view/278. [Accessed: 26-Jan-2021].

[24] "Attachment browser: ESC Efficiency.jpg by matttay - RC Groups," Rcgroups.com. [Online]. Available: https://www.rcgroups.com/forums/attachment.php?attachmentid=2389256. [Accessed: 26-Jan-2021].

[25] J. Grasmeyer and M. Keennon, "Development of the black widow micro air vehicle," in 39th Aerospace Sciences Meeting and Exhibit, 2001.

[26] "Brushless Motor KV To RPM Calculator," Rcdronegood.com, 16-Aug-2017. [Online]. Available: http://www.rcdronegood.com/brushless-motor-kv-to-rpm/. [Accessed: 26-Jan-2021].

[27] "UIUC Airfoil Data Site," Illinois.edu. [Online]. Available: https://m-selig.ae.illinois.edu/ads/coord_database.html. [Accessed: 24-Mar-2021].

[28] "XFLR5," Xflr5.tech. [Online]. Available: http://www.xflr5.tech/xflr5.htm. [Accessed: 24-Mar-2021].

[29] "7 Denier ultralight coated ripstop nylon fabric (sold per yard)," Rockywoods.com. [Online]. Available: https://www.rockywoods.com/7D-Ultralight-Coated-Ripstop-Nylon-Fabric. [Accessed: 29-Mar-2021].

[30] "0.74 oz MTN 7D Ripstop Nylon," Ripstopbytheroll.com. [Online]. Available: https://ripstopbytheroll.com/products/0-74-oz-mtn-7d-ripstop-nylon. [Accessed: 29-Mar-2021].

[31] M.-Y. Chu, L. De Jonghe, and S. Visco, "High specific power lithium polymer rechargeable battery," in Proceedings of 11th Annual Battery Conference on Applications and Advances, 2002, pp. 163–165.

[32] Europa.eu. [Online]. Available: https://ec.europa.eu/home-affairs/sites/default/files/e-library/documents/policies/security/pdf/uav_study_element_2_en.pdf. [Accessed: 01-Apr-2021].

[33] R. Madhavan, T. Silva, F. Farina, R. Wiebbelling, L. Renner, and E. Prestes, "Unmanned aerial vehicles for environmental monitoring, ecological conservation, and disaster management," in Technologies for Development, Cham: Springer International Publishing, 2018, pp. 31–39.

[34] Rechargeable Li-ion Polymer Battery, "Specification of product," Custompower.com. [Online]. Available: https://www.custompower.com/documents/SPB463048.pdf. [Accessed: 16-Apr-2021].

[35] Murrieta Mendoza, Alejandro. (2013). Vertical and lateral flight optimization algorithm and missed approach cost calculation.

[36] Jacob, J. D., Simpson, A., & Smith, S., Design and Flight Testing of Inflatable Wings with Wing Warping (SAE Technical Paper No. 2005-01–3392), 2005. https://doi.org/10.4271/2005-01-3392

[37] A. Simpson, J. Jacob, and S. Smith, “Inflatable and Warpable Wings for Meso-Scale UAVs,” in Infotech@Aerospace, 2005.

[38] “ch11,” Nasa.gov. [Online]. Available: https://history.nasa.gov/SP-4308/ch11.htm. [Accessed: 22-Apr-2021].

[39] “Rogallo,” Kitehistory.com. [Online]. Available: http://www.kitehistory.com/Miscellaneous/rogallo.htm. [Accessed: 22-Apr-2021].

[40] “Why aren’t Rogallo wings or parafoils used in aircraft with fuselages?,” Stackexchange.com. [Online]. Available: https://aviation.stackexchange.com/questions/32622/why-arent-rogallo-wings-or-parafoils-used-in-aircraft-with-fuselages. [Accessed: 22-Apr-2021].

[41] “Rogallo wing definitions and diagrams,” Hghistory.org, 15-Mar-2020. [Online]. Available: https://hghistory.org/hang-gliding-2/rogallodefns/. [Accessed: 22-Apr-2021].

[42] Aiaa.org. [Online]. Available: https://www.aiaa.org/docs/default-source/uploadedfiles/aiaadbf/previous-competitions/top-reports/2017topreports.pdf?sfvrsn=4aecc31f_0. [Accessed: 22-Apr-2021].

[43] J. D. Allen Jr, “Folding solid-membrane wing structure for a micro air vehicle,” Wvu.edu. [Online]. Available: https://researchrepository.wvu.edu/cgi/viewcontent.cgi?article=1562&context=etd. [Accessed: 23-Apr-2021].

[44] N. H. Rosid, E. Irsyad Lukman, M. Ahmad Fadlillah, and M. Agoes Moelyadi, “Aerodynamic characteristics of tube-launched tandem wing unmanned aerial vehicle,” J. Phys. Conf. Ser., vol. 1005, p. 012015, 2018.

[45] J. Jacob and S. Smith, “Design limitations of deployable wings for small low altitude UAVS,” in 47th AIAA Aerospace Sciences Meeting including The New Horizons Forum and Aerospace Exposition, 2009.

[46] R. L. K. Woodland, “Sonotube compatible unmanned aerial vehicle and system,” 6056237, 02-May-2000.

[47] B. Johnson, D. Claxton, B. Stanford, V. Jagdale, and P. Ifju, “Development of a composite bendable-wing micro air vehicle,” in 45th AIAA Aerospace Sciences Meeting and Exhibit, 2007.

[48] “Types of wood,” The-warren.org. [Online]. Available: https://www.the-warren.org/GCSERevision/resistantmaterials/wood.html. [Accessed: 27-Apr-2021].

[49] Builderology.com. [Online]. Available: https://builderology.com/types-of-wood/. [Accessed: 27-Apr-2021].

[50] O. Tkachuk, “Detailed design of a forest surveillance UAV,” Ulisboa.pt. [Online]. Available: https://fenix.tecnico.ulisboa.pt/downloadFile/281870113704610/Oleh_87746_Extended_Abstract.pdf. [Accessed: 27-Apr-2021].

[51] “The basics: Polymer definition and properties,” Americanchemistry.com. [Online]. Available: https://plastics.americanchemistry.com/plastics/The-Basics/. [Accessed: 27-Apr-2021].

[52] “Composite Materials,” Sciencedirect.com. [Online]. Available: https://www.sciencedirect.com/topics/engineering/composite-materials. [Accessed: 27-Apr-2021].

[53] “What are composites? - composites 101,” Compositeslab.com, 18-May-2015. [Online]. Available: http://compositeslab.com/composites-101/what-are-composites/. [Accessed: 27-Apr-2021].

[54] D. Ozkan, M. S. Gok, and A. C. Karaoglanli, “Carbon fiber reinforced polymer (CFRP) composite materials, their characteristic properties, industrial application areas and their machinability,” in Advanced Structured Materials, A. Öchsner and H. Altenbach, Eds. Cham: Springer International Publishing, 2020, pp. 235–253.

[55] “Fiber Reinforced Polymers - characteristics and behaviors,” Princelund.com. [Online]. Available: https://www.princelund.com/fiber-reinforced-polymers.html. [Accessed: 27-Apr-2021].

Appendix A: Sizing and Estimation

A.1. Fatigue (Determination of the hinge diameter)

Force requires to retract the wing should exceed the weight of the wing??

Weight of the wing = 0.16775 N

Centre of gravity from the hinge rotation centre =110mm

Torque =force ×Perpendicular distance = 110×0.167751=18.45261N-mm

Therefore, Torque for each hinges $\tau = 9.2263$ Nmm

A: Load Analysis

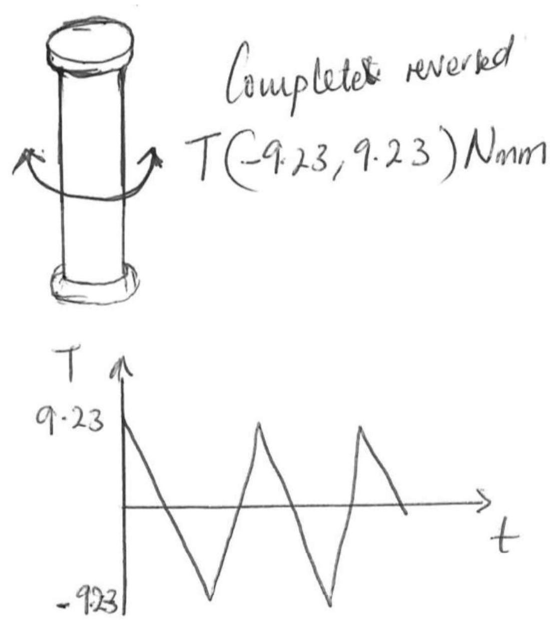

Figure A.1.1: Load Analysis (Torque)

$T \sim (-9.23, 9.23) Nmm$

$T_m = \frac{T_{max}+T_{min}}{2}$ and $T_a = \frac{T_{max}-T_{min}}{2}$

$$T_m = \frac{9.23 + -9.23}{2} = 0$$

$$T_a = \frac{9.23 - -9.23}{2} = 9.23\ Nmm$$

B: Stress Analysis

Critical point at the walls, upper middle and below

$$\tau_m = \frac{16T_m}{\pi d^3} = 0$$

$$\tau_a = \frac{16T_a}{\pi d^3} = \frac{16 \times 9.23}{\pi d^3} = \frac{47.01}{d^3}\ MPa$$

C: Material Properties

Material Type: Reinforced Carbon fibre(lowest grade)

$S_{ut} = 7MPa$

$S_{yt} = 6.62MPa$

$S_{us} = 0.8S_{ut} = 5.6MPa$

$S_{ys} = 0.5777S_{yt} = 3.82MPa$

$S_f = 3.5\ MPa$

D: Design Equation and Solution: Modified Goodman

Operating Point, $P\left(0, \frac{47.01}{d^3}\right)$

Safety factor = 2

Failure by Fatigue

$$\frac{1}{n} = \frac{\tau_m}{S_{us}} + \frac{\tau_a}{S_f} = \frac{1}{2} = \frac{47.01}{3.5d^3}$$

$d^3 = \frac{47.01 \times 2}{3.5}$ therefore d = 4.99mm

Failure by Yield

$$\frac{1}{n} = \frac{\tau_m}{S_{ys}} + \frac{\tau_a}{S_{ys}} = \frac{1}{2} = \frac{47.01}{3.82d^3}$$

$d^3 = \frac{47.01 \times 2}{3.5}$ therefore d = 4.91mm

Since the diameter determined by fatigue is greater than diameter determined by yield, it will fail fatigue.

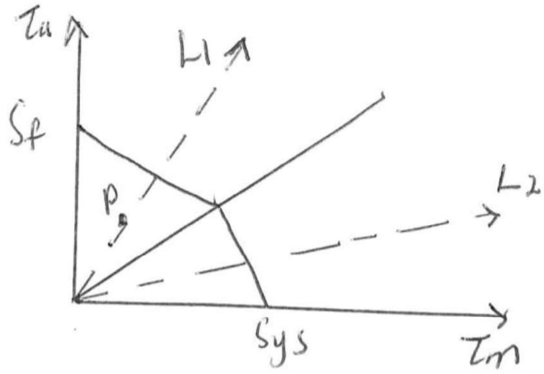

Figure 61: DE-Goodman graph

Standardising = d=5mm

Calculating the actual factor of safety

$\frac{1}{n} = \frac{47.01}{3.5 \times 3^3}$; n(actual)=2.01

A.2. Aircraft Structure Weight Estimation

After material selection and determining the sizes of the aircraft components, the mass of each component is calculated using the traditional formula:

$Mass = density(\rho) \times volume(V)$

The density is of each component is known since the material has been selected.

A.2.1. Weight of the wings

Weight of ripstop nylon

Wing span =480mm

Average cord length$\frac{70+50}{2} = 60mm$

Wing area (excluding the rods)= chord length × wing span length =480×60×2=57600mm^2

Surface area on the rods $= 2\pi \times r \times h \times 2 = 2\pi \times 2 \times 480 \times 2$

Total area of the ripstop nylon $= 57600 + 2\pi \times 2 \times 480 \times 2 = 69663.72mm^2$

There total weight of ripstop nylon= $\bar{A} \times A = 0.000024 \times 69663.72 = 1.672g$

Weight of wing supporting carbon rods

Density of carbon rod = 0.002267 g/mm3

Volume of the rods $= 2 \times \pi \frac{d^2}{4} h = \pi \times \frac{3^2}{4} \times 480 = 6785.84mm^3$

Weight of rods in the wing $=0.002267 \times 6785.84 = 15.38g$

Thus, total weight of the wing $= 15.38g + 1.672g = 17.1g$

A.2.2. Tail weight estimation

Weight of Ripstop on the Elevator and Fin

Elevator area $= 2 \times 3570mm^2$

Fin area$= 2 \times 1035mm^2$

Total area$= 2 \times 1035mm^2 + 2 \times 3570mm^2 = 9210mm^2$

Mass of ripstop at the tail,$= 0.000024 \times 9210 = 0.221g$

Weight of tail supporting carbon rods

Volume of rods $= \pi \frac{d^2}{4} h = \pi \times 1^2(70 + 70 + 10 + 60 + 52) = 823.1mm^3$

Mass of rods at the tail $= 823.1mm^3 \times 0.002267 = 1.865g$

$M_{tail} = 1.865g + 0.221g = 2.1g$

A.2.3. Main carbon square rod support weight estimation

Volume $= Ah = 10 \times 10 \times 200 = 20000mm^3$

Mass of Carbon support $= 20000 \times 0.002267 = 45.3g$

Estimation Weight of hinges = 5.5g

Appendix B: FXLR5 Aerodynamic Results

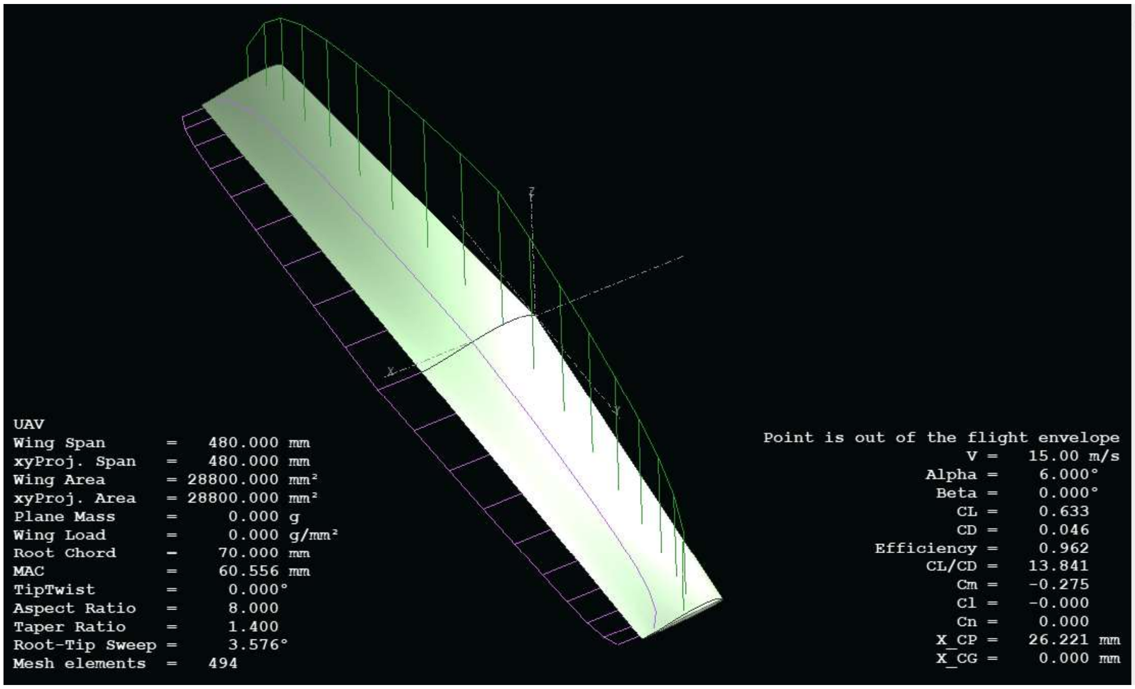

Figure 62.1:drag and lift

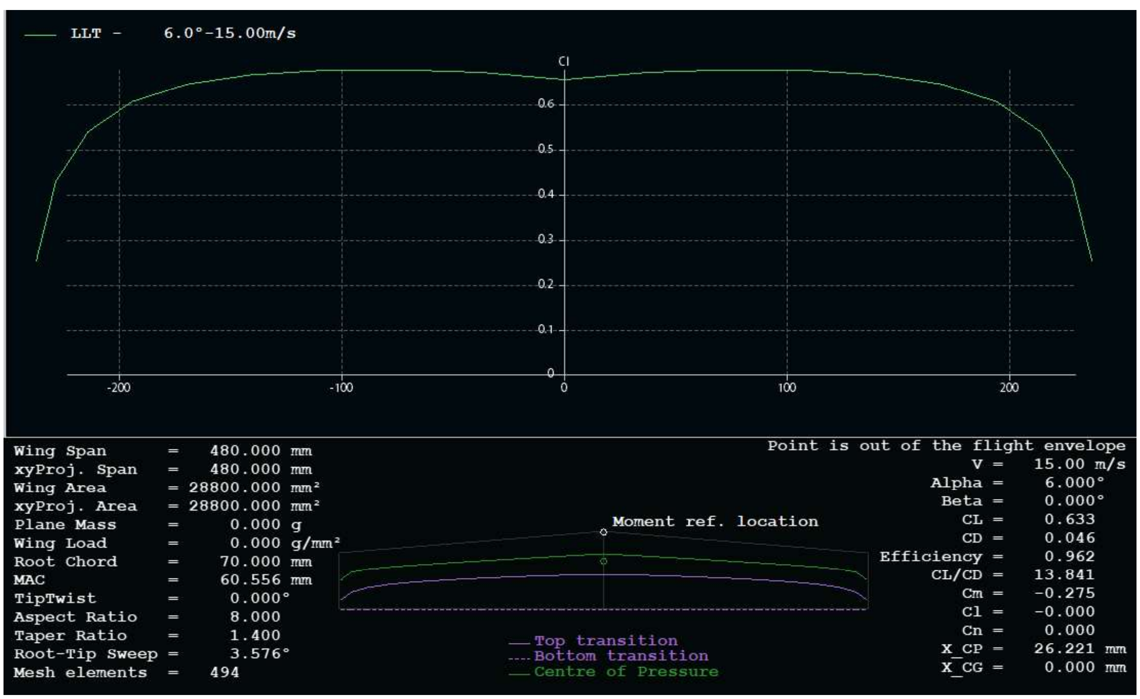

Figure 63: Cl vs Wingspan

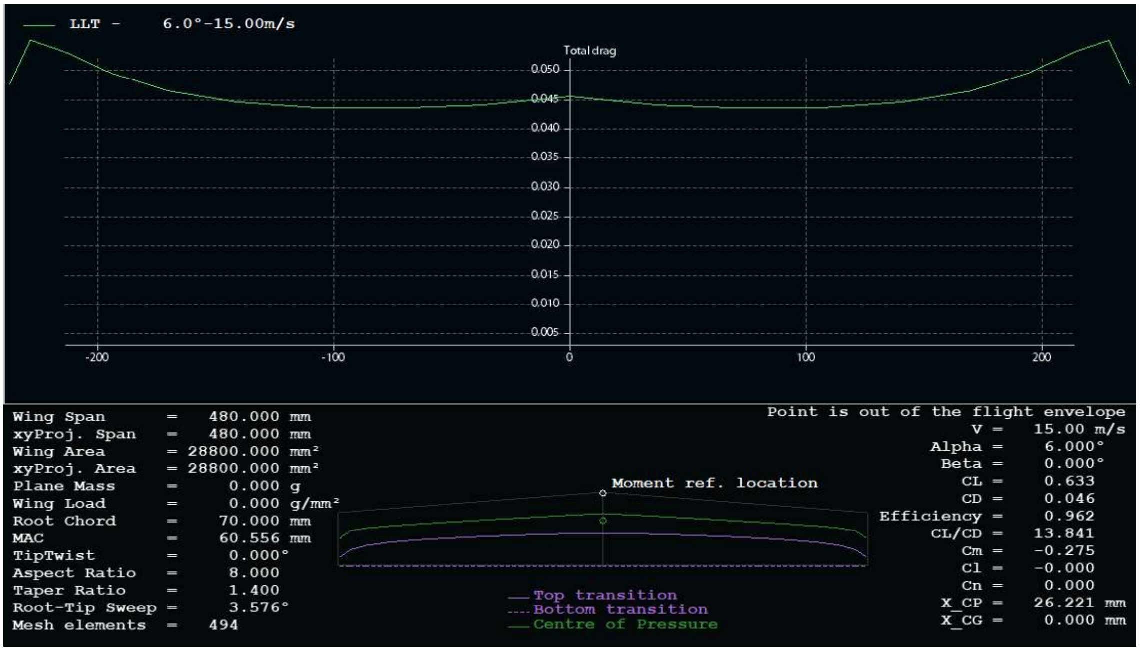

Figure 64: Total drag vs Wingspan

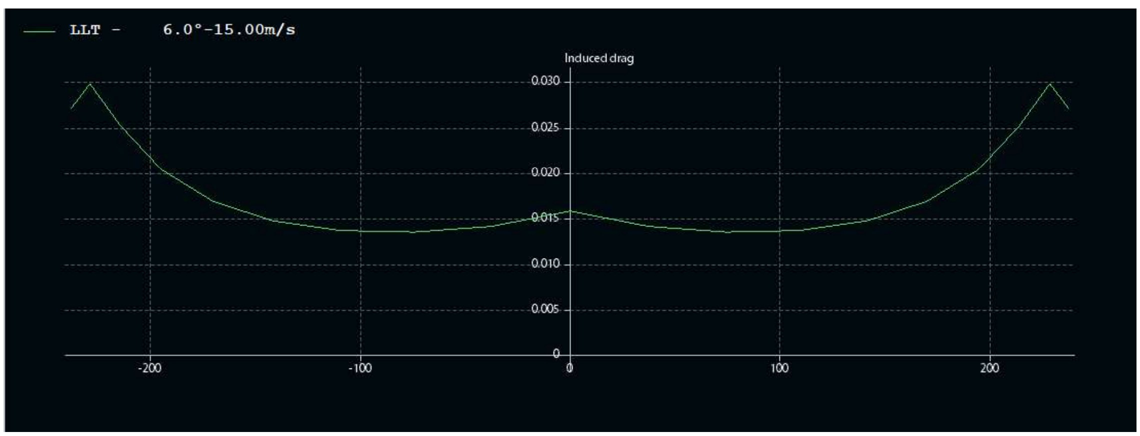

Figure 65: Induced drag vs Wingspan

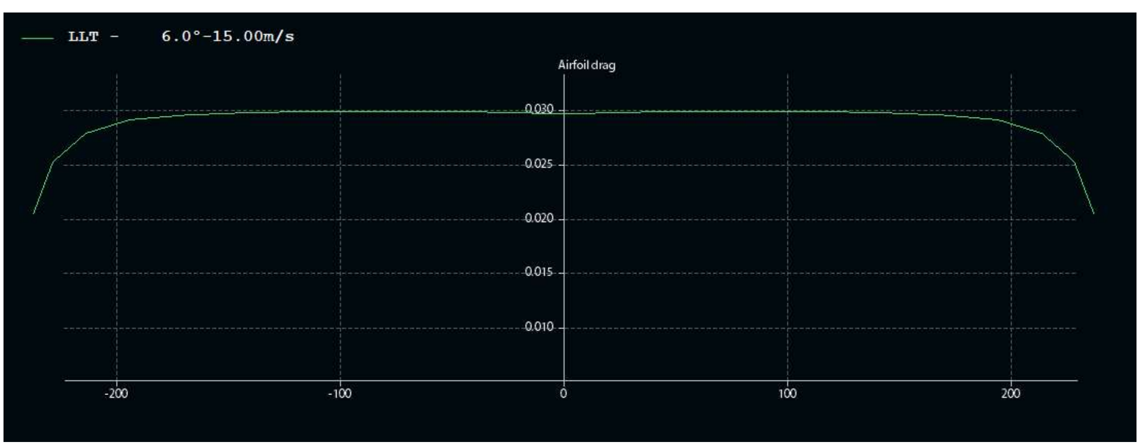

Figure 66 Aerofoil drag vs wingspan

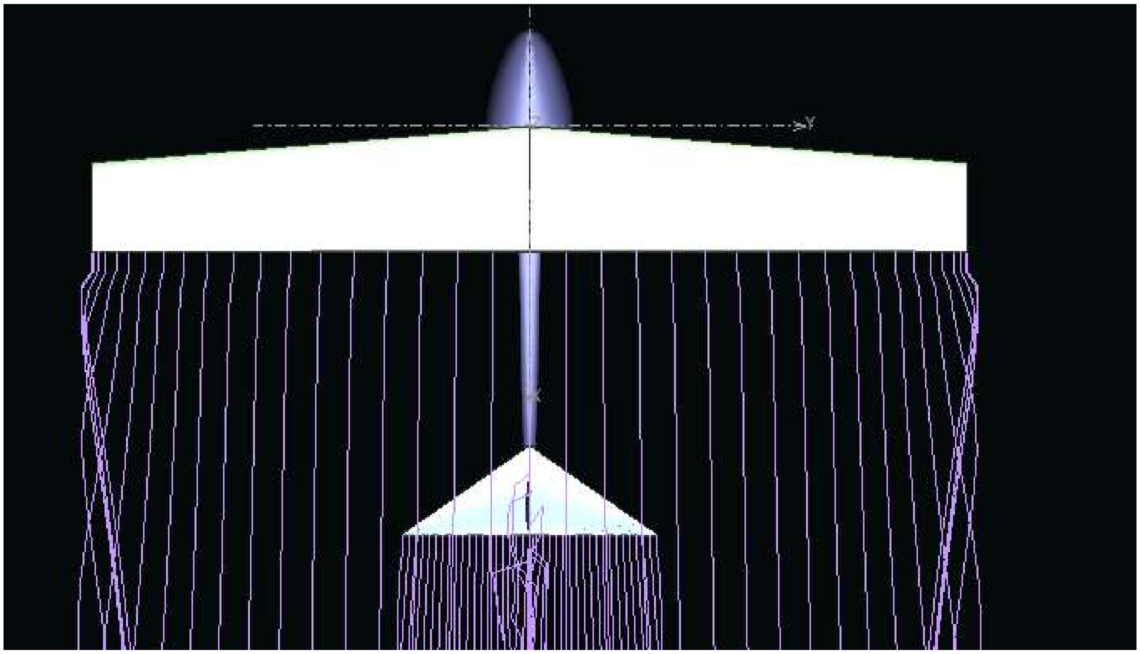

Figure 67: Streamlines

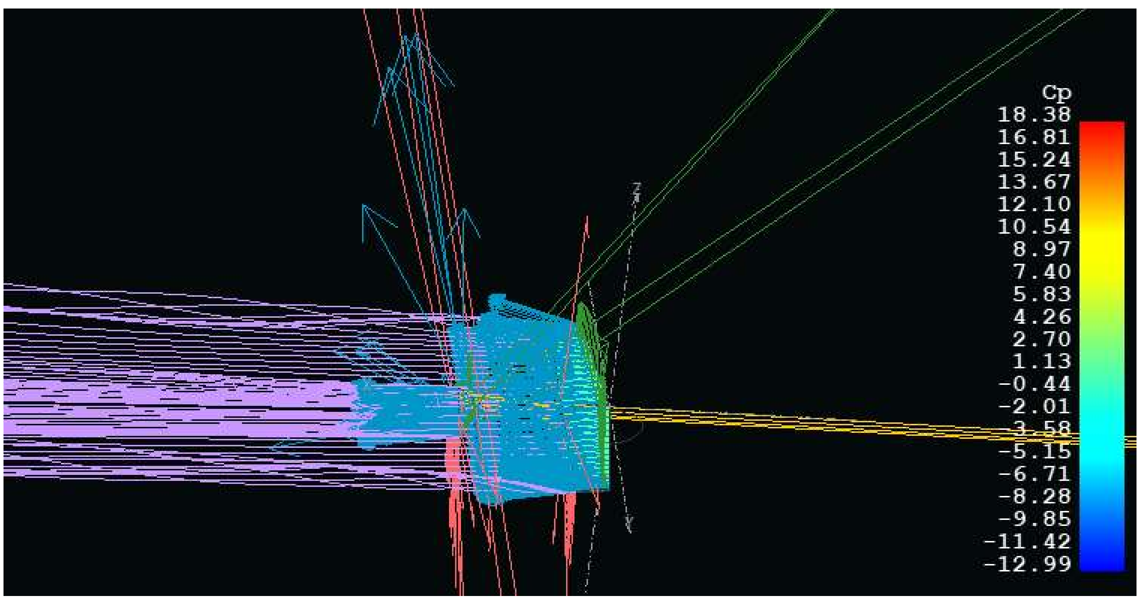

Figure 68: All Aerodynamic Properties

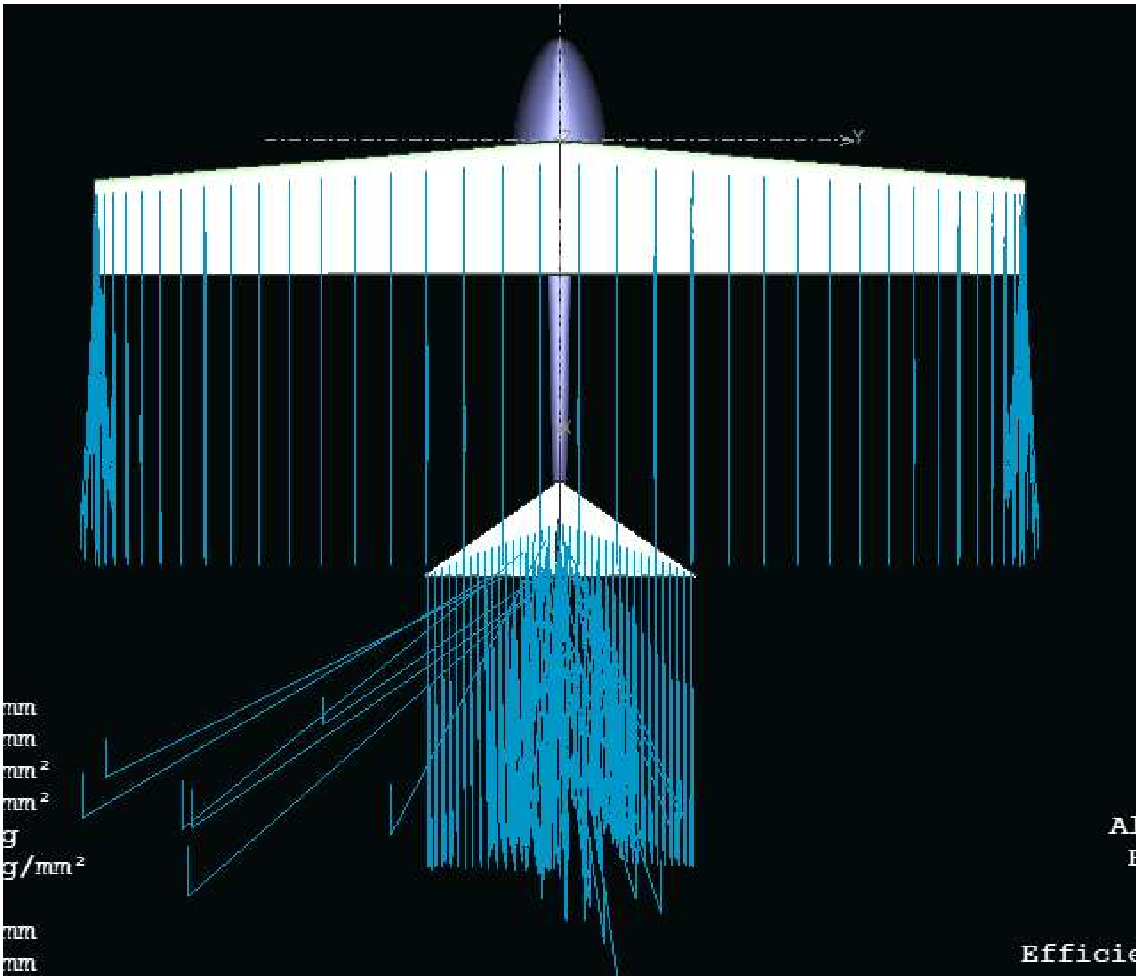

Figure 698: Surface Velocity vector

Appendix C: CAD Files

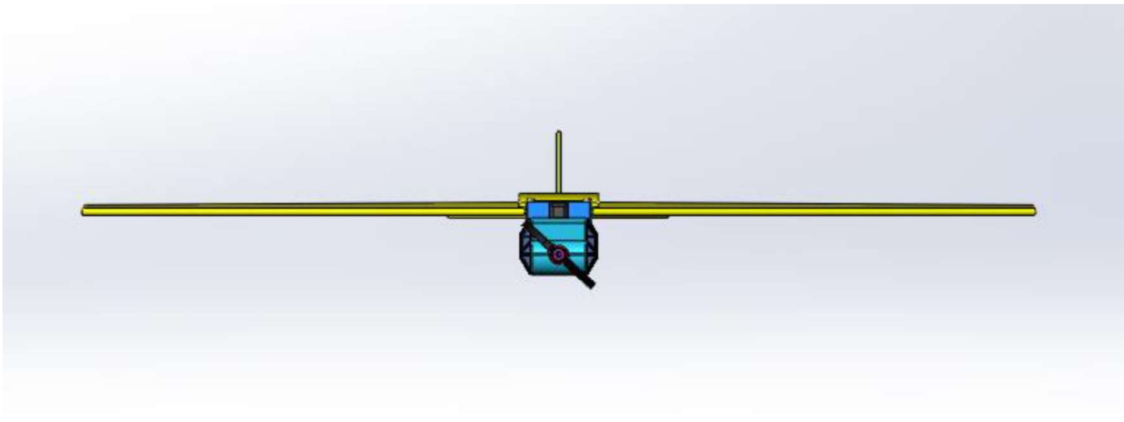

Figure 70Front View

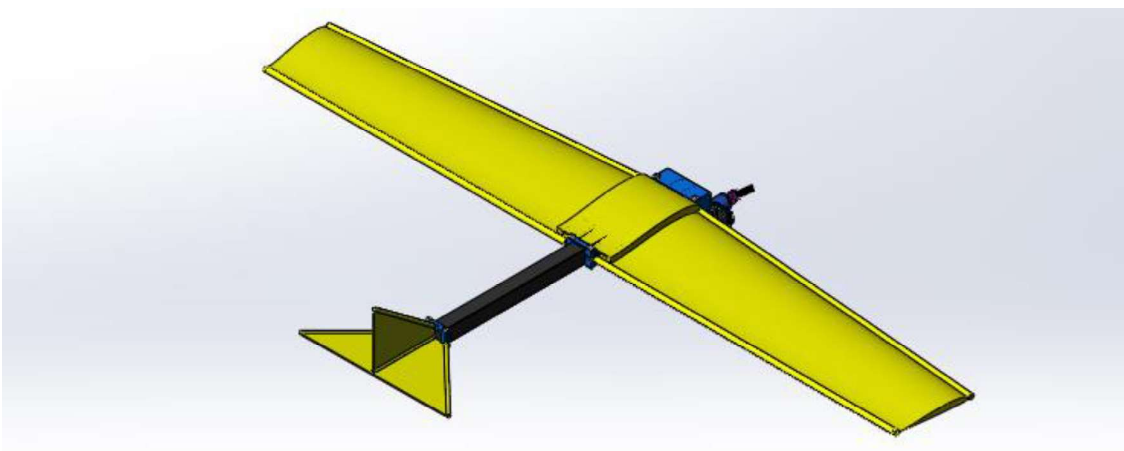

Figure 71: Isometric View

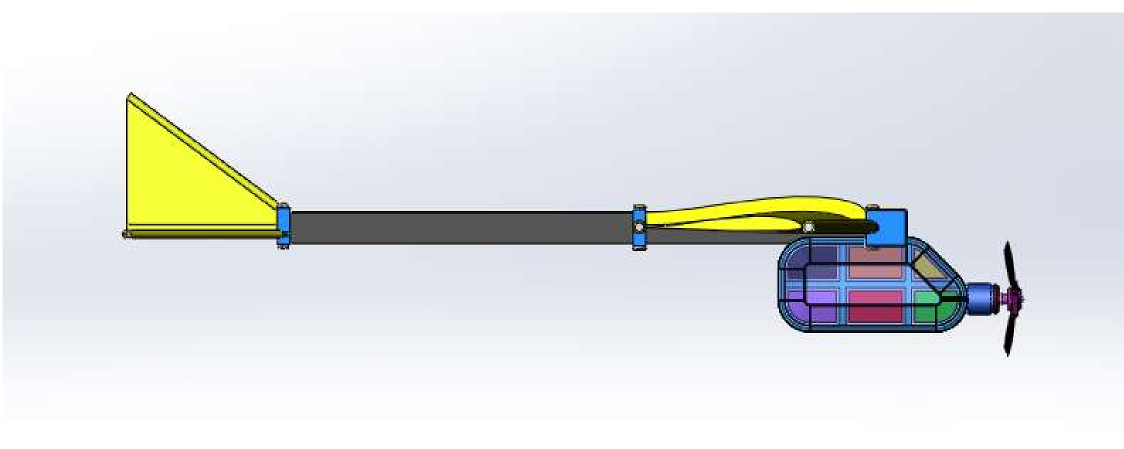

Figure 72: Side View

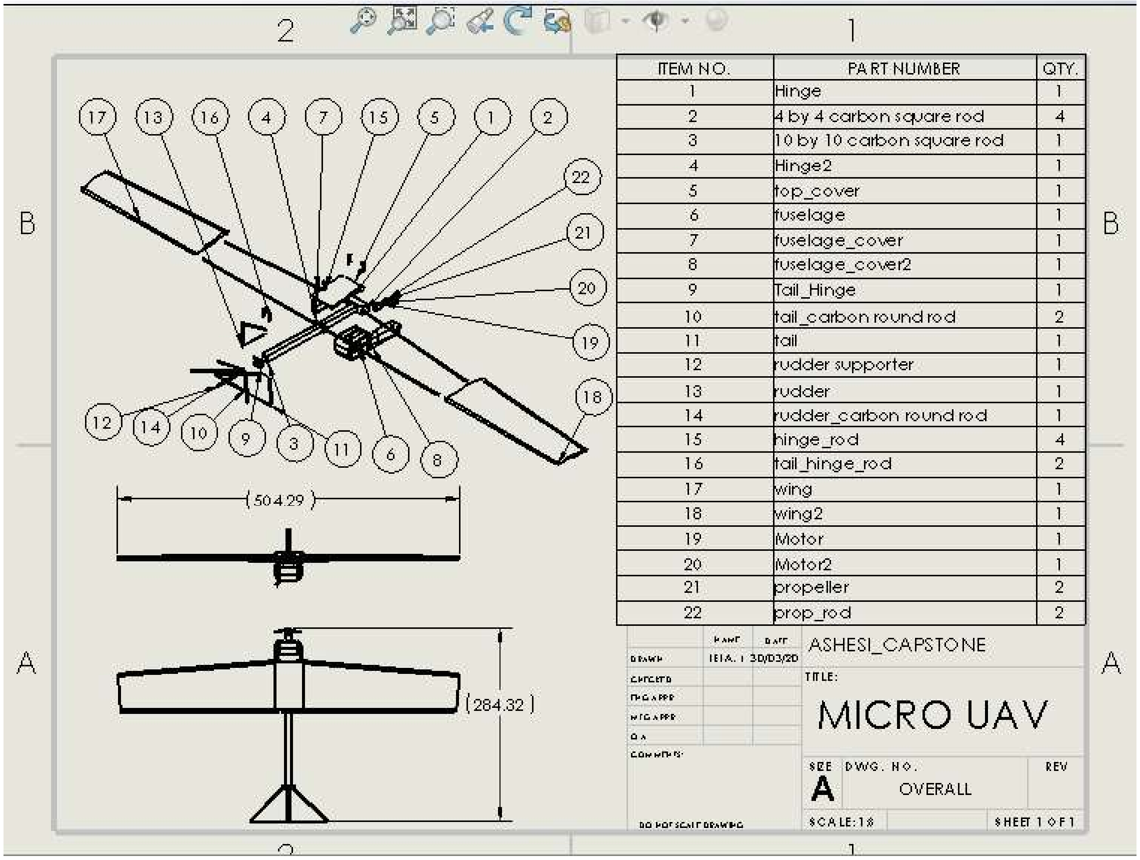

ITEM NO.	PART NUMBER	QTY.
1	Hinge	1
2	4 by 4 carbon square rod	4
3	10 by 10 carbon square rod	1
4	Hinge2	1
5	top_cover	1
6	fuselage	1
7	fuselage_cover	1
8	fuselage_cover2	1
9	Tail_Hinge	1
10	tail_carbon round rod	2
11	tail	1
12	rudder supporter	1
13	rudder	1
14	rudder_carbon round rod	1
15	hinge_rod	4
16	tail_hinge_rod	2
17	wing	1
18	wing2	1
19	Motor	1
20	Motor2	1
21	propeller	2
22	prop_rod	2

Figure 73 Assembly drawing